uOttawa

L'Université canadienne
Canada's university

FACULTÉ DES ÉTUDES SUPÉRIEURES ET POSTOCTORALES

uOttawa

L'Université canadienne
Canada's university

FACULTY OF GRADUATE AND POSDOCTORAL STUDIES

Fatima Maksoud

AUTEUR DE LA THÈSE / AUTHOR OF THESIS

M.Sc. (Cellular and Molecular Medicine)

GRADE / DEGREE

School of Cellular and Molecular Medicine

FACULTÉ, ÉCOLE, DÉPARTEMENT / FACULTY, SCHOOL, DEPARTMENT

Characterizing the Role of the MRTF-A/SRF Pathway in Shear Induced Cytoskeletal Remodeling

TITRE DE LA THÈSE / TITLE OF THESIS

J. Copeland

DIRECTEUR (DIRECTRICE) DE LA THÈSE / THESIS SUPERVISOR

CO-DIRECTEUR (CO-DIRECTRICE) DE LA THÈSE / THESIS CO-SUPERVISOR

EXAMINATEURS (EXAMINATRICES) DE LA THÈSE / THESIS EXAMINERS

C. Kennedy

J.Lee

Gary W. Slater

Le Doyen de la Faculté des études supérieures et postdoctorales / Dean of the Faculty of Graduate and Postdoctoral Studies

Characterizing the Role of the MRTF-A/SRF Pathway in Shear Induced Cytoskeletal Remodeling

Fatima Maksoud

Thesis submitted to the
Faculty of Graduate and Postdoctoral Studies
In partial fulfillment of the requirements
For the MSc degree in Cellular and Molecular Medicine

Cellular and Molecular Medicine
Faculty of Medicine
University of Ottawa

Your file Votre référence
ISBN: 978-0-494-61192-0
Our file Notre référence
ISBN: 978-0-494-61192-0

Abstract

Laminar shear stress is atheroprotective mainly due to its effect on endothelial cell morphology. Endothelial cells subjected to laminar flow elongate, align in the direction of flow and form robust stress fibers which align along with microtubules parallel to the direction of flow. We investigated the role of the actin/MRTF-A/SRF pathway in mediating the endothelial remodeling response. We hypothesize that MRTF-A is required for shear induced cytoskeletal remodeling to occur.

We were able to show that MRTF-A translocates to the nucleus within 3 hours of shear stress application. The duration of nuclear translocation was short term lasting only 6 hours. After 6 hours of flow, MRTF-A was predominantly cytoplasmic. The inhibition of ROCK abolished shear induced MRTF-A nuclear translocation and cytoskeletal remodeling. The inhibition of PI-3 kinase, myosin II and GSK-3β attenuated shear induced MRTF-A nuclear translocation and cytoskeletal remodeling whereas the inhibition of Rac1 and MEK had no effect. Shear induced MRTF-A nuclear translocation and the cytoskeletal remodeling response appear to be largely ROCK dependent.

In addition, we investigated the requirement of MRTF-A for cell migration. HUVECs infected with adenovirus expressing a dominant negative form of MRTF-A were unable to migrate in a scratch wound assay. Moreover, HUVECs expressing DN MRTF-A were unable to form a capillary network consisting of dispersed cells in a matrigel assay but formed networks where cells remained in clumps.

Table of Contents

List of Tables

Chapter 2

List of Figures

Chapter 1

Chapter 3

Chapter 4

List of Abbreviations

ARP 2/3: Actin Related Proteins 2 and 3

BAEC: Bovine Aortic Endothelial Cells

BSAC: Basic, SAP and coiled coil domain

CA: Constitutively Active

CoIP: Co-Immunuprecipitation

DAPI: 4',6-diamidino-2-phenylindole

Dia: Diaphanous

DRF: Diaphanous Related Formin

DSRF: Drosophila Serum Response Factor

DN: Dominant Negative

EC: Endothelial Cell

ECM: Extracellular matrix

EGTA: Ethyleneglycol-*bis*(β-aminoethyl)-N,N,N′,N′-tetraacetic Acid

ERK: Extracellular Signal Related Kinase

ES: Embryonic Stem

FBS: Fetal Bovine Serum

FHOD: Formin Homology Domain-Containing Protein

GDP: Guanosine Diphosphate

GFP: Green Fluorescent Protein

GSK-3β: Glycogen Synthase Kinase 3β

GTP: Guanosine Triphosphate

HUVEC: Human Umbilical Vein Endothelial Cells

JNK: c-Jun N-terminal Kinase

MADS: MCM-1, Agamous, Deficiens, SRF

MAPK: Mitogen-Activated Protein Kinase

MRTF: Myocardin Related Transcription Factor

MTOC: Microtubule Organizing Center

PECAM-1: Platelet Endothelial Cell Adhesion Molecule-1

PBS: Phosphate Buffered Saline

PI-3K: Phosphatidylinositol 3-Kinase

ROCK: Rho-Associated Kinase

RGD: Arginine-Glycine-Aspartic acid

RPEL: Arginine, Proline, Glutamic Acid, Leucine

SAP: SAF-A/B, Acinus, PIAS

siRNA: Small Interfering Ribonucleic Acid

SMC: Smooth Muscle Cells

SRE: Serum Response Element

SRF: Serum Response Factor

TCF: Ternary Complex Factor

VEGFR2: Vascular Endothelial Growth Factor Receptor 2

Acknowledgements

I would like to dedicate this thesis to my parents who supported and encouraged me throughout my academic journey. Only now am I beginning to understand the struggles parents go through and the sacrifices they make to ensure their children get the best of everything. Thank you mom and dad for giving me the best of everything.

I am deeply grateful for having had the privilege to conduct my research under the supervision of Dr. John Copeland. I would like to thank him for his patience, advice and his constant enthusiasm and positive attitude. His love for science and breadth of knowledge continually inspire me.

I would like to thank the members of my advisory committee Dr. Chris Kennedy and Dr. Christina Addison for their advice, helpful suggestions and support for my project. I am grateful to the late Dr. Lowell Langille for inviting me to his lab at the University of Toronto to conduct the long term flow and magnetic beads experiments, both of which were conducted with the aid of Marc Chretien.

I would like to thank Beth, Sarah, Dominique, Susan, Dominic and David as well as the many summer students that have passed through the Copeland lab for their friendship, help and advice throughout this project.

I could not have survived graduate studies had it not been for a very special group of friends who are too numerous to mention individually (Lunde, I couldn't have done it without you!).

Finally, who can I thank more than my beloved husband Walid and my little princess Noura. Thank you حبيبي for your unconditional love, patience and support. It was a long trip and you were always there for me.

Chapter 1: Introduction

This thesis will investigate the involvement of the actin/MRTF-A/SRF pathway in shear induced cytoskeletal remodeling in HUVECs. This investigation aims to:

1- Determine if shear stress activates the MRTF-A/SRF transcriptional response.

2- Identify whether MRTF-A is required for shear induced cytoskeletal remodeling.

3- Determine the components acting upstream of MRTF-A in the shear induced remodeling response.

Chapter 1 will introduce the transcription factor, serum response factor (SRF) and describe the actin/MAL/SRF pathway. A detailed description of the structure, knockout phenotypes and mechanism of regulation of the SRF cofactor MRTF will also be provided. Also in this section, the requirement for MRTFs in tension/force associated processes such as Drosophila border cell migration and skeletal muscle hypertrophy is discussed. The subsequent part of the chapter will deal with the endothelial actin cytoskeleton and its associated structures (focal contacts, adherens junctions). Also detailed in this chapter is how endothelial cells sense and respond to shear stress and the different signalling pathways triggered by the onset of shear stress. The last part of this chapter will discuss the requirement for SRF activity in endothelial cells during angiogenesis.

1.1 Serum Response Factor

SRF is a member of the MADS box family of transcription factors. SRF regulates muscle specific and growth factor inducible genes by binding to a 10 base pair CArG

box located within a region of the promoter called the serum response element (SRE) (reviewed in Miano, 2003). The naming of SRF came through the discovery that SRF bound a serum response element in the promoter of the immediate early gene c-fos (Norman et al., 1988, Treisman R, 1986). Serum response elements similar to that of c-fos were later found in the promoters of other immediate early genes.

SRF regulates the transcription of genes required for cell growth as well as a subset of genes encoding cytoskeletal and contractile proteins. The ability of SRF to control two mutually exclusive programs of gene expression resides in the use of cofactors that control the spatial and temporal expression of SRF target genes.

SRF null models in *C.elegans, D. melanogaster* and *M. musculus* show that SRF is indispensable for the expression of cytoskeletal and contractile genes. Processes requiring the expression of these genes, such as cell spreading, adhesion and migration are greatly impaired in the absence of SRF. However, SRF inactivation does not impair cell growth and proliferation suggesting that SRF is not essential for these processes (Schratt et al., 2001, Schratt et al., 2002, Li et al., 2005, Niu et al., 2005 also reviewed in Miano, 2003).

SRF knockdown in *C. elegans* by siRNA resulted in locomotion defects ranging from uncoordinated movement to paralysis (Fraser at al, 2000). Loss of SRF function in *Drosophila* led to defects in formation of the larval tracheal system and wing differentiation. DSRF, the *Drosophila* SRF homologue, is expressed in terminal tracheal cells which extend cytoplasmic processes to oxygen deprived tissue. In larvae homozygous for the pruned allele of DSRF, the terminal cells are unable to extend these processes, giving rise to a defective respiratory phenotype (Guillemin et al., 1996).

DSRF is also expressed in regions of the wing imaginal disc that gives rise to intervein tissue. DSRF(-/-) Drosophila fail to form intervein tissue in the wing. DSRF (-/+) Drosophila form excess vein tissue in the wing. This indicates that DSRF is required for the suppression of vein tissue and the formation of intervein tissue (Montagne et al., 1996) Mouse embryos lacking SRF fail to form mesoderm and lack proper folding of the endoderm and ectoderm leading to their death before completing gastrulation (Day 12.5 of development) (Arsenian et al., 1998).

SRF knockout in ES cells leads to altered cellular spreading, adhesion and migration. SRF(-/-) ES cells are unable to form cytoskeletal structures such as focal adhesions and actin stress fibers (Schratt et al, 2001). This is probably due to the significantly reduced expression of β-actin causing a shift in the actin treadmilling equilibrium leading to a deficit in actin filament formation. Indeed, expression of a constitutively active derivative of SRF, SRF-VP16, is sufficient to re-establish the formation of focal adhesions and actin stress fibers (Schratt et al, 2002).

1.2 Rho-Actin-MAL-SRF Pathway

SRF dependent transcription is activated via the MAPK/TCF signalling pathway or the Rho/MRTF pathway. Growth related genes such as c-fos and egr-1 are activated through the formation of a ternary complex between SRF and members of a family of Ets domain proteins known as ternary complex factors (TCFs). The activity of these proteins is controlled by MAPK signalling (Treisman R, 1994). The Rho/actin/MRTF pathway activates cytoskeletal and immediate early genes through activated Rho GTPase which promotes changes in actin cytoskeletal dynamics leading to the activation of a second

group of SRF co-factors, the myocardin related proteins (MRTF-A and MRTF-B) (Miralles et al., 2003). TCF and MRTF compete for the same binding site on SRF such that activation of one cofactor excludes the possibility of activating the other (Cen et al., 2004, Murai et al., 2002).

Actin treadmilling plays a key role in RhoA mediated SRF activation. Drugs such as latrunculin and C2 toxin that prevent actin polymerization inhibit SRF activation (Sotiropoulos et al., 1999). Conversely, drugs that promote F-actin polymerization in the absence of other stimuli result in SRF activation (Geneste et al., 2002, Gineitis et al., 2001, Mack et al., 2001, Tominaga et al., 2000). Also, over expression of a non-polymerizable actin (actin G13R) inhibits SRF activation in the presence of an active derivative of the actin nucleating protein, mDia1 (Copeland JW and Treisman R, 2002). These data suggest that it is the overall level of G actin, rather than F-actin, which governs the activation of this pathway.

1.3 Myocardin Related Transcription Factors (MRTFs)

Myocardin related transcription factors are a family of SRF transcriptional co-activators that consists of the founding member myocardin, MRTF-A (aka MAL22, MKL1), and MRTF-B (aka MAL16, MKL2). The ancestral gene is thought to be similar to Drosophila, MAL-D, which closely resembles MRTF-A (Han et al., 2004) Myocardin was discovered during a bioinformatics screening for cardiac specific genes and is expressed exclusively in the cardiovascular system while MRTF-A and MRTF-B are ubiquitously expressed. MRTF-A and MRTF-B are thought to be largely functionally redundant, although MRTF-B is not as potent a transcriptional activator as MRTF-A

(Wang et al., 2002) and there are other apparent differences in their behaviour as described below.

1.3.1 Structure of Myocardin and MRTFs

Members of the myocardin family of transcription factors have conserved N termini and divergent C termini. The C terminus of these proteins functions as a transcriptional activation domain that recruits general transcription factors and RNA pol II to the target promoter. At the N terminus of these proteins, there are several conserved domains; an RPEL motif, two basic domains (B1 and B2), a glutamine rich domain, a SAP domain and a leucine zipper. These domains mediate nuclear import, association with SRF and MRTF dimerization (Figure 1.1) (reviewed in Cen et al., 2004).

The RPEL motifs bind monomeric actin and regulate the cellular localization and activity of MRTF-A and B. Deletion of this domain renders either protein constitutively active and localized to the nucleus. The RPEL motifs of myocardin are unable to bind G-actin which likely accounts for its constitutive nuclear localization (Miralles et al., 2003). The nuclear import of MRTF-A is also mediated by the two basic regions, B1 and B2. Binding of G-actin to the RPEL motifs masks B2 causing MRTF-A to be sequestered to the cytoplasm. The release of G-actin from MRTF-A unmasks the B2 region enabling MRTF-A nuclear accumulation. The exact mechanism of MAL export however remains unknown (Miralles et al., 2003).

Association of myocardin and MRTF-A/B with SRF is mediated by the basic domain B1 (Wang et al., 2001, Zaromytidou et al., 2006). The leucine zipper enables homo and hetero dimerization between family members. Myocardin and its related transcription factors all contain a SAP domain. This domain is a conserved region of 35

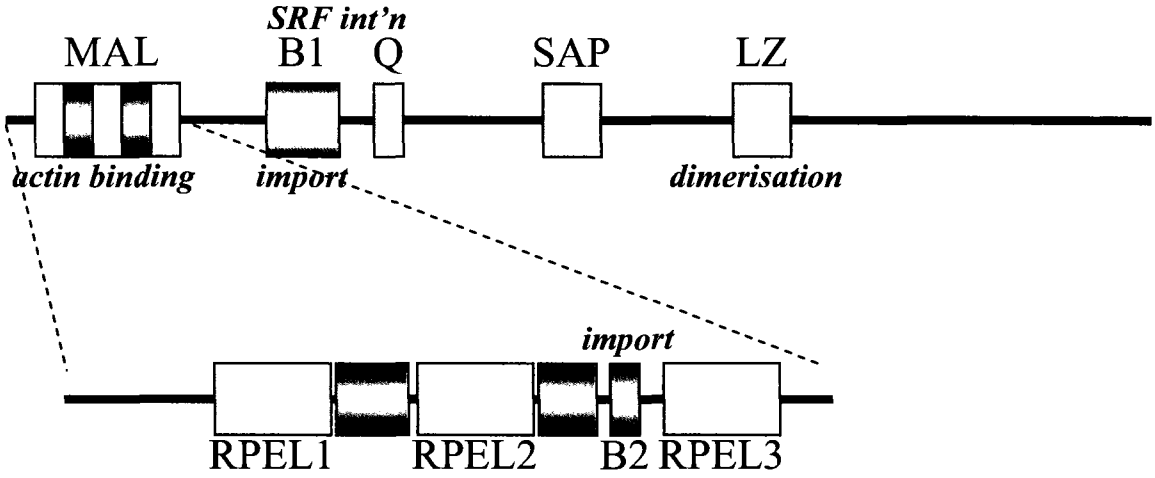

Figure 1.1: **MRTF structure.** MRTFs are characterized by the presence of highly conserved RPEL motifs that serve to bind G-actin. Basic regions B1 and B2 are necessary for nuclear import. Basic region B1 and glutamine rich domain Q are required for interaction with SRF. Leucine zipper (LZ) permits the homo and heterodimerization between family members.

amino acids named after nuclear proteins which also possess a similar domain; SAF-A/B, Acimus and PIAS. The function of the SAP domain in MRTFs remains unclear (Cen et al., 2004).

1.3.2 MRTF Knockout Phenotypes

MRTF-A and B are thought to be functionally redundant. The two proteins are very similar at the structural level and both are ubiquitously expressed. Indeed, both MRTF-A and MRTF-B activity must be blocked in order to inhibit Rho-induced activation of SRF-dependent transcription (Cen et al., 2003). However, knockout mice with single gene null mutations for either MRTF exhibit unique phenotypes. Mice homozygous for a loss of function mutation of MRTF-A are viable and fertile, however, 40% of homozygous embryos die during embryogenesis (Sun et al., 2006). Further examination of the embryos isolated between stages E10-E18.5 shows that 35% suffer from dilation of atrial and ventricular chambers of the heart as well as dilation of outflow vessels of these chambers (Sun et al., 2006). The surviving MRTF-A mice appear normal except for the inability to nurse their pups. During early lactation stages, expression of genes encoding SMC markers (e.g. SM α actin, SM myosin) decreased in mammary myoepithelial cells. This was followed by the apoptosis of these cells. These data suggest that mammary gland myoepithelial cells are unable to maintain their differentiated state due to the absence of SMC markers leading to the inability of these cells to perform their proper function during lactation. This implies that MRTF-A is required for the differentiation and maintenance of mammary gland myoepithelial cells (Sun et al., 2006, Li et al., 2006).

MRTF-B mutant mice die at mid-gestation. These embryos display a spectrum of defects in cardiac outflow tracts as well as defects in pharyngeal arch remodeling. These are accompanied by the failure of neural crest cells to differentiate into vascular SMCs. Restoring MRTF-B expression in the neural crest (by neural crest specific expression of Cre) is enough to generate viable mice and rescue cardiac outflow defects in MRTF-B mutants (Oh et al., 2005, Li et al., 2005). This indicates that MRTF-B is required for the differentiation of cardiac neural crest derivatives into SMCs. Normal SMC differentiation ensures the proper patterning of cardiac outflow tracts and pharyngeal arches.

The difference in the MRTF-A versus MRTF-B knockout phenotypes could indicate that each plays a unique non-redundant role in the affected tissues. Alternatively, it may be that MRTF-A and MRTF-B are largely redundant, but certain tissues are particularly sensitive to total MRTF activity. Hence, knocking out one MRTF brings total MRTF activity below a required threshold. It will be of interest to determine if knock-in of MRTF-A for MRTF-B is able to rescue the MRTF-B phenotype and vice versa.

1.4 Regulation of MRTF Activity

1.4.1 MRTF Regulation in NIH3T3 and Smooth Muscle cells

In serum starved NIH3T3 cells, MRTF-A is almost exclusively cytoplasmic. Serum stimulation, activation of RhoA or actin polymerization causes MRTF-A to translocate to the nucleus. MRTF-A is extremely dynamic in unstimulated cells and shuttles continuously between the cytoplasm and the nucleus. Hence, the cytoplasmic

localization of MRTF-A in unstimulated cells reflects the high basal nuclear export rate of MRTF-A (Vartiainen et al., 2007). The N-terminus of MRTF-A consists of regulatory RPEL motifs which are able to bind monomeric actin. It is this interaction that causes the apparent "retention" of MRTF-A in the cytoplasm. Deletion or mutation of RPEL motifs 2 and 3 gives rise to MRTF mutants that are constitutively nuclear, thus supporting the regulatory role of the RPEL motifs. It is thought that the binding of G-actin to the RPEL motifs masks the B1 domain which has been shown to be required for nuclear import. Actin polymerization depletes the G-actin pool, leading to dissociation of the MRTF-A: actin complex which unmasks the B1 domain and allows MRTF-A to translocate to the nucleus.

Upstream of MRTF-A, RhoA regulates the activation of the MRTF-A/SRF pathway through its downstream effectors ROCK and mDia which promote actin nucleation, polymerization and stabilization. The formin protein mDia drives actin nucleation and polymerization through its conserved FH2 domain (Li and Higgs., 2003). ROCK activates LIM kinase which phosphorylates cofilin thus inhibiting its activity (Maekawa et al., 1999). In its unphosphorylated form cofilin, promotes the dissociation of ADP bound actin monomers from the minus end of the actin filament. Hence, ROCK activity serves to stabilize F-actin filaments. ROCK induced F-actin stabilization and mDia1 induced actin polymerization both contribute to the depletion of the G-actin pool enabling MRTF-A to translocate to the nucleus and activate SRF dependent transcription (Figure 1.2) (Miralles et al., 2003).

In addition to regulating MRTF-A nuclear import, the G-actin pool also regulates MRTF-A nuclear export and the transcriptional activation of SRF target genes

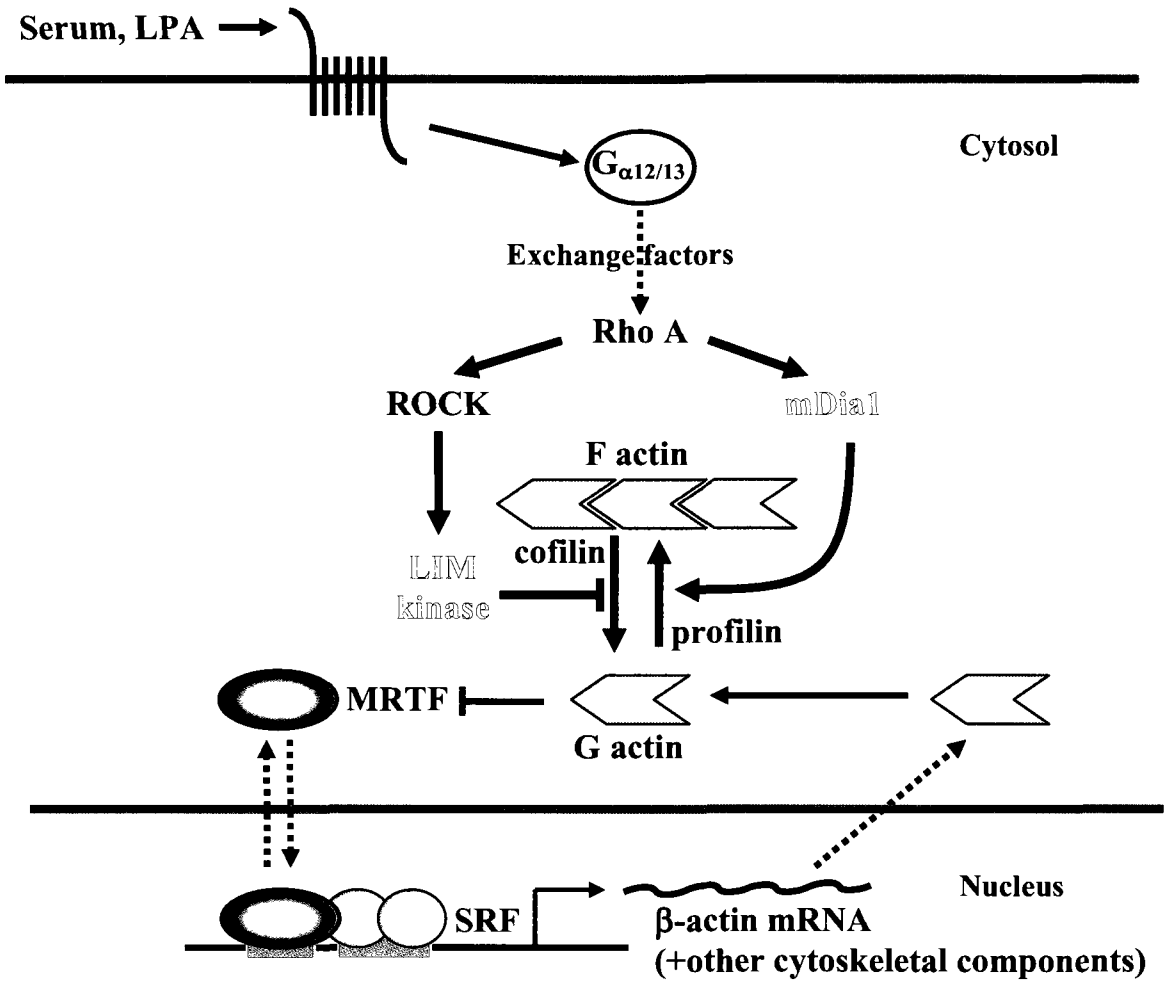

Figure 1.2: **Actin/MRTF/SRF Pathway.** Serum stimulation activates Rho through GPCR. Rho activates ROCK and mDia1 which cooperate to induce actin polymerization and stabilization. mDia1 works with the G-actin binding protein cofilin to promote actin polymerization. ROCK activates LIM kinase which phosphorylates and inactivates cofilin promoting filament stabilization. Depletion of the G-actin pool induces nuclear translocation of MAL and SRF dependent transcription.

(Vartiainen et al., 2007). The interaction of G-actin with MRTF-A through its conserved RPEL motifs is required for export via the nuclear exportin Crm-1. This interaction, however, represses SRF activity once MRTF-A is in the nucleus (Vartiainen et al., 2007). The presence of G-actin bound to MRTF-A could hinder the assembly of a transcriptional complex or could prevent MRTF-A from associating with parts of the general transcription machinery thus preventing SRF from driving transcription. Therefore, the dissociation of the actin:MRTF complex is required for RhoA/SRF dependent transcription.

SRF is a key regulator of SMC differentiation. It regulates SMC specific transcription by binding to CArG boxes found in the promoters of SMC differentiation marker genes. The expression of these genes was found to be regulated by RhoA/actin signalling (Mack et al., 2001). MRTF-A is expressed in various SMC types which prompted the investigation into its involvement in SRF signalling as well as its regulation in SMCs.

MRTF cellular localization was investigated as a regulator of SMC specific transcription. An EGFP/MRTF-A fusion protein was transfected into 10T1/2 and SMCs to track MRTF-A localization in real time. MRTF-A was still detected in the nucleus of a proportion of 10T1/2 cells following serum starvation. Nuclear MRTF-A was detected in even higher proportions in SMCs subjected to serum deprivation. Most cells however displayed an intermediate phenotype where MRTF-A was diffusely distributed throughout the cell. Treatment of 10T1/2 cells with an agonist prompted MRTF-A translocation to the nucleus in cells where it was initially cytoplasmic within 45-60 mins. This nuclear translocation was further translated into activation of the SM α actin

promoter. MRTF-A translocated to the nucleus at a faster rate in SMCs (within 10-60 mins). The requirement for nuclear localization of MRTF-A for SMC differentiation marker gene expression was further demonstrated with the use of a DN form of MRTF-A. This DN (MRTF-A ΔB1ΔB2) lacked the N-terminal basic regions B1 and B2 necessary for nuclear translocation. MRTF-A ΔB1ΔB2 dimerizes to endogenous MRTF-A, retaining it in the cytoplasm thus inhibiting its activity. SM α actin expression levels decreased with increasing amounts of MRTF-A ΔB1ΔB2 (Hinson et al., 2007).

MRTF-B is thought to function very similarly to MRTF-A (Selvaraj et al., 2003) although the regulation of its activity has not been extensively studied. MRTF-B is known to be a weaker activator of SRF than MRTF-A which is probably due to an N terminal domain, absent in MRTF-A, which inhibits MRTF-B/SRF interaction (Mack CP and Hinson JS, 2005).

Cell type specific differences exist in some aspects of MRTF regulation such as basal MRTF localization and how fast MRTF translocates to the nucleus in response to a stimulus. The regulation of MRTF by RhoA and the MRTF/SRF interaction however, seem to be conserved.

1.4.2 Regulation of MRTF Activity Through Calcium Dependent Dissociation of Epithelial Cell Contacts.

Dissociation of epithelial cell contacts through calcium depletion of the extracellular media triggers the nuclear translocation of MRTF-A. The endogenous distribution of MRTF-A in LLC-PK1 cells was investigated using a polyclonal antibody raised against BSAC, an isoform of the mouse homologue of MRTF-A. In untreated

cells, MRTF-A is exclusively cytoplasmic whereas calcium depletion results in an increase in MRTF-A nuclear localization (16% increase) (Fan el al., 2007).

SRF activation by calcium withdrawal involves signalling via G-actin. Transfection of wild type actin and non polymerizable actin mutant R62D leads to a reduction in SRF activation (measured by reporter gene induction) in a reduced calcium environment. Expression of G15S actin, an F-actin stabilizing mutant activated SRF to a similar extent under physiological and reduced calcium levels. Also, the actin:MAL complex is disrupted upon calcium withdrawal as demonstrated by CoIP studies (Busche et al., 2008).

MRTF-A nuclear translocation and SRF reporter gene induction upon calcium dependent dissociation of cell contacts correlated with the transcriptional induction of endogenous SRF target genes such as vinculin and SM α-actin (Fan et al., 2007, Busche et al., 2008).

Both RhoA and Rac are activated upon calcium withdrawal (Fan et al., 2007, Busche et al., 2008). However, it was shown that Rac is required for SRF activation in epithelial cell monolayers following calcium depletion. Tat-C3, a cell permeable toxin which specifically inhibits RhoA did not inhibit SRF activation by calcium reduction. TcdB and TcdBF which inhibit RhoA/Rac/cdc41 and Rac/R-Ras respectively reduced SRF activation by calcium reduction in a dose dependent manner (Busche et al., 2008). Thus, calcium dependent dissociation of epithelial cell contacts induces activation of SRF through Rac, MRTF-A and G-actin signalling.

1.5 Mechanical Stress and MRTFs

The SRF cofactor MRTF-A has been shown to be necessary for several tension/force associated processes. It is believed that one aspect of the MRTF/SRF pathway function is to provide cells with reinforcement allowing them to cope with mechanical stress. In this section, we will examine examples of this concept in Drosophila border cell migration and load induced hypertrophy of skeletal muscle.

1.5.1 MAL-D is Required for Drosophila Border Cell Migration

Border cells are a group of 8 follicle cells located at the anterior of the *Drosophila* egg chamber. These cells delaminate from the epithelial layer surrounding the nurse cells and migrate from the anterior end of the egg chamber to the border between the nurse cells and the oocyte. Wild type border cells migrate as a tight cluster through the substratum and the surrounding nurse cells. Migration initiates with the extension of actin rich filopodia from one cell within the cluster that pulls the rest of the group with it. Border cells mutant for MAL-D are able to extend the long actin rich filopodia, but fail to complete their migration due to the fragmentation of the filopodia. Large fragments of cytoplasm break off from the cellular extension and continue to migrate toward the oocyte leaving behind the cluster of border cells (Somogyi K and Rorth P, 2004). This has been taken to suggest that MAL-D is required for the transcription of cytoskeletal and contractile genes required for the filopodia to withstand the physical strain exerted upon it during migration.

In actively migrating wild type cells, MAL-D is localized to the nucleus. It is also observed that migrating border cell clusters with a high proportion of cells with nuclear

MAL-D are more likely to have an elongated shape. Clusters with no or few cells with nuclear MAL-D have a more rounded phenotype (Somogyi K and Rorth P, 2004). The elongated phenotype suggests that the cell is being subjected to external forces as well as to tension from within. Mutations in other genes required for migration causes MAL-D to remain cytoplasmic. For example, the activity of the transcription factor slbo is required to initiate migration. Border cells mutant for slbo do not accumulate nuclear MAL-D. However the slbo mutant cells are able to accumulate nuclear MAL-D if pulled along by wild type border cells within the same cluster (Somogyi K and Rorth P, 2004). This indicates that force/tension exerted on the cells within the cluster can induce MAL-D nuclear translocation. Thus, tension induced MAL-D activity provides Drosophila border cells with the cytoskeletal reinforcement needed during migration.

1.5.2 MRTF-A is Required for Load Induced Hypertrophy of Skeletal Muscle

Skeletal muscle specific deletion of SRF leads to the death of mutant mice within a few days after birth. These mutant mice display a deficiency in muscle growth which probably disrupts breathing and/or nursing leading to their death. A similar although less severe phenotype is displayed by mice expressing a dominant negative mutant of MRTF-A which consists of the N-terminus containing the SRF binding domain and lacks the C terminal transcriptional activation domain rendering the protein unable to potentiate transcription. This dominant negative works by dimerizing to endogenous MRTF inhibiting their transcriptional activity. These mice exhibited a similar muscle myopathy, but are viable, surviving to adulthood (Li et al., 2005). This is probably due to the inability of dominant negative MRTF-A to shutdown SRF activity completely. Close

examination of dominant negative MRTF-A transgenic mice shows muscle damage and degeneration characterized by fibrosis of myofibrils (Li et al., 2005). As a result, MRTF-A transgenic mice appear runted in comparison with wild type mice. It is likely that inhibition of MRTF activity disrupts the expression of SRF genes which are necessary for the synthesis of sarcomeric proteins which enable muscle cells to withstand the force associated with load induced hypertrophy.

1.6 The Endothelial Actin Cytoskeleton

1.6.1 Actin Structures

Endothelial cells in mature blood vessels are in a quiescent state, but they retain their ability to divide and migrate, this is necessary for the repair of any damage done to the endothelial layer of a blood vessel. Also, formation of new blood vessels is necessary to support growing embryonic tissues as well as to reconstruct damaged adult tissues. The process of new vessel formation "angiogenesis" also requires coordinated cell movement. Endothelial cell movement is made possible by the dynamic remodeling of the actin cytoskeleton into different structures essential for cell migration such as filopodia, lamellipodia and stress fibers.

Filopodia are finger like structures that protrude from the cells leading edge. These structures consist of parallel bundles of actin filaments packed tightly together. Filopodia are believed to be important for sensing the external environment and providing the cell with directional cues (Alberts et al., 2002).

Lamellipodia are sheet like cellular extensions in the cells leading edge. This structure is essential for providing the cell with the necessary traction force for movement. Lamellipodia consist of a web like network of cross linked actin filaments.

Stress fibers are parallel bundles of actin filaments cross linked to myosin filaments rendering them contractile. Stress fibers are required for the retraction of the rear part of the cell during migration (Alberts et al., 2002).

Filopodia formation is initiated by the Rho GTPase cdc42 whereas lamellipodia and stress fibers are formed through the activation of Rac and Rho GTPases respectively.

1.6.2 Actin-Associated Endothelial Cell Junctions

Actin filaments of endothelial cells extend to the cell periphery to form attachments with the extracellular matrix and with neighbouring cells via focal adhesions and adherens junctions. At focal adhesions, actin filaments are linked to integrins by anchor proteins such as α-actinin, talin, filamin and vinculin. Integrins participate in cellular signalling and provide cells with a strong attachment to the extracellular matrix. Adherens junctions are a specialized type of intracellular junction consisting of transmembrane cadherins and cytoplasmic catenins. In endothelial cells, VE-cadherin is an adhesive glycoprotein comprised of a transmembrane domain, a cytoplasmic tail and an extracellular domain. VE cadherins are found as homodimers in the endothelial plasma membrane. The cytoplasmic tail of VE cadherin binds to α and β catenins that link VE cadherin to actin filaments. The extracellular domain of each VE cadherin dimer is able to bind to the extracellular domain of a neighbouring cell hence forming an adherens junction between the two cells. The association of adherens junction

components with actin is essential for junction stabilization as well as junction opening and closing.

1.7 Shear Stress and Endothelial cells

1.7.1 Forces Acting on Endothelium and Flow Patterns

Endothelial cells are subjected to three main forces as a result of blood flow and pressure. Blood pressure exerts a force perpendicular to the cell surface which results in a compressive force. Blood flowing through blood vessels exposes endothelial cells to a frictional force tangential to the cell surface termed "shear stress". A small force is generated from the stretching of the blood vessel due to pulsatile blood flow. This stretching force is sensed by all components of the blood vessel including the extracellular matrix (Figure 1.3) (Davies P, 1997).

Shear stress can be either laminar or turbulent depending on the geometry of the vasculature. Areas of the vasculature that are straight and uncurved are subjected to laminar flow where blood flows in undisturbed parallel layers. In areas containing branches and bifurcations, steady laminar flow is disrupted and becomes turbulent. Turbulent flow can also include separated flow where blood re-circulates at regions near branch points (Davies P, 1997).

Laminar flow causes transient activation of signalling pathways that promote inflammation and cell proliferation. Extended exposure of the endothelium to laminar flow results in the down regulation of these signalling pathways whereas turbulent flow promotes their sustained activation (Chien S, 2008). The sustained activation of pro-inflammatory and proliferative pathways in areas of disturbed flow predispose these

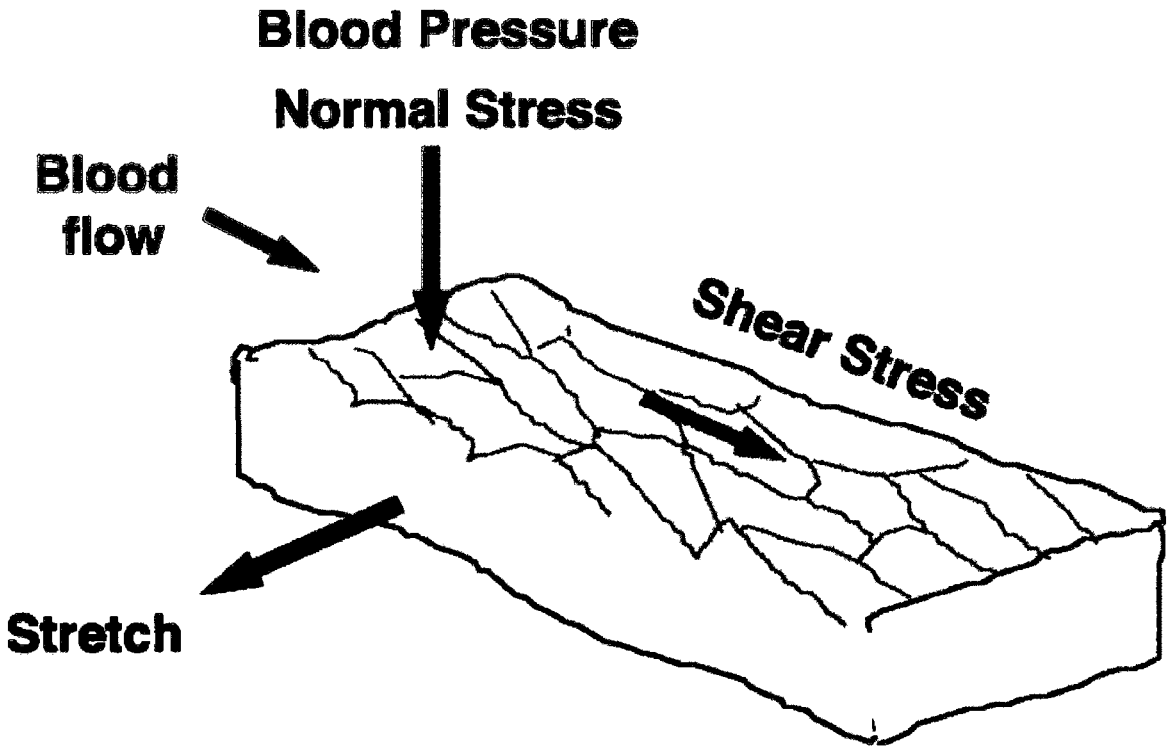

Figure 1.3: **Forces acting on the endothelium.** Endothelial cells are subjected to many different forces. Blood pressure acts normal to the endothelial cell surface whereas blood flow exerts a frictional force tangential to the endothelial cell surface termed shear stress. Blood flow also exerts a force on the whole blood vessel resulting in a stretching force. Reproduced from Chiu et al. 2008 Vascular endothelial responses to altered shear stress: Pathologic implications for atherosclerosis, Annals of Medicine.

areas to the formation of atherosclerotic plaques. Areas of the vasculature subjected to laminar flow are spared from the development of atherosclerotic plaques, thus laminar shear stress is termed "atheroprotective" (Chien S, 2008).

1.7.2 Morphological Changes in Response to Shear Stress

The ability of endothelial cells to align in the direction of flow was first demonstrated by the repositioning of an arterial patch at a 90 degree angle from its original position. Endothelial cells on the patch changed their orientation to align themselves parallel to the direction of flow (Flaherty et al., 1972, Davies, 1995). The structural reorganization endothelial cells undergo in response to shear stress is thought to minimize shear induced trauma to the cell. Elongated endothelial cells show an increased resistance to micropipette deformation (Osborn et al., 2006).

The first prominent change upon the onset of shear stress is the redistribution of cellular F-actin. In static cultures, F-actin is distributed as a dense peripheral band. After application of shear stress, F-actin is reorganized to form parallel stress fibers spanning the length of the cell. Microtubules as well as the MTOC also redistribute to align themselves in the direction of flow (McCue et al., 2006). It is the simultaneous rearrangement of the actin filaments and microtubules that drives the change in cellular morphology (i.e elongation and alignment parallel to the direction of flow) (McCue et al., 2006, Noria et al., 2004). The redistribution of microtubules is thought to be important for the distribution of proteins via myosin motors to the sites where remodeling is occurring (McCue et al., 2006).

Components of junctional complexes (adherens junctions, focal adhesions) are also reassembled in response to flow in order to accommodate changes in cell shape. After 16hrs of shear stress application, adherens junctions display a punctuate staining pattern. Continuous junctions are restored after 96hrs of flow (Noria et al., 1999).

1.7.3 Mechanotransduction and the Endothelial Mechanosensory Complex

The ability of endothelial cells to transform mechanical stimuli into biochemical responses requires a mechanism that senses the mechanical stimulus. A number of candidates have been put forth as the shear stress receptor. The apical surface of endothelial cells is coated with a thin layer of glucosaminoglycans 300-400 nm thick called the glycocalyx (Smith et al., 2003, Vink et al., 2000). The glucosaminoglycan chains of the glycocalyx layer extend through the plasma membrane and are thought to be implicated in the transmission of the shear stress signal.

Embedded in the plasma membrane are a variety of receptor proteins that may play a role in transmitting the shear stress stimulus. These proteins include receptor tyrosine kinases such as VEGFR, G proteins and G protein coupled receptors (Salit et al., 2002, Gudi et al., 1998, Chachisvilis et al., 2006). Integrins on the basal side of endothelial cells have also been implicated as possible candidates of mechanotransduction (Jalali et al., 2001). Integrins undergo rapid conformational change in response to shear stress leading to an increase in integrin binding to the ECM which transiently inactivates Rho. The transient inactivation of Rho is necessary for proper cytoskeletal alignment to occur (Tzima, et al., 2001). Invaginations in the plasma membrane known as caveolae are also thought to mediate mechanotransduction through

sensing changes in plasma membrane tension (Yu et al., 2006). Caveolae were found to be more numerous in cells subjected to laminar shear stress than in static cells (Rizzo et al., 2003). There is evidence that ion channels are also possible mediators of mechanotransduction. Increasing flow results in an extremely rapid increase in intracellular calcium and potassium. Cation TRP and potassium channels have been suggested as possible sensors of shear stress (Folgering et al., 2008, Hoger et al., 2002).

A mechanosensory pathway essential to mediating the shear stress response has been detailed by Tzima et al (2005). This pathway is initiated upon phosphorylation of the cytoplasmic domain of PECAM-1 in response to the application of shear stress. Phosphorylated PECAM-1 is able to directly bind and activate Src kinase which activates VEGFR2 in a ligand independent manner. VEGFR2 is able to bind PI-3 kinase directly through phosphorylation sites on the receptor leading to PI-3 kinase phosphorylation and subsequent activation. Binding of VEGFR2 to PI-3 kinase however does not occur in cells lacking VE cadherin. This indicates the involvement of VE cadherin in the formation of a complex between PI-3 kinase and VEGFR2 for PI-3 kinase activation to occur. The association between VE cadherin and VEGFR2 is thought to be indirect, mediated by β-catenin. Activated PI-3 kinase is then able to activate integrins which activate signalling pathways that mediate cell and stress fiber alignment in the direction of flow.

The described mechanosensory complex consisting of PECAM-1, VEGFR2, and VE-cadherin is both necessary and sufficient to transduce shear stress. Endothelial cells lacking PECAM-1 and VE-cadherin are unable to align actin filaments in the direction of flow. Transfection of PECAM-1, VE cadherin and VEGFR2 into a non endothelial cell

type (COS-7 African green monkey cells) results in endothelial like behaviour upon exposure to shear stress. Only cells expressing all three receptors align in the direction of flow following 16hrs of shear stress application. Control untransfected cells retain their static phenotype even after 16hrs of flow application.

1.7.4 Signalling Molecules Activated by Shear Stress

Rho dynamics alternate between the active and inactive state during the application of shear stress. Rho translocates to the cell membrane immediately upon the onset of shear stress and is thought to correlate with its activation (Li et al 1999). Decreased Rho activity follows shortly after flow application correlating with a decrease in stress fibers. The peak in Rho activity 60 mins after the onset of flow correlates with an increase in stress fibers (Tzima et al., 2001). Endothelial cells expressing constitutively active V14Rho are unable to orient themselves in the direction of flow. Cytoskeletal reorientation is also inhibited (Tzima et al., 2001). Therefore, the initial down regulation of Rho is essential for alignment of cells and stress fibers parallel to the direction of flow. A downstream effector of Rho, Rho kinase (ROCK) is also activated in response to shear stress. Unlike Rho, ROCK activity increase rapidly in response to shear stress application. This activation peaks at 30 mins following flow after which ROCK activity returns to basal levels (Lin et al., 2003).

Rac1 is transiently activated within 30 mins of shear stress application, after which Rac1 levels drop back to basal (Tzima et al., 2002). Activated Rac1 seems to localize to the downstream edges of sheared cells. Expression of constitutively active V12Rac inhibits the downstream polarization of Rac1 and cells are unable to align in the

direction of flow. Similarly, expression of a dominant negative Rac1 construct, N17Rac results in the random distribution actin stress fibers even after extended periods of flow (Tzima et al., 2002). These observations indicate that spatial localization of Rac1 at the downstream edge of endothelial cells is necessary for shear induced cell and stress fiber alignment to occur. It has been demonstrated that PI-3 kinase, a downstream effector of Rac1, is activated in response to shear stress and cyclic strain (Tzima et al., 2005, Li el al., 2005, Haga el al., 2003). AKT phosphorylation levels reach a peak 30 mins after the application of shear stress (Sumpio et al., 2005).

MAP kinases represent possible candidates mediating the effects of shear stress on endothelial cells. ERK, JNK and p38 MAP kinases are all activated by shear stress (Azuma et al., 2000, Azuma et al., 2001). p38 MAP kinase is required for proper cell alignment and elongation (Kadohama et al., 2006). Endothelial cells fail to reorient in the direction of flow when subjected to shear stress in the presence of a p38 MAP kinase inhibitor, SB203580. Also, cell shape remains similar to that of cells in static culture (Kadohama et al., 2006).

GSK-3β is involved in the regulation of planar cell polarity and microtubule stability. Phosphorylation of GSK-3β inhibits its kinase activity (Harwood et al., 2001). Active (unphosphorylated) GSK-3β disrupts microtubule stability through its ability to inactivate microtubule stabilizing proteins such as APC (Zumbrunn et al., 2001). Shear stress induces the phosphorylation of GSK-3β hence inhibiting its kinase activity. Complete inhibition of GSK-3β activity using LiCl and SB415286 and expression of constitutively active GSK-3β derivatives lead to a failure in endothelial cell elongation and reorientation in the direction of flow (McCue et al., 2006). This indicates that GSK-

3β activity is tightly controlled in the morphological responses to shear stress. Total inhibition of GSK-3β also results in the reversal of MTOC polarity. MTOC reorient upstream of the nucleus in the presence of GSK-3β inhibitors whereas in the absence of exogenous inhibitors, MTOC orient downstream of the nucleus (McCue et al., 2006).

1.8 SRF is Required for Angiogenesis

EC specific deletion of SRF in mouse embryos results in the development of aneurysms and haemorrhages leading ultimately to embryonic death. Mutant embryos are still able to form the first primitive vascular plexus. However, the capillary density of this plexus is reduced, indicating a defect in sprouting angiogenesis. Analysis of endothelial tip and stalk cells in mutant embryos show reduced levels of cortical actin in comparison to tip and stalk cells of wild type embryos. The number of tip cells is similar in both wild type and mutant embryos however, mutant tip cells have significantly less filopodia extensions when compared to wild type tip cells. Also, phalloidin staining shows that F-actin at the base of filopodia extensions appears to be in aggregates suggesting disorganization of the actin cytoskeleton (Franco et al., 2008).

The role of SRF in cell migration can be assessed by means of in vitro angiogenesis assays. The aortic ring assay uses intact vascular explants, which more accurately simulates the environment in which angiogenesis takes place in vivo. Aortic rings cultured in matrigel give rise to microvascular networks composed of branching endothelial channels (Auercach et al., 2003). Mosaic deletion of SRF in EC of mice hinders the sprouting of vessels in an aortic ring assay. SRF deficient cells impede the migration and elongation of these vessels. Also, knockdown of SRF in EC in vitro using

siRNA impairs cell migration and inhibits the formation of endothelial cell networks in a matrigel assay (Franco et al., 2008). Together, these data demonstrate the importance of SRF for unimpaired vessel migration.

In addition to defects in endothelial actin networks and cell migration, mutant embryos also display a significant decrease in EC specific expression of β-actin and VE-cadherin. Knockdown of SRF using siRNA in EC cultured in vitro also leads to a decrease in VE-cadherin and β-actin mRNA levels. Endothelial cell junctions also appear modified in small vessels of mutant embryos. The number of adherens junctions appears reduced in comparison to those of wild type embryos. Also, large gaps are detected between the membranes of mutant EC in contrast to the tight attachment observed between membranes of wild type EC (Franco et al., 2008). These data point to the importance of SRF for the proper formation of junctions in EC. SRF inactivation seems to disrupt EC junctions leading to the formation of brittle vasculature which gives rise to the haemorrhages and aneurysms seen in the mutant embryos.

Chapter 2: Materials and Methods

Cell Culture

Human Umbilical Vein Endothelial Cells (HUVECs) were cultured in EGM-2 basal media (Cambrex) supplemented with hEGF, Hydrocortisone, GA-1000 (Gentamicin, Amphotericin-B), VEGF, hFGF-B, R3-IGF-1, Ascorbic Acid, Heparin and 2% FBS. Cell cultures were maintained in a humidified 95% air/5% CO_2 incubator. HUVECs were seeded at a density of 2000-5000 cells/cm^2 and used between passages 2-4.

Shear Stress

HUVECs were grown on 75mm x 25mm x 1mm collagen I coated glass culture slides (Flexcell International Corporation). Cells were seeded at a density of $1x10^6$ cells per 100 x 15mm dish (3 slides/dish) and grown to confluence with one media change 48 hrs after seeding. Cells infected with adenovirus were infected prior to this media change.

A flow system (Flexflow apparatus, Flexcell International Corporation) was used to impose shear stress on cultured cells. Experimental slides were slotted into a parallel plate chamber and media was pumped through the chamber from a reservoir by means of a peristaltic pump. Cells were subjected to 3 hrs of laminar shear stress (3dynes/cm^2) at 37°C, 5% CO_2. Control static slides were left in the incubator at 37°C, 5% CO_2 after the media on them had been changed. This media change was to control for nuclear translocation of MRTF-A occurring in response to the addition of fresh media. After 3 hrs, cells were fixed in 4% formaldehyde in 1X PBS for 15 mins and permeabilized in

0.3% Triton X-100 in 1X PBS for 10 mins. MRTF-A staining was visualized by immunofluorescence with 1:100 goat-anti-MRTF-A antibody (Santa Cruz Biotechnologies) and 1:200 donkey-anti-goat Alexafluor 594 (Molecular Probes). F-actin was visualized with 1:200 fluorescein phalloidin (Molecular Probes). Nuclei were stained using Vectashield with DAPI (Vector Labs).

For subjecting cells to longer term shear stress, HUVECs were grown to confluence on glass slides (Corning, Corning, NY) and coated with collagen type I (Inamed). Cells were subjected to laminar shear stress of 7-8 dynes/ cm^2 in a parallel plate flow chamber as described by Frangos et al. (1988). Briefly, the flow system consists of a parallel plate flow chamber placed between an upper and a lower reservoir. The vertical distance between the two reservoirs creates hydrostatic pressure that drives the media into the flow chamber. Varying the distance between the two reservoirs allows for the application of different flow rates. The flow system was kept in a 37°C environmental room and 5% humidified CO_2 was bubbled into the media. Cells were fixed, permeabilized and stained as described above.

For inhibitor treatment, inhibitors were added to EGM-2 complete media at the indicated concentrations. Cells were preincubated with the inhibitors 1hr prior to flow or 2hrs for LiCl. Flow experiments were performed as described above.

Table 1. Inhibitors used in flow experiments

Inhibitor	Target	Concentration	Supplier
NSC23766	Rac1	50 μM	Calbiochem
LY294002	PI-3 kinase	20 μM	Calbiochem
U0126	MEK	10 μM	Calbiochem
Y27632	ROCK	10 μM	Calbiochem
Blebbistatin	Myosin II	30 μM	Sigma
LiCl	GSK-3β	30 mM	Calbiochem

siRNA Transfection

Integrated DNA Technologies DICER substrate duplexes targeting the gene of interest along with a Cy3 conjugated transfection control RNA duplex and a scrambled universal negative control were tested according to the instructions .The RNA duplex that showed the best knockdown results using western blotting and immunofluoresence was used for subsequent experiments.

siRNA duplexes were reconstituted to 20μM using RNase free buffer. The RNA duplex as well as the negative control duplex was transfected into 1 x 10^6 HUVECs at a concentration of 2nM. For two culture slides, 730 μl optimem (Gibco) was added to 20 μl of siRNA duplex (2 μM) in one centrifuge tube. In another centrifuge tube, 735 μl of optimem was added to 15 μl Dharmafect transfection reagent (Dharmacon). The two tubes were incubated for 5 minutes at room temperature. The contents of tubes 1 and 2 were then combined and incubated for 20 minutes at room temperature. Culture media

was removed from the dishes and replaced by 18.5 ml of antibiotic free complete EBM-2 media. siRNA transfection complexes were then added dropwise onto cells of two culture slides. Experiments were performed 48hrs after transfection of the siRNA duplexes.

Immunofluoresence

HUVECs were fixed with 4% formaldehyde in 1X PBS for 15 minutes, washed twice with 1X PBS and permeabilized with 0.3% Triton X-100 for 10 minutes. Cells were then incubated with primary antibody (in 5% FBS, 1X PBS) at 37°C for 30-60 minutes. Cells were then washed 3 times for 5 minutes in 1X PBS. HUVECs were then incubated with secondary antibody (in 5% FBS, 1X PBS) and phalloidin at 37°C for 30 minutes. Cells were then washed 3 times for 5 minutes in 1X PBS and mounted using VectaShield mounting media with DAPI (Vector Labs). Pictures were taken using a Zeiss Axio Imager Z1 microscope equipped with an AxioCam HRm camera. Pictures were captured using a 40X dry objective (ECPlan-NeoFluor, 0.75 NA). Images were processed with Axiovision 4.5.

Western Blotting

For immunoblotting with PECAM-1 antibody, HUVECs from flow and static slides were washed in 1X PBS at the end of the flow experiment and scraped in 1X SDS. Samples were then boiled for 3-5 minutes and stored at -20°C. For immunoblotting, a 10% acrylamide gel was prepared and samples were boiled for 3-5 minutes prior to loading. After loading, the gel was run for 1hr at 185 V and transferred onto a

nitrocellulose membrane at 100 V for 1hr. The blot was blocked in 5% milk powder in 1X PBS for 1 hr. The blot was then incubated overnight at 4°C with anti-PECAM-1 antibody (1/5000) diluted in 5% milk powder in 1X PBS followed by donkey-anti-mouse secondary antibody, conjugated to horseradish peroxidase diluted (1:5000) in 5% milk powder in 1X PBS. Immunoreactive proteins were visualized by chemiluminesence (Western Lighting Plus reagent, Perkin Elmer). Blots were exposed on autoradiographic film (Kodak). For immunoblotting with anti-tubulin antibody, the same blot was stripped in stripping buffer (0.1M Glycine, 0.5% SDS, pH 2.5) for 40 mins, blocked in 5% milk powder in 1X PBS for 1 hr and reprobed overnight at 4°C with anti-tubulin antibody, diluted (1:1000) in 5% milk powder in 1X PBS. The blot was further probed with donkey-anti-mouse secondary antibody, conjugated to horseradish peroxidase as above.

For testing MRTF-A and MRTF-B siRNA knockdown levels by immunoblotting, HUVECs were transfected with siRNA duplexes as previously described. Cells were harvested in 1X SDS and samples were boiled for 3-5 minutes prior to loading onto a 10% acrylamide gel. The gel was run and transferred and the blot was blocked as described previously. Anti-MRTF-A and anti-MRTF-B were used at 1:1000 dilution (blots were probed overnight at 4 °C). Donkey anti-goat HRP was diluted (1:5000) in 5% milk powder and 1X PBS. Reagent proteins were visualized by chemiluminesence and the blot was exposed onto autoradiographic film as above. Blots were stripped and reprobed with anti-tubulin antibody as described above.

Magnetic Beads

HUVECs were seeded onto glass coverslips placed in a 60mm dish (450,000 cells/dish for RGD peptide experiment and 350,000 cells/dish for PECAM-1 experiment).

To prepare anti-PECAM-1 coated magnetic beads, 1ml of carbonate buffer ($NaHCO_3$, pH 9.4) was added to 50mg iron filings and 20 µl anti-PECAM-1 antibody. The mixture was sonicated briefly and placed on a rotator at 4°C overnight. The next day, a 300 µl aliquot of beads was taken and washed 3 times in carbonate buffer. After washing, the beads were resuspended in 300 µl of carbonate buffer, sonicated again and added to 50ml of complete EGM-2 media.

To prepare RGD peptide coated magnetic beads, 0.86 ml of carbonate buffer ($NaHCO_3$, pH 9.4) was added to 50mg iron filings and 2.5mg RGD peptide (Peptides International). The mixture was sonicated briefly and placed on a rotator at 4°C overnight. The next day, a 300 µl aliquot of beads was taken and washed 3 times in carbonate buffer. After washing, the beads were resuspended in 300 µl of carbonate buffer, sonicated again and added to 45ml of complete EGM-2 media.

Bead binding and force application was identical in the case of PECAM-1 coated beads and RGD peptide coated beads. Briefly, cells were rinsed once with 3ml of media. Following rinsing of cells, 3ml of bead suspension was added to each dish while shaking to ensure that the beads were evenly distributed on the cells. Cells were placed in 37°C incubator for 15 minutes after which the media on the cells was aspirated and 3ml of fresh media was added. Cells were replaced in 37°C incubator for 1hr. Following the incubation period, cells were exposed to lateral magnetic force for 1hr, 2hr or 4hr after

which cells were fixed in 4% paraformaldehyde for 15 minutes. Cells were then permeabilized in 0.3% Triton X-100 for 10 minutes and stained for MRTF-A and F-actin.

"Calcium Switch" Assay

HUVECs were seeded onto glass coverslips in 6 well plates at 150,000 cells/well. Cells were grown until 2 days post confluent in order to ensure full formation of adherens junctions. Media on the cells was changed to EGM-2 (without FBS and supplements) with 4mM EGTA. Cells were fixed at various time points to monitor MRTF-A localization during adherens junction dissolution.

For adherens junction reformation, cells were prepared as above. At 2 days post-confluency, adherens junctions were dissolved by incubating cells in EGM-2 with 4mM EGTA for 40 mins. Media was then replaced with complete EGM-2 and cells were fixed at various time points to monitor the progression of adherens junction reformation.

Coverslips were prepared for immunofluoresence as described above. Briefly, adherens junctions were visualized using goat-anti-VE cadherin (1:100) (Santa Cruz Biotechnologies). MRTF-A was visualized using goat-anti-MRTF-A (1:100) (Santa Cruz Biotechnologies). Secondary antibodies were donkey-anti-goat AlexaFluor 594 and donkey-anti-goat AlexaFluor 488 (1:200). Nuclei were visualized with DAPI in Vectashield mounting media (Vector Labs).

Adenoviral Infection

HUVECs were infected with adenovirus (MOI=200) 48hrs after seeding. Briefly, the media was aspirated and replaced with the appropriate volume of adenoviral suspension (diluted in DMEM). Cells were incubated with the adenoviral suspension for 1 hr. Culture plates were gently shaken every 15 minutes to ensure even distribution of the adenovirus. After 1 hr, the adenoviral suspension in DMEM was aspirated and replaced with fresh EBM-2 media.

Scratch Wound Assay

HUVECs were seeded on collagen I coated glass coverslips in 6 well plates at 200,000 cells per well. Collagen was diluted 1:200 in 30% ethanol. Coverslips were then coated with 0.5ml of diluted collagen and left overnight under low flow in a laminar flow hood to dry.

HUVECs were infected with either flag-tagged MRTF-A(ΔB1ΔB2) or GFP-expressing adenovirus (MOI=200) 48hrs after seeding. Cells were then wounded 48hrs after infection with a p200 pipet tip and fixed at the indicated times. Coverslips were prepared for immunofluoresence as described above. Briefly, epitope tagged MRTF-A(ΔB1ΔB2) was visualized using 1:500 mouse-anti-flag antibody (Sigma). Endogenous MRTF-A was visualized using 1:100 goat-anti-MRTF-A (Santa Cruz Biotechnologies). Secondary antibodies used include donkey-anti-mouse AlexaFluor 350 and donkey-anti-goat AlexaFluor 594 (1:200).

Matrigel Assay

Glass coverslips were placed into a 6 well plate and coated with 250 μl of matrigel (BD Biosciences). The matrigel coat was immediately aspirated and the remaining film was allowed to solidify. HUVECs were grown in 60mm dishes and infected as above, with either MRTF-A(ΔB1ΔB2) or GFP-expressing adenovirus 48hrs prior to seeding onto matrigel. HUVECs were trypsinized and reseeded (200,000 cells/well) onto the matrigel coated coverslips after media was added into the wells of the plate. Cells were fixed in 4% paraformaldehyde for 15 minutes 24hrs after seeding onto matrigel. Cells were then permeabilized in 0.3% Triton X-100 for 10 minutes and stained with 1:500 mouse-anti-flag antibody to detect cells infected with flag-MRTF-A(ΔB1ΔB2) and 1:100 goat-anti- MRTF-A to detect endogenous MRTF-A.

SRF Reporter Gene Assay

SRF reporter gene assays were performed in NIH3T3 cells. Cells were cultured in 6 well plates (100,000 cells/well) and transfected 24hrs following seeding.

Cells are transfected with a luciferase reporter plasmid 3DA.luc which contains three SRF binding sites in its promoter (Geneste et al., 2002) as well as MLV-LacZ which is a constitutively active reporter plasmid used to monitor transfection efficiency.

Each well was transfected with 50ng 3DA.luc and 250ng MLV-LacZ expressing plasmids. 0.1μg SRFVP16 expressing plasmid was included as a positive control. Cells were also transfected with an empty pEF.Flag plasmid to ensure that each well was transfected with a total of 1.5μg of DNA.

DNA was added to 50 µl of optimem. To this mixture, 4 µl of lipofectamine in 50 µl optimem was added. The solutions were mixed thoroughly and incubated at room temperature for 30 minutes to allow for lipid-DNA complex formation. The DNA was added dropwise onto optimem washed cells. DNA was left on cells for 5hrs after which the transfection media was removed and replaced with 0.5% serum. For CCG-1423 treatment, the inhibitor was added at the indicated concentrations and incubated with the cells for 19hrs. Following the 19hr preincubation period, selected samples were serum stimulated for 6hrs. Cells were washed in 1X PBS, scraped in 400 µl 1X PBS and centrifuged for 5 minutes at 5000 rpm (4 °C) to pellet cells. The supernatant was removed and the cells were lysed in 100 µl of 1X reporter lysis buffer (Promega). Lysates were stored at -20 °C overnight.

Cell lysates were thawed and vortexed for 30 seconds to ensure efficient lysis. Samples were centrifuged at 13,000 rpm for 10 minutes to clear cell debris. The assays were performed as follows: β-galactosidase (β-gal) reactions were performed by adding 30µl of cleared lysate to 200 µl of 4mg/ml chlorophenol red β-D galactopyranosidase (CPRG-Calbiochem) diluted 1:10 in β-gal buffer (10mM $MgSO_4$, 0.5% β-mercaptoethanol in PBS). The β-gal reactions were developed and absorbance values at OD_{594} were measured with a SpectraMax M2 plate reader (Molecular Devices). Luciferase reactions were performed by adding 30 µl of cleared lysate to 30 µl of luciferin. Luciferase samples were read with an LMAX II (Molecular Devices) immediately after luciferin was added. Relative SRF activation is obtained by calculating the luminescence to absorbance ratio. SRF activation by the constitutively active SRF VP16 construct is set to 100% activation against which the other activities are compared.

Statistical Analysis

A student *t*-test was performed to compare results obtained from two different experiments. A value of $P<0.05$ was considered statistically significant.

Chapter 3: Results

Part I: Shear Stress, MRTF, Cytoskeletal Remodeling

3.1 MRTF-A and MRTF-B Nuclear Translocation in Response to Shear Stress

Upon exposure to shear stress, endothelial cells elongate and replace their cortical actin ring with thick actin stress fibers that extend throughout the cell. Stress fiber formation requires the activity of MRTF-A in NIH3T3 cells (Morita et al., 2007). We wished to investigate whether shear stress could induce the activation of the MRTF-A/SRF pathway in HUVECs. MRTF-A nuclear translocation correlates with activation of the MRTF-A/SRF pathway, therefore monitoring of MRTF-A sub-cellular localization provides a measure of the activation status of the pathway. The endothelium in vivo consists of a confluent monolayer of endothelial cells thus confluent cultures of HUVECs were used in all flow experiments (McCue et al., 2004).

HUVECs were subjected to 3hrs of shear stress at 3 dynes/cm^2. The cells elongated, formed parallel stress fibers and began to align in the direction of flow. Concomitant with stress fiber formation, we see nuclear MRTF-A in approximately 65% of cells (Figure 3.2). Intermediate distribution of MRTF-A, i.e. MRTF-A dispersed evenly throughout the cytoplasm and the nucleus, was observed in 14% of cells and cytoplasmic distribution of MRTF-A was observed in 21% of cells. In contrast, cells in static culture retain their distinct cobblestone shape and cortical ring of actin at the cell periphery. MRTF-A remained predominantly cytoplasmic (74%) in these cells (Figure 3.1).

It has been suggested that MRTF-A and MRTF-B are functionally redundant (Cen et al., 2003). Therefore, we wished to investigate the cellular localization of MRTF-B in

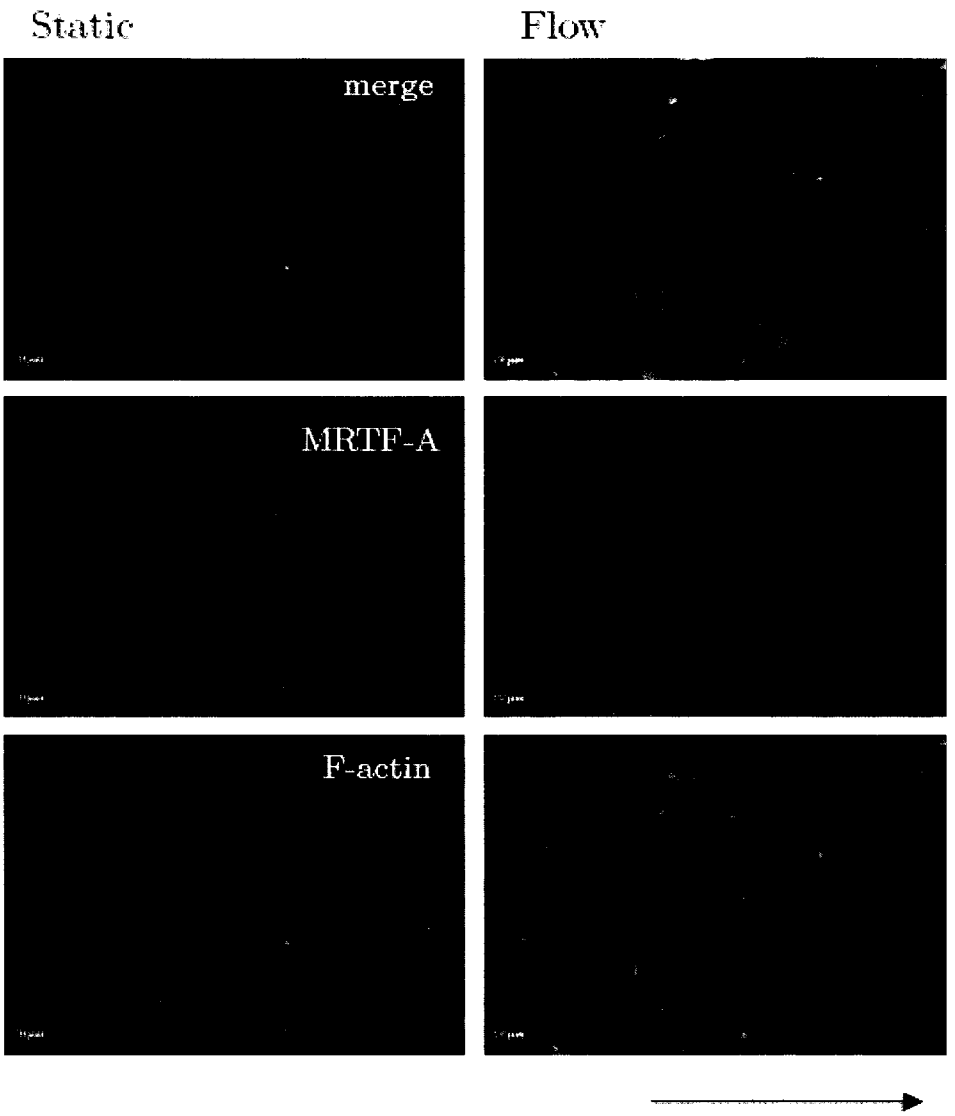

Figure 3.1. Shear stress induces MAL nuclear translocation and remodeling of actin stress fibers.

HUVEC were subjected to a flow rate of 3 dynes/cm^2 for 4 hours. Arrow indicates direction of flow. Cells were stained for MAL (red) and F-actin (green). The nuclei are marked by DAPI staining (blue).

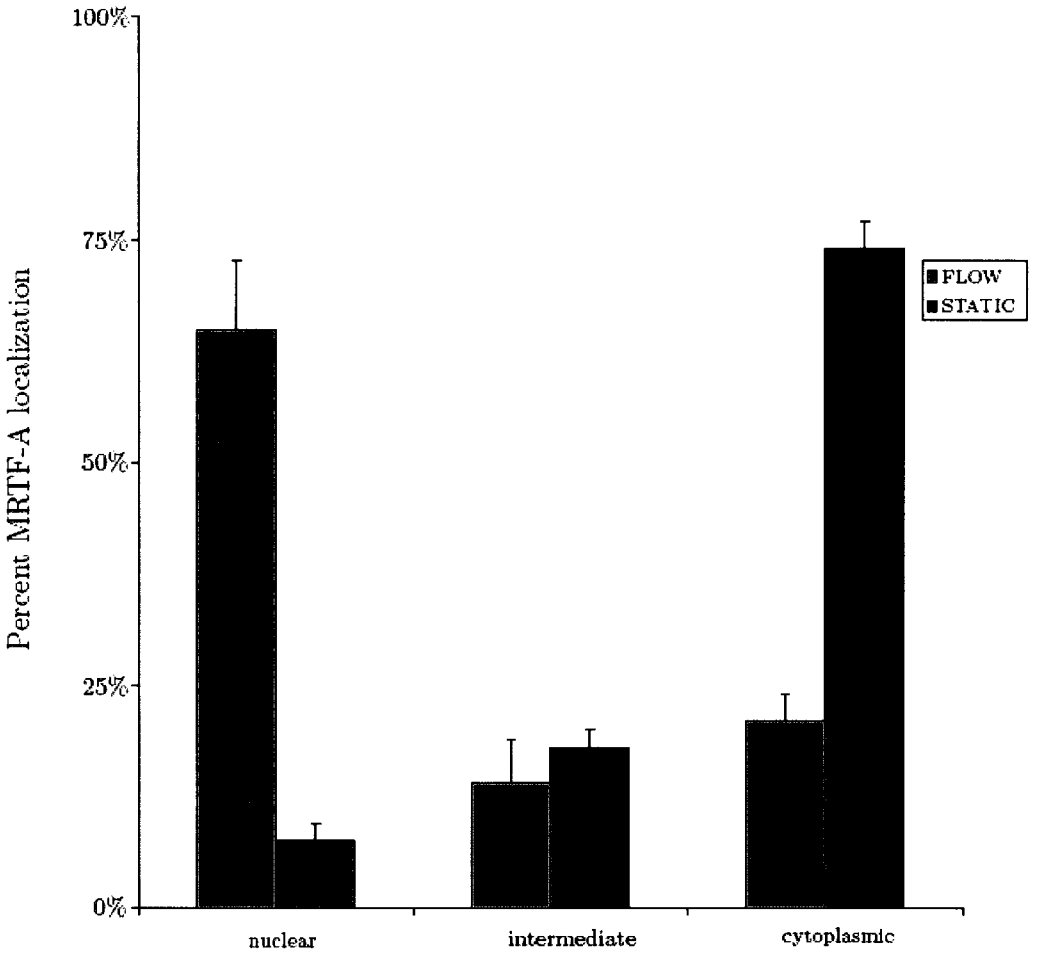

Figure 3.2. MRTF-A sub-cellular localization in response to flow. HUVEC were grown to confluence and subjected to 3hrs of shear stress (3dynes/cm^2) 48 hrs after the last maintenance media change, >200 cells were counted. Mean values from three separate trials are plotted. Error bars represent standard deviation from the mean.

HUVECs in response to shear stress. As above, HUVECs were subjected to flow and MRTF-B sub-cellular localization was assessed by immunofluoresence. MRTF-B was found to translocate to the nucleus in response to flow (Figure 3.3) however, translocation was to a much lesser extent (in 14% of cells) than that seen in the case of MRTF-A (Figure 3.4). Moreover, there were a large proportion of cells with "intermediate" (~51%) as well as cytoplasmic MRTF-B (~ 35%). These results are similar to previous observations in NIH 3T3 fibroblasts where serum stimulation only induces moderate translocation of MRTF-B to the nucleus (Morita et al., 2007).

3.2 Down Regulation of MRTF-A In Response to Long Term Shear Stress

The onset of shear stress activates many signalling pathways which are subsequently down regulated with the sustained application of laminar flow. We sought to determine whether shear induced MRTF-A nuclear translocation would be sustained or down regulated with prolonged shear stress application. As above, confluent HUVEC cultures were subjected to shear stress for 4hr, 8hr, 24hr and 48hrs and MRTF-A sub-cellular localization was assessed by immunofluoresence. MRTF-A was mostly nuclear at 4hrs of flow, but became predominantly cytoplasmic by 8hrs and remained cytoplasmic at longer time points (Figures 3.5-3.8). In a second repeat of this experiment HUVECs were subjected to flow for 4hrs, 6hrs, 8hrs and 14hrs and a similar trend was observed. MRTF-A accumulated in the nucleus of most cells after 4hrs of flow. Following 6hrs of flow, MRTF-A was seen to be either dispersed evenly throughout the cell or nuclear in the majority of cells (Figure 3.9). MRTF-A was almost exclusively cytoplasmic following 8hrs of flow and remained cytoplasmic at the longer time points

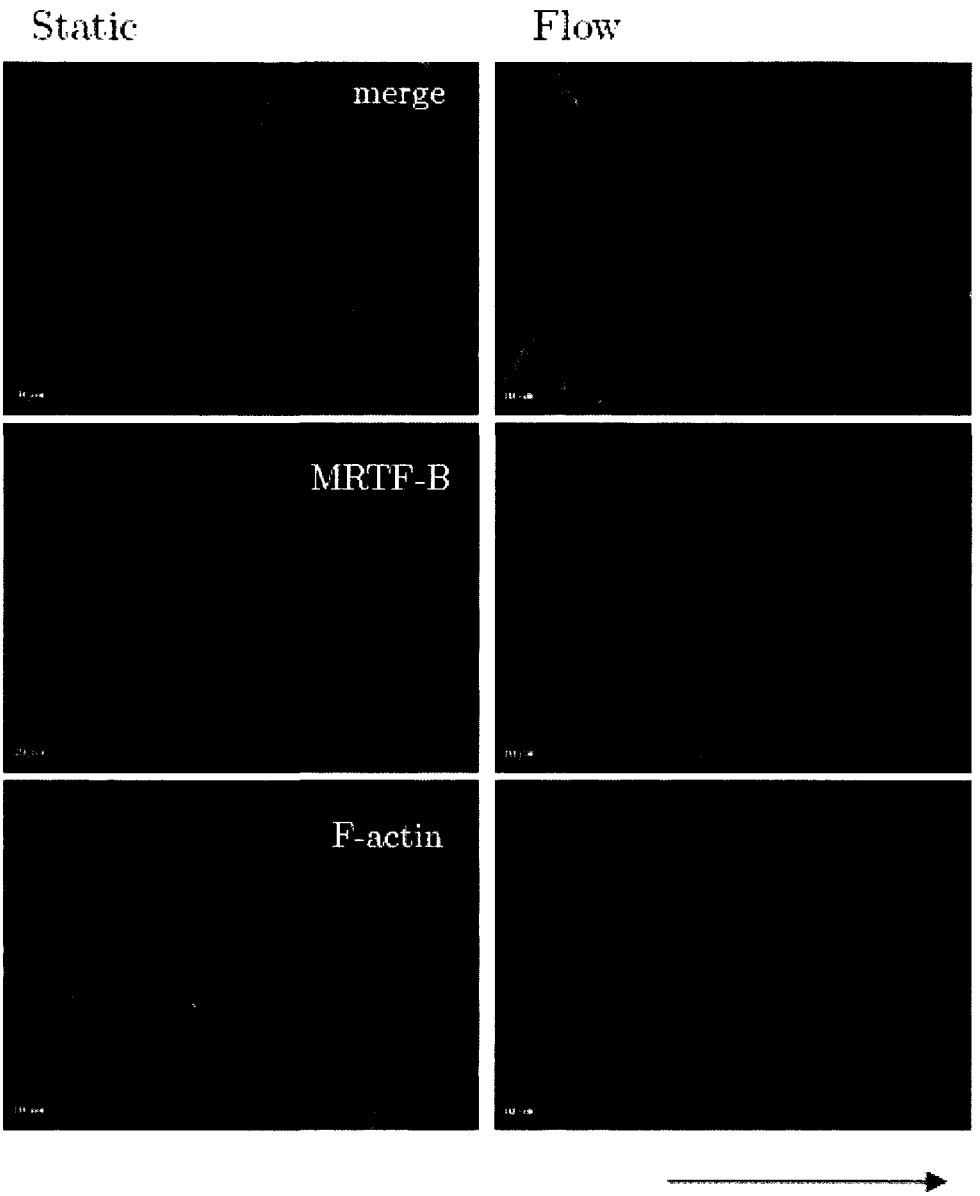

Figure 3.3 MRTF-B sub-cellular localization in response to flow
HUVEC were grown to confluence and subjected to 3hrs of shear stress (3dynes/cm^2) 48 hrs after the last maintenance media change. Endogenous MRTF-B was detected using anti-MRTF-B antibody (red); F-actin was detetcted with fluorescein phalloidin (green). Arrow indicates direction of flow.

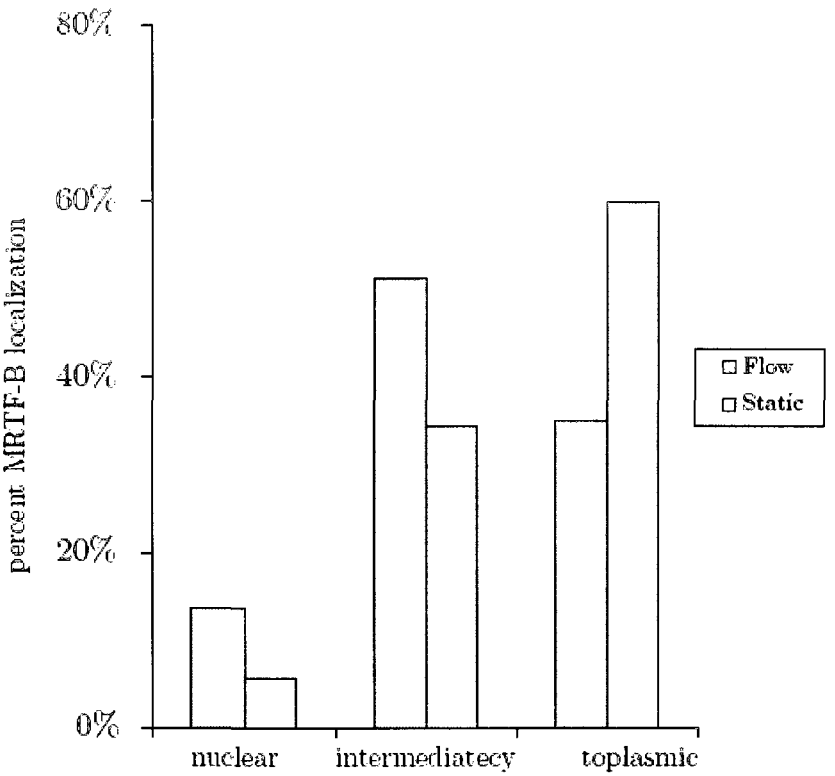

Figure 3.4. MRTF-B sub-cellular localization in response to flow
HUVEC were grown to confluence and subjected to 3hrs of shear stress (3dynes/cm^2) 48 hrs after the last maintenance media change, >100 cells were counted from one trial.

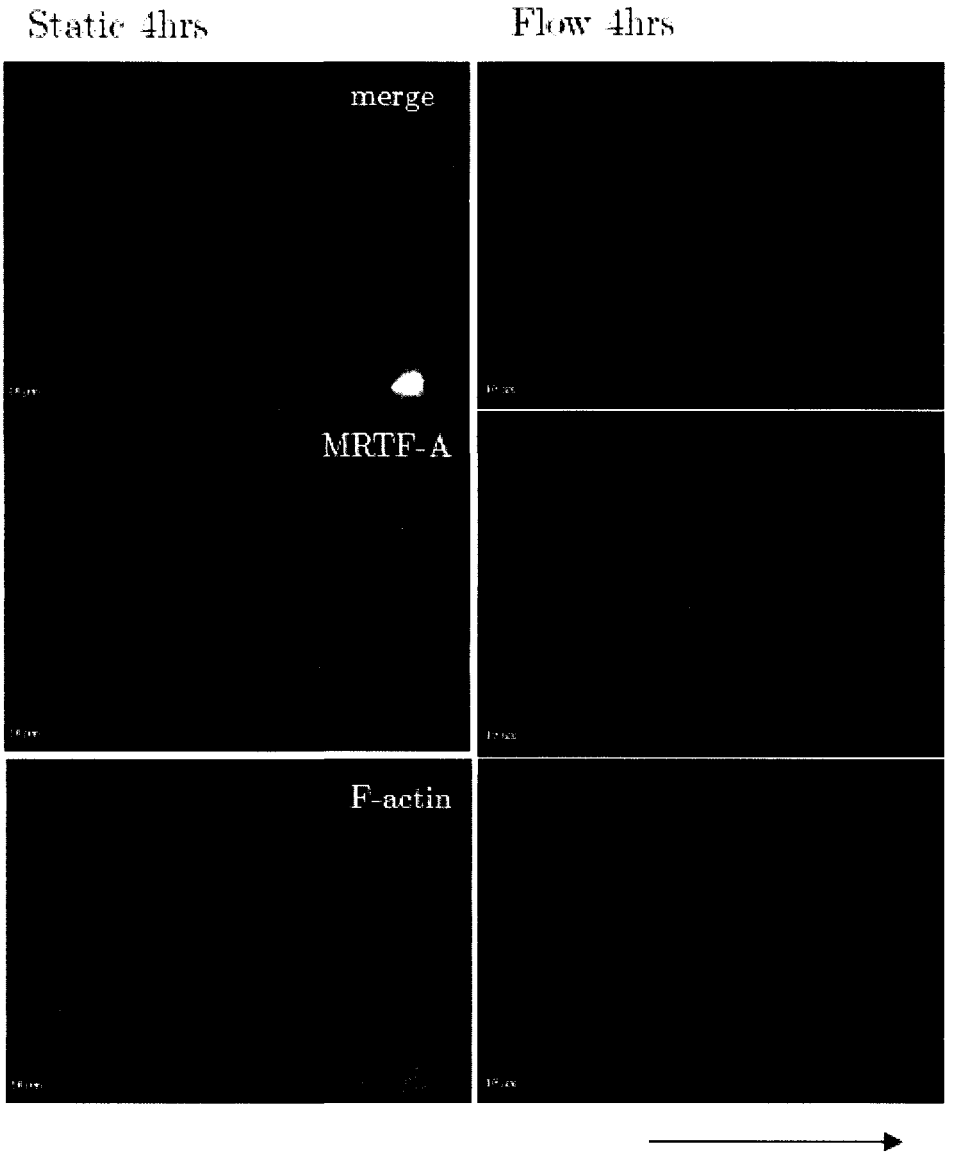

Figure 3.5. MRTF-A sub-cellular localization in response to long term flow. HUVEC were grown to confluence and subjected to 4hrs of shear stress (~6 dynes/cm2) 48hrs after after the last maintenance media change. Humidified CO_2 was bubbled into media throughout time of flow. Endogenous MRTF-A was detected using anti-MRTF-A antibody (red); F-actin was detetcted with fluorescein phalloidin (green).

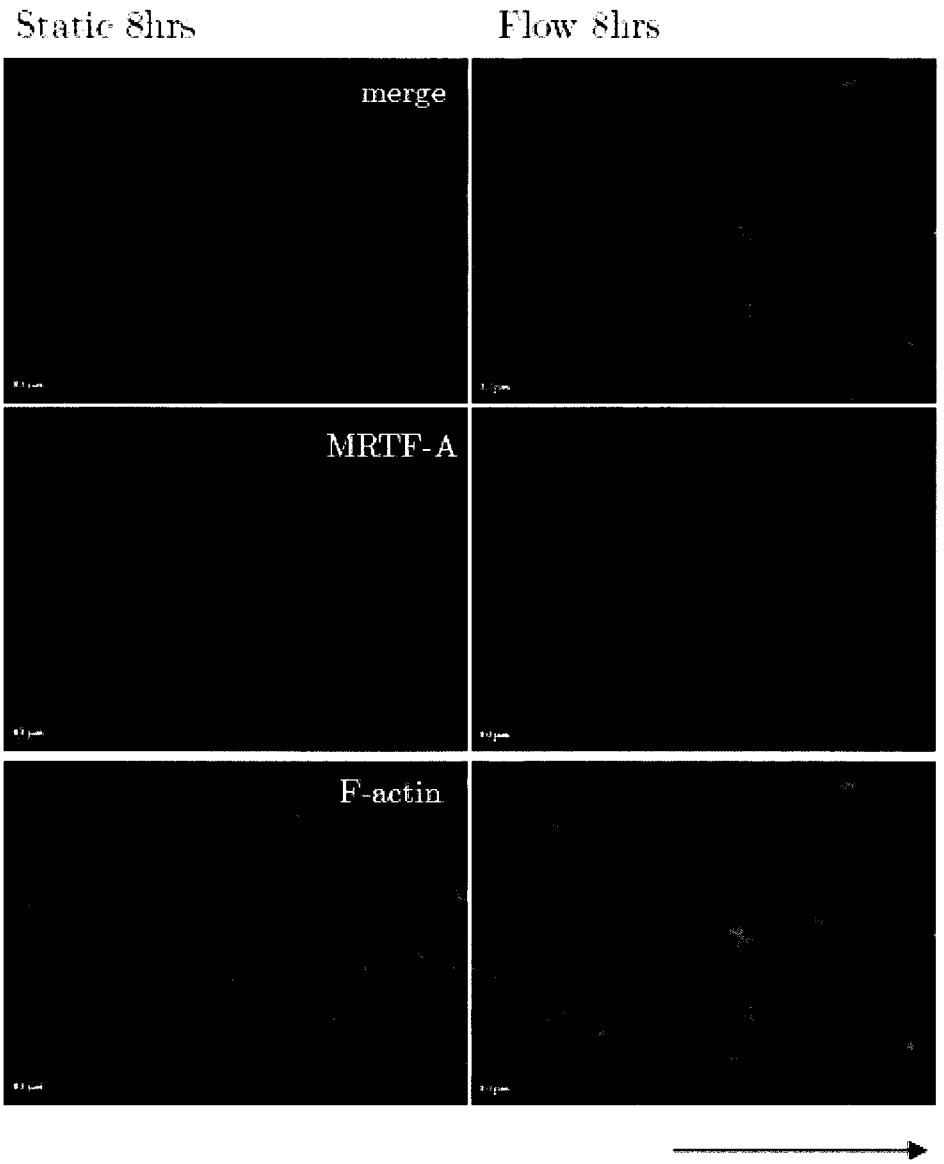

Figure 3.6. MRTF-A sub-cellular localization in response to long term flow. HUVEC were grown to confluence and subjected to 8hrs of shear stress (~6 dynes/cm2) 48hrs after after the last maintenance media change. Humidified CO_2 was bubbled into media throughout time of flow. Endogenous MRTF-A was detected using anti-MRTF-A antibody (red); F-actin was detetcted with fluorescein phalloidin (green).

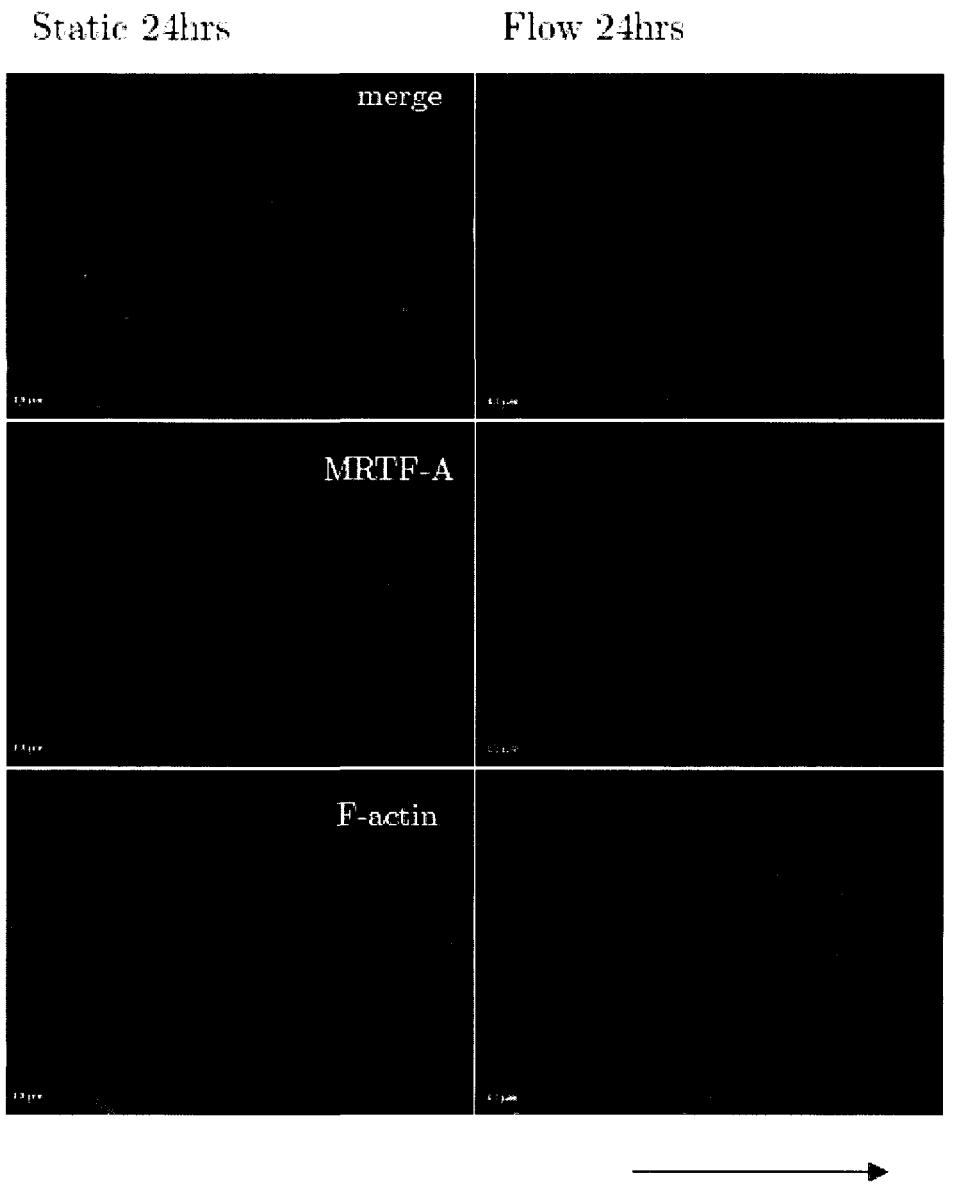

Figure 3.7. MRTF-A sub-cellular localization in response to long term flow. HUVEC were grown to confluence and subjected to 24hrs of shear stress (~6 dynes/cm2). Humidified CO_2 was bubbled into media throughout time of flow. Endogenous MRTF-A was detected using anti-MRTF-A antibody (red); F-actin was detetcted with fluorescein phalloidin (green).

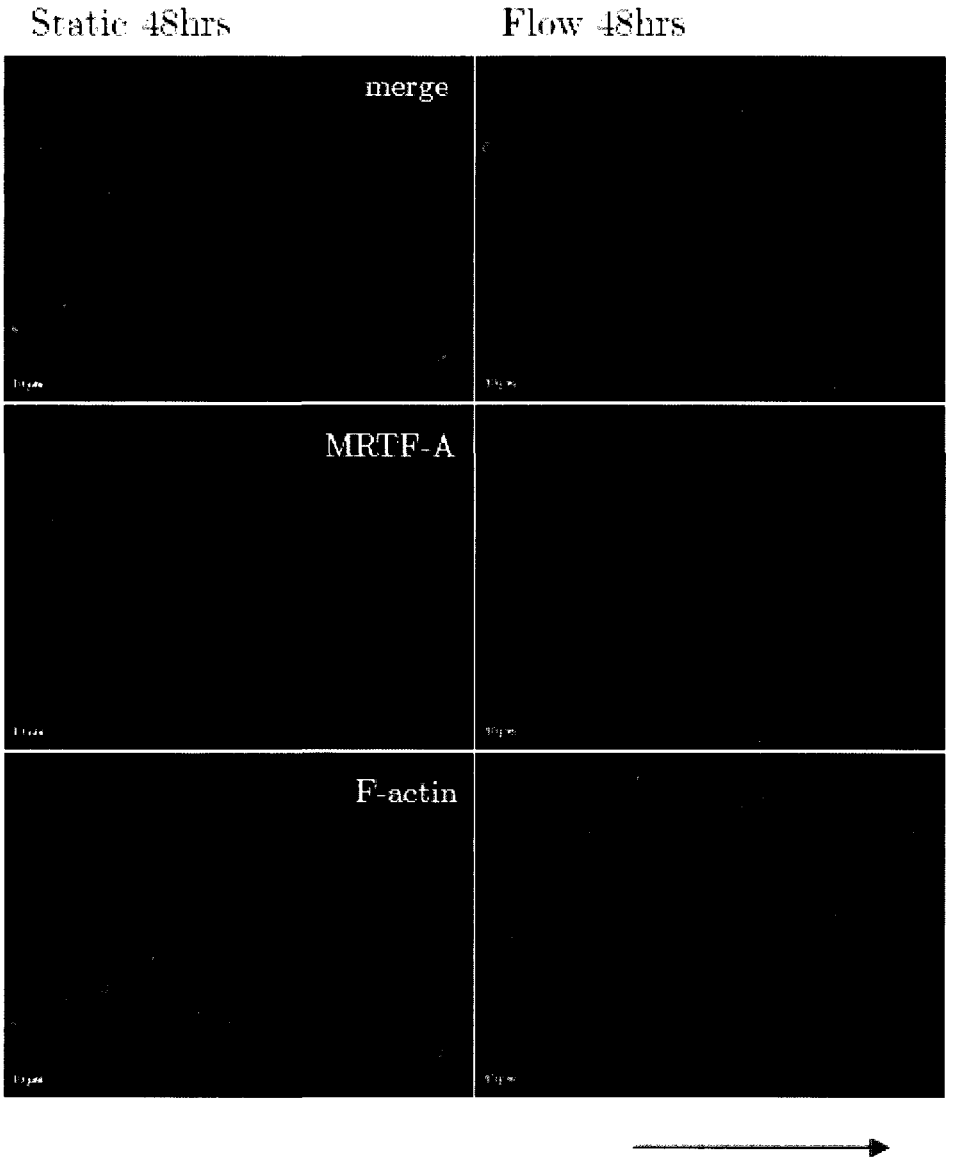

Figure 3.8. MRTF-A sub-cellular localization in response to long term flow. HUVEC were grown to confluence and subjected to 48hrs of shear stress (~6 dynes/cm2) 48hrs after after the last maintenance media change. Humidified CO_2 was bubbled into media throughout time of flow. Endogenous MRTF-A was detected using anti-MRTF-A antibody (red); F-actin was detected with fluorescein phalloidin (green).

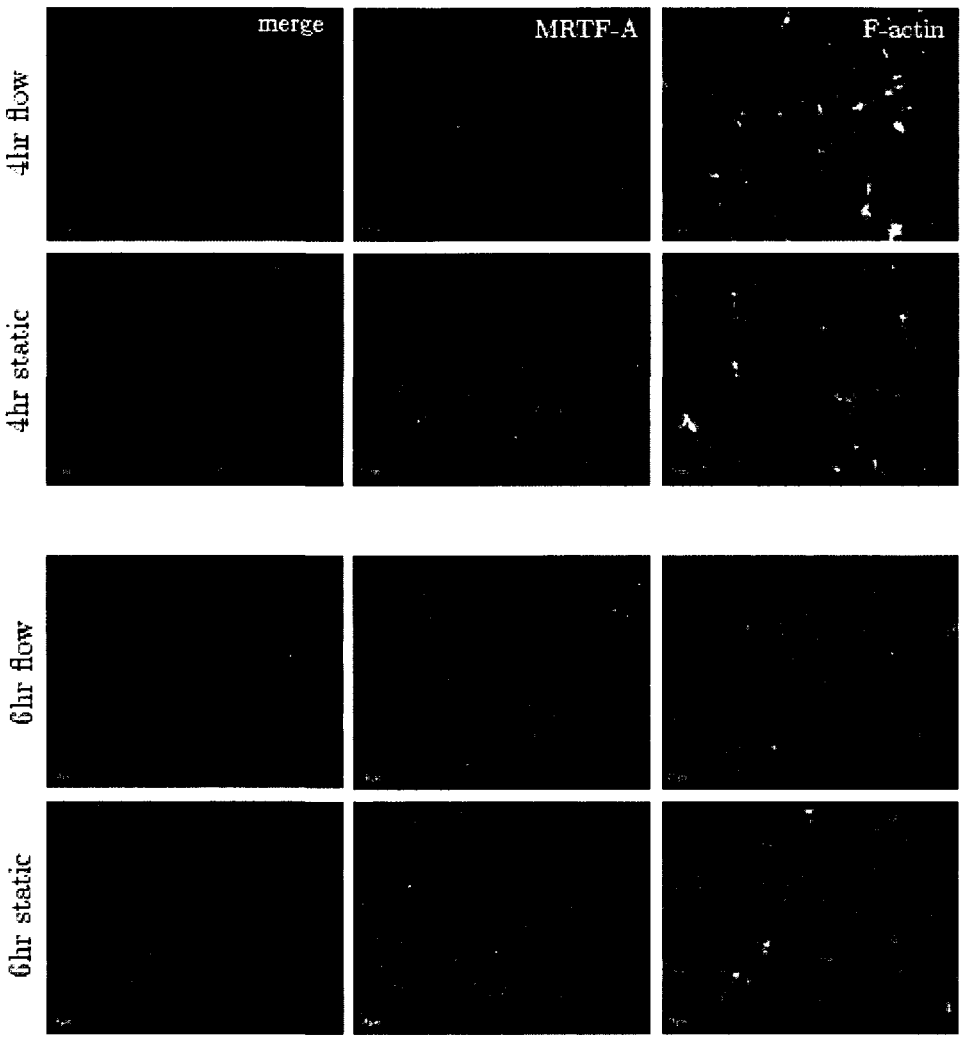

Figure 3.9. MRTF-A sub-cellular localization in response to long term flow. HUVEC were grown to confluence and subjected to 4hrs and 6hrs of shear stress (3 dynes/cm^2) 48hrs after after the last maintenance media change. Humidified CO_2 was bubbled into media throughout time of flow. Endogenous MRTF-A was detected using anti-MRTF-A antibody (red); F-actin was detetcted with fluorescein phalloidin (green). Nuclei were stained with DAPI.

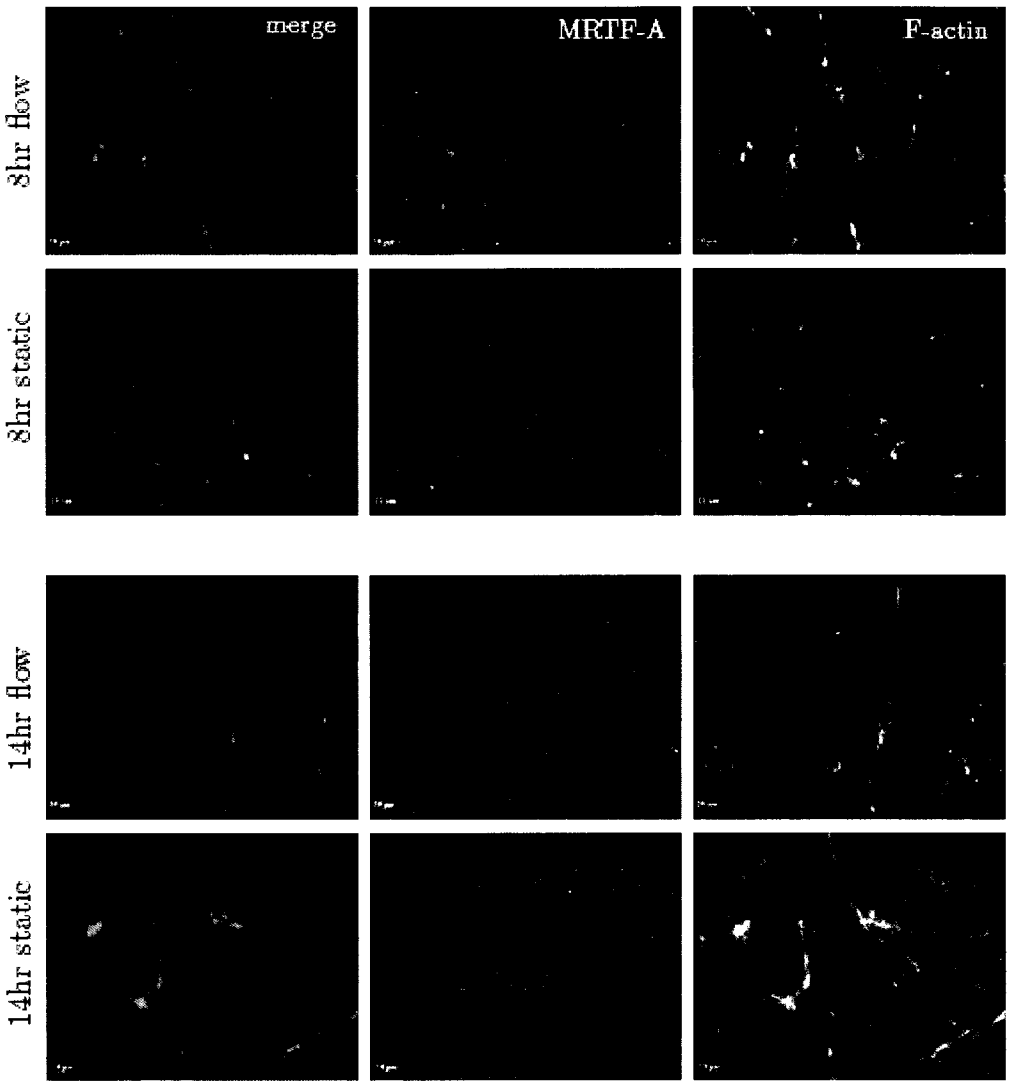

Figure 3.10. MRTF-A sub-cellular localization in response to long term flow. HUVEC were grown to confluence and subjected to 8hrs and 14hrs of shear stress (3 dynes/cm^2) 48hrs after after the last maintenance media change. Humidified CO_2 was bubbled into media throughout time of flow.Endogenous MRTF-A was detected using anti-MRTF-A antibody (red); F-actin was detetcted with fluorescein phalloidin (green). Nuclei were stained with DAPI.

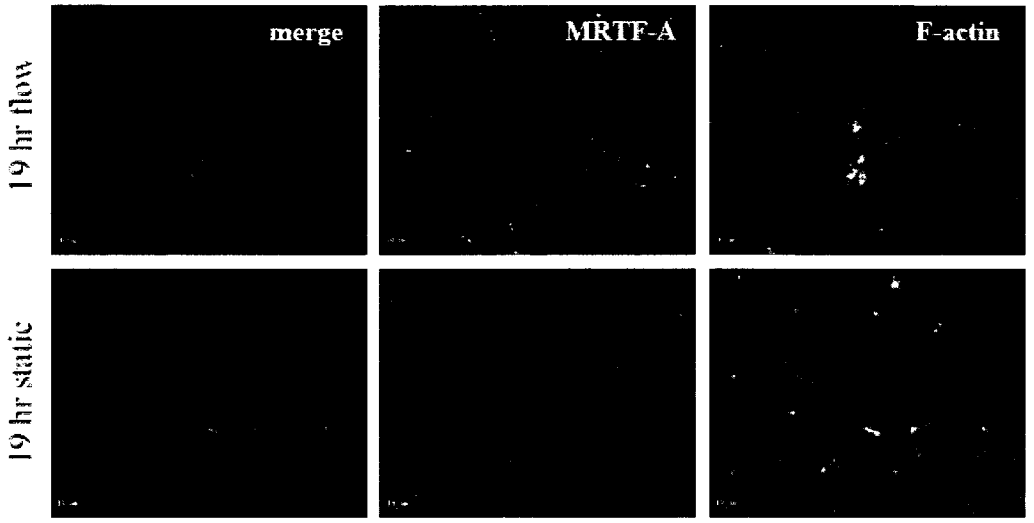

Figure 3.11. MRTF-A sub-cellular localization in response to long term flow. HUVEC were grown to confluence and subjected to 19 hrs of shear stress (3 dynes/cm^2) 48hrs after after the last maintenance media change. Humidified CO_2 was bubbled into media throughout time of flow.Endogenous MRTF-A was detected using anti-MRTF-A antibody (red); F-actin was detetcted with fluorescein phalloidin (green). Nuclei were stained with DAPI

(Figure 3.10-3.11). This suggests that as with other shear activated pathways, MRTF-A is down regulated with the sustained application of shear stress. To our surprise, at the longer time points, cells did not align parallel to the direction of flow as expected. Instead, they aligned perpendicular to the direction of flow. The unusual perpendicular alignment was not due to the setup of the flow apparatus since the same experiment was performed twice using two slightly different setups both of which yielded similar results in terms of HUVEC alignment following shear stress application and MRTF-A down regulation following 4 hrs of flow. This issue will be addressed further in Chapter 4 (Discussion).

We attempted to asses the effects of oscillating flow on MRTF-A nuclear translocation. There have been reports in the literature stating that cells subjected to oscillating flow retain the cobblestone morphology typical of static cells and do not elongate or display any stress fiber remodeling (Thoumine et al., 1995). An osciflow device (Flexcell International Corporation) was used to subject HUVECs to oscillating flow (1Hz). Unfortunately we were unable to obtain consistent results in these experiments. Half of the trials showed cells elongating and nuclear translocation of MRTF-A while the other half of trials showed no cell elongation and MRTF-A remained cytoplasmic (Figure 3.12 and Figure 3.13).

3.3 Regulation of Shear Induced MRTF-A Nuclear Localization

To aid in understanding the role of the MRTF/SRF pathway in the shear stress response we sought to identify the signalling pathways that lead to its activation. Shear stress induces activation of a number of signalling pathways that are known to regulate

actin dynamics and are therefore likely to participate in the activation of the MRTF pathway.

3.3.1 Rac1

In fibroblasts, Rac1 is sufficient to activate MRTF-A/SRF (Hill et al., 1995). Rac1 is transiently activated by shear stress with activation peaking at 30 mins after the onset of flow. In order to study the involvement of Rac1 in shear induced MRTF-A nuclear translocation in HUVECs, cells were pre-treated with Rac1 inhibitor (NSC23766) and subjected to shear stress in the presence of NSC23766. MRTF-A sub-cellular localization

was assessed by immunofluoresence. MRTF-A nuclear translocation was seen in 55% of cells and was not significantly different between NSC23766 treated cells and untreated cells subjected to shear stress (student *t*-test, Pvalue =0.3, Figure 3.15). Cells subjected to shear stress were still able to elongate and form parallel actin stress fibers in response to flow (Figure 3.14). MRTF-A subcellular localization was not affected by NSC23766 treatment in static controls. These data demonstrate that shear induced MRTF-A nuclear translocation appears to be largely Rac1 independent.

3.3.2 PI-3 kinase

The PI-3 kinase/AKT pathway is activated in response to shear stress and cyclic strain in BAECs (Li et al, 2005, Haga et al., 2003). PI-3 kinase is a downstream effector of Rac implicated in mediating MRTF-A activation in response to specific extracellular stimuli (Gineitis and Treisman, 2001). To assess the role of PI-3 kinase in shear induced

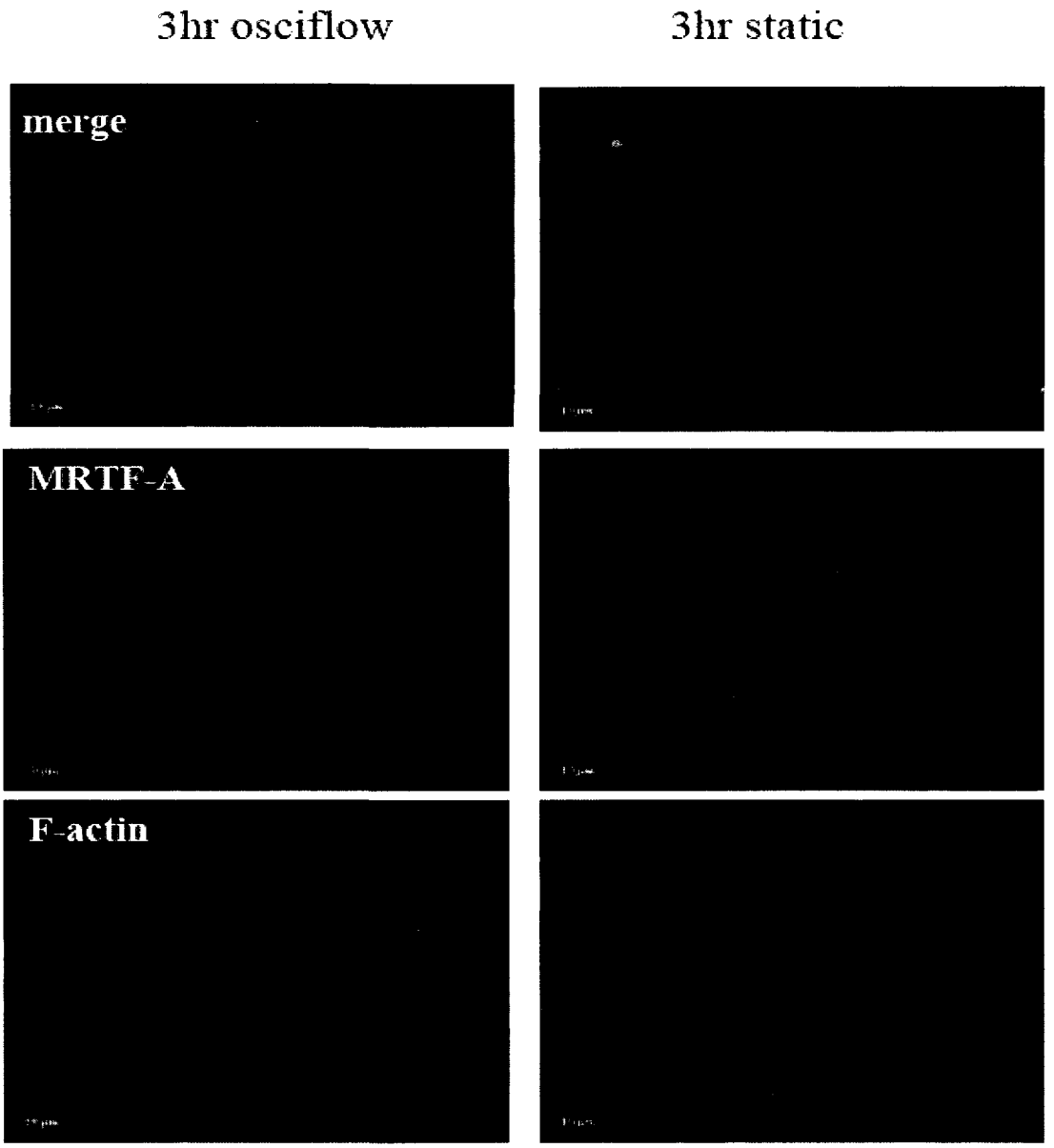

Figure 3.12. MRTF-A localization in response to oscillatory flow
HUVECs were grown to confluence and subjected to 3hrs of oscillatory flow (3 dynes/cm^2, 1Hz) 48hrs after the last maintenance media change. MAL was detected using anti-MRTF-A antibody. F-actin was detected with fluorescein phalloidin. Nuclei were stained with DAPI.

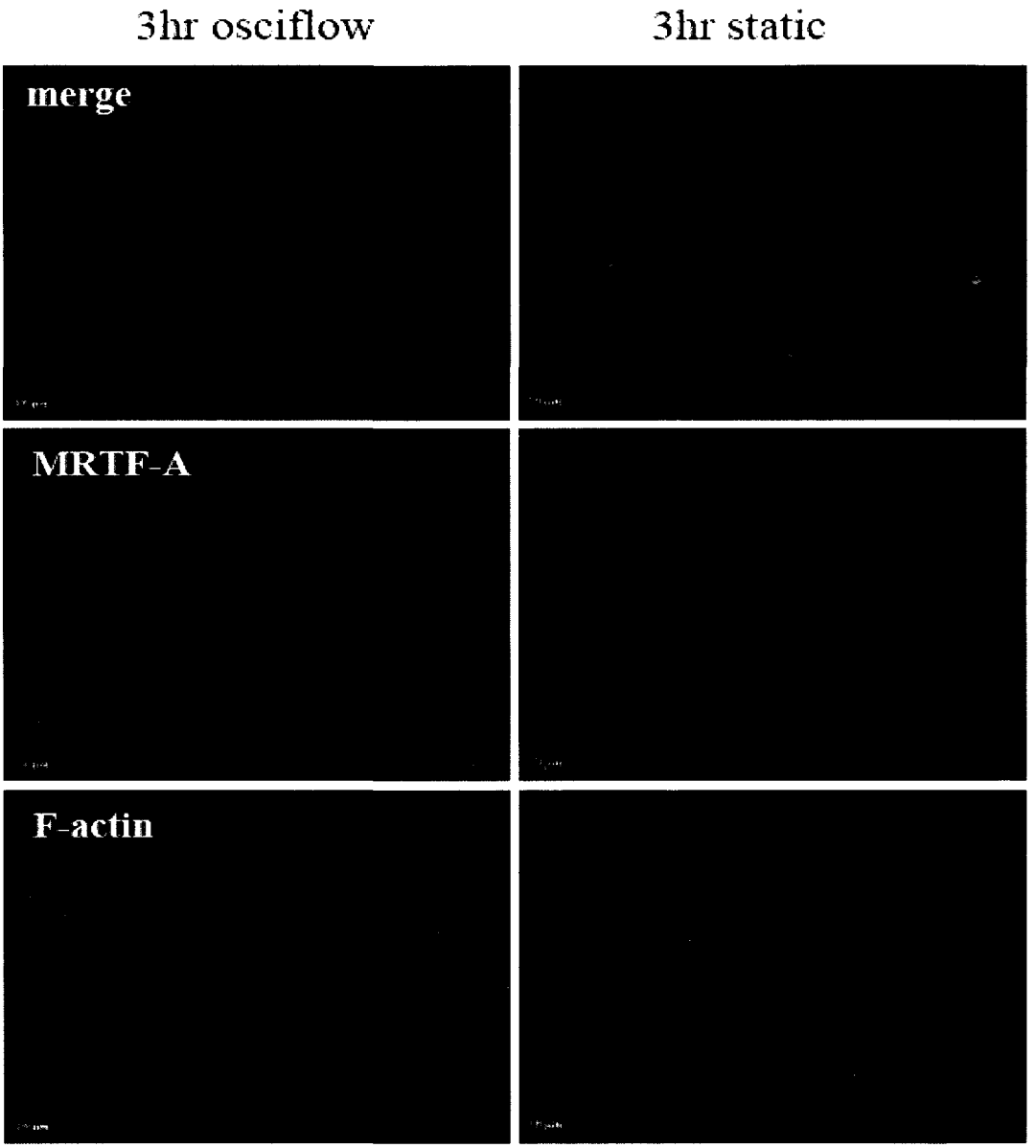

Figure 3.13. MRTF-A localization in response to oscillatory flow

HUVECs were grown to confluence and subjected to 3hrs of oscillatory flow (3 dynes/cm^2, 1Hz) 48hrs after the last maintenance media change. MAL was detected using anti-MRTF-A antibody. F-actin was detected with fluorescein phalloidin. Nuclei were stained with DAPI.

MRTF-A nuclear translocation, HUVECs were pre-treated with PI-3 kinase inhibitor (LY294002) and later subjected to shear stress in the presence of LY294002. MRTF-A sub-cellular localization was assessed by immunofluoresence. The majority of cells subjected to shear stress displayed intermediate MRTF-A distribution (41%). MRTF-A was nuclear in 35% of cells and cytoplasmic in 24% of cells subjected to shear stress (Figure 3.17). In addition, actin stress fibers appeared significantly reduced in these cells (Figure 3.16). MRTF-A was unaffected in static control cells treated with LY294002. These results indicate that, as is the case in fibroblasts, PI-3 kinase plays some role in shear-induced MRTF-A nuclear translocation as well as in cytoskeletal remodeling.

3.3.3 GSK-3β

Endothelial cells are unable to elongate and align in the direction of flow when GSK-3β activity is inhibited (McCue et al., 2006). The elongation and alignment of endothelial cells in the direction of flow has been attributed to the assembly and reorientation of actin stress fibers as well as MTOC and microtubule realignment (McCue et al., 2006, Noria, et al., 2004). The role of GSK-3β in shear induced MRTF-A nuclear translocation and cytoskeletal remodeling was assessed as above using LiCl- an inhibitor of GSK-3β. HUVECs subjected to 3hrs of shear stress were unable to remodel their actin cytoskeleton. Actin remained in a cortical ring following exposure to shear stress (Figure 3.16). MRTF-A nuclear translocation was also reduced as a result of LiCl treatment as only 18% of cells subjected to shear stress displayed nuclear MRTF-A. MRTF-A was intermediate in 63% of sheared cells and cytoplasmic in 19% of cells

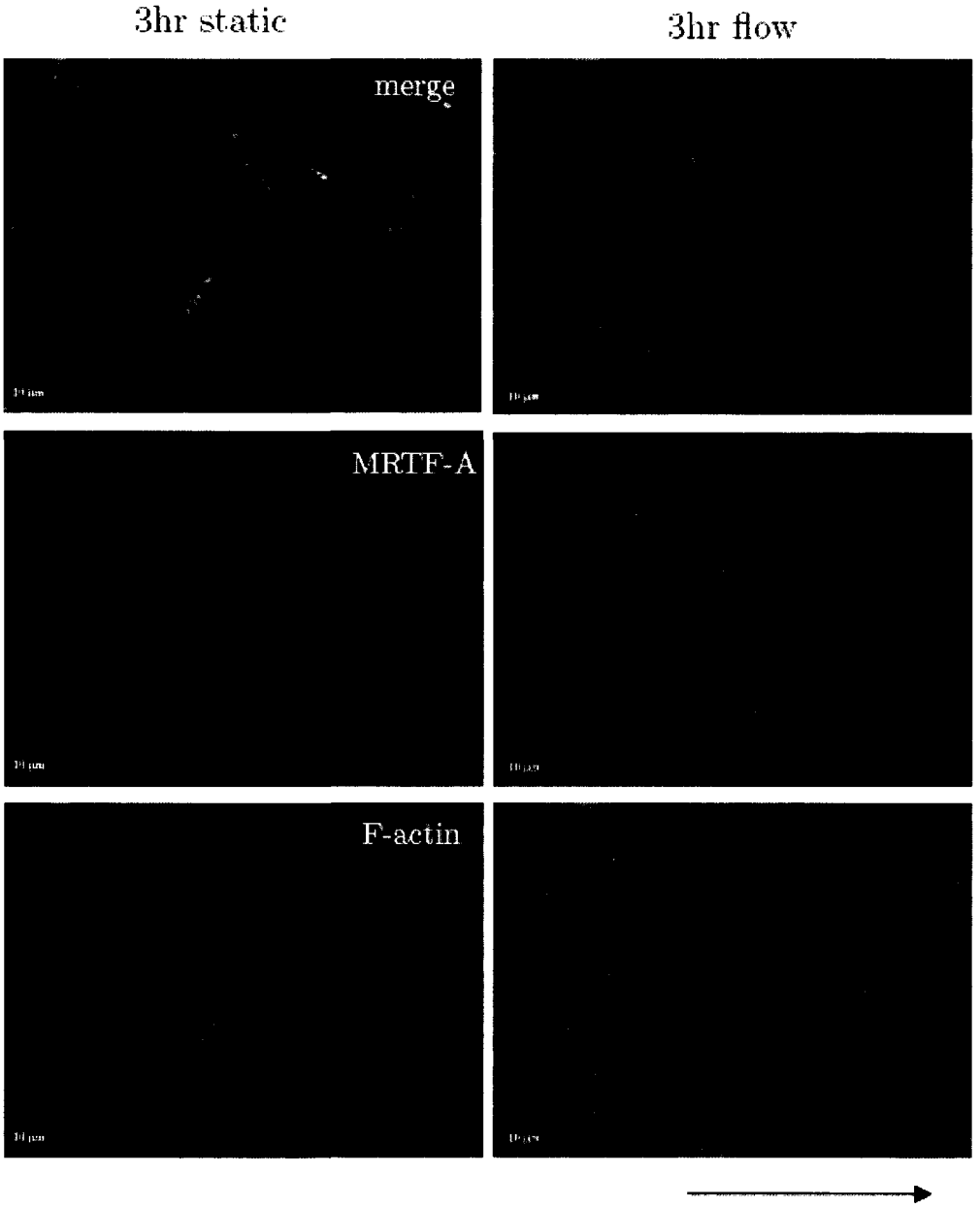

Figure 3.14. Rac 1 inhibitor (NSC23766) has no effect on shear induced MRTF-A nuclear translocation.

HUVEC were preincubated with 50μM of Rac 1 inhibitor for 1hr prior to being subjected to 3hrs of shear stress (3 dynes/cm^2) in the presence of 50μM of Rac1 inhibitor. Endogenous MRTF-A was detected using anti-MRTF-A antibody (red); F-actin was detetcted with fluorescein phalloidin (green). Arrow indicates direction of flow.

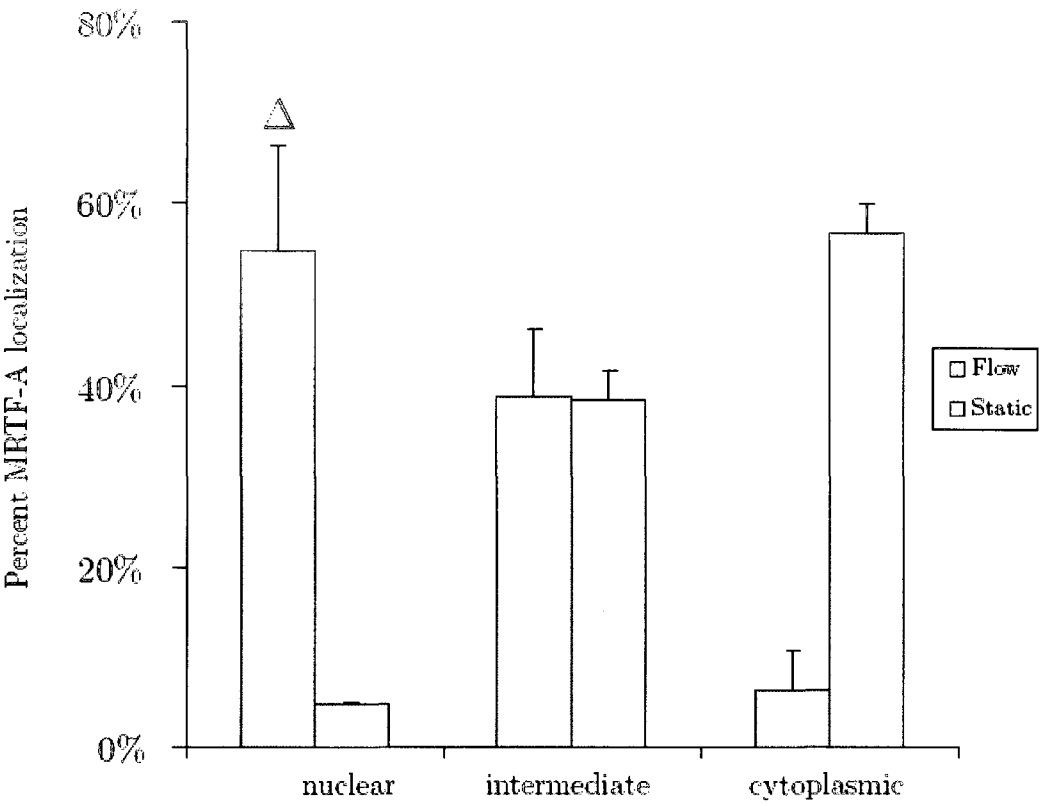

Figure 3.15 Rac 1 inhibitor (NSC23766) has no effect on shear induced MRTF-A nuclear translocation.

HUVEC were preincubated with 50μM of Rac 1 inhibitor for 1hr prior to being subjected to 3hrs of shear stress (3 dynes/cm^2) in the presence of 50μM of NSC23766. Error bars indicate standard deviation from the mean (>100 cells counted from two separate experiments). Δ Indicates no significant difference when compared with percentage of cells with nuclear MRTF-A in untreated HUVEC subjected to flow P=0.3

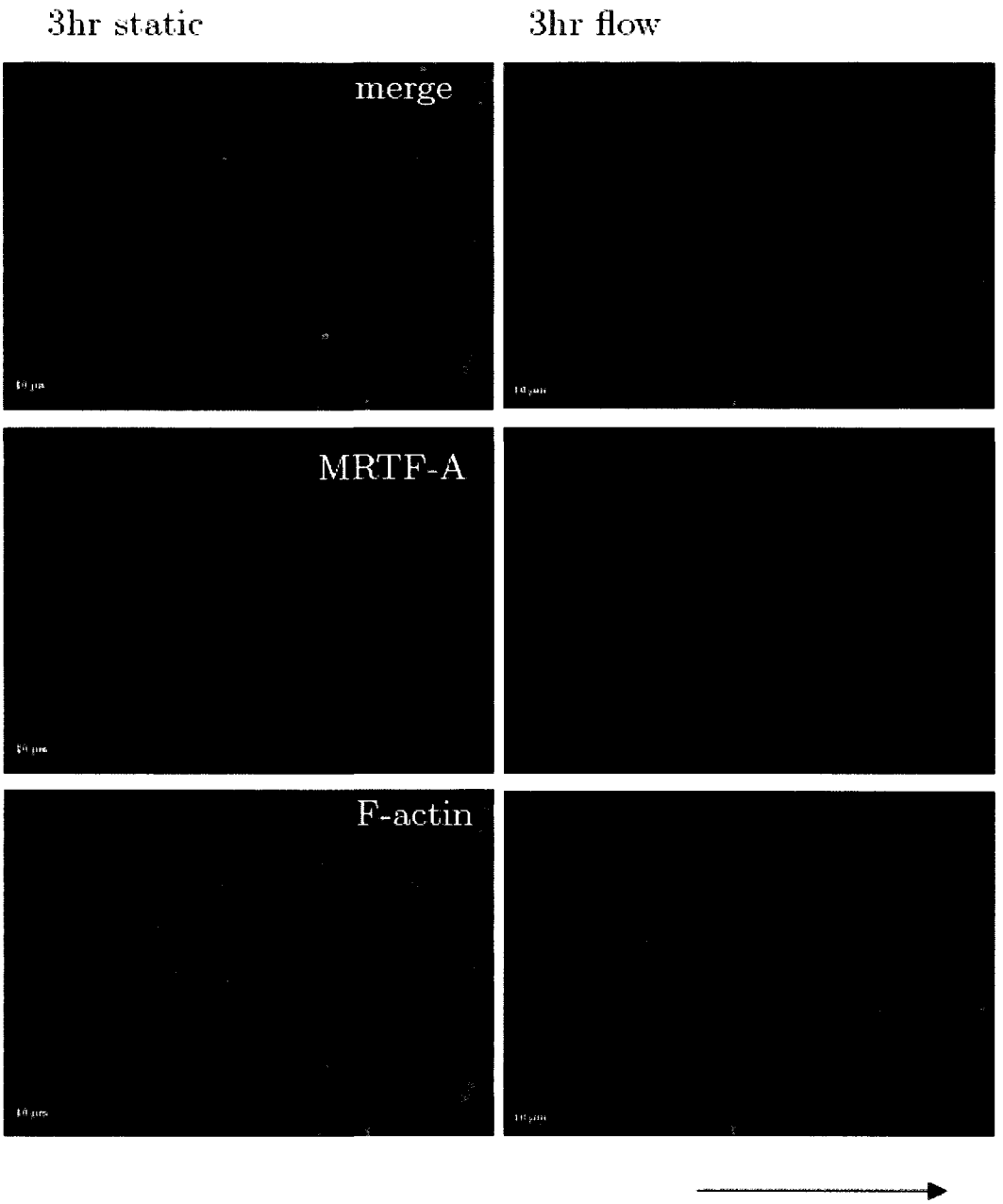

Figure 3.16. PI-3 kinase inhibitor LY294002 reduces shear induced MRTF-A nuclear translocation.

HUVEC were preincubated with 20μM of LY294002 for 1 hr prior to being subjected to 3hrs of shear stress (3 dynes/cm^2) in the presence of 20μM of LY294002. Endogenous MRTF-A was detected using anti-MRTF-A antibody (red); F-actin was detetcted with fluorescein phalloidin (green). Arrow indicates direction of flow.

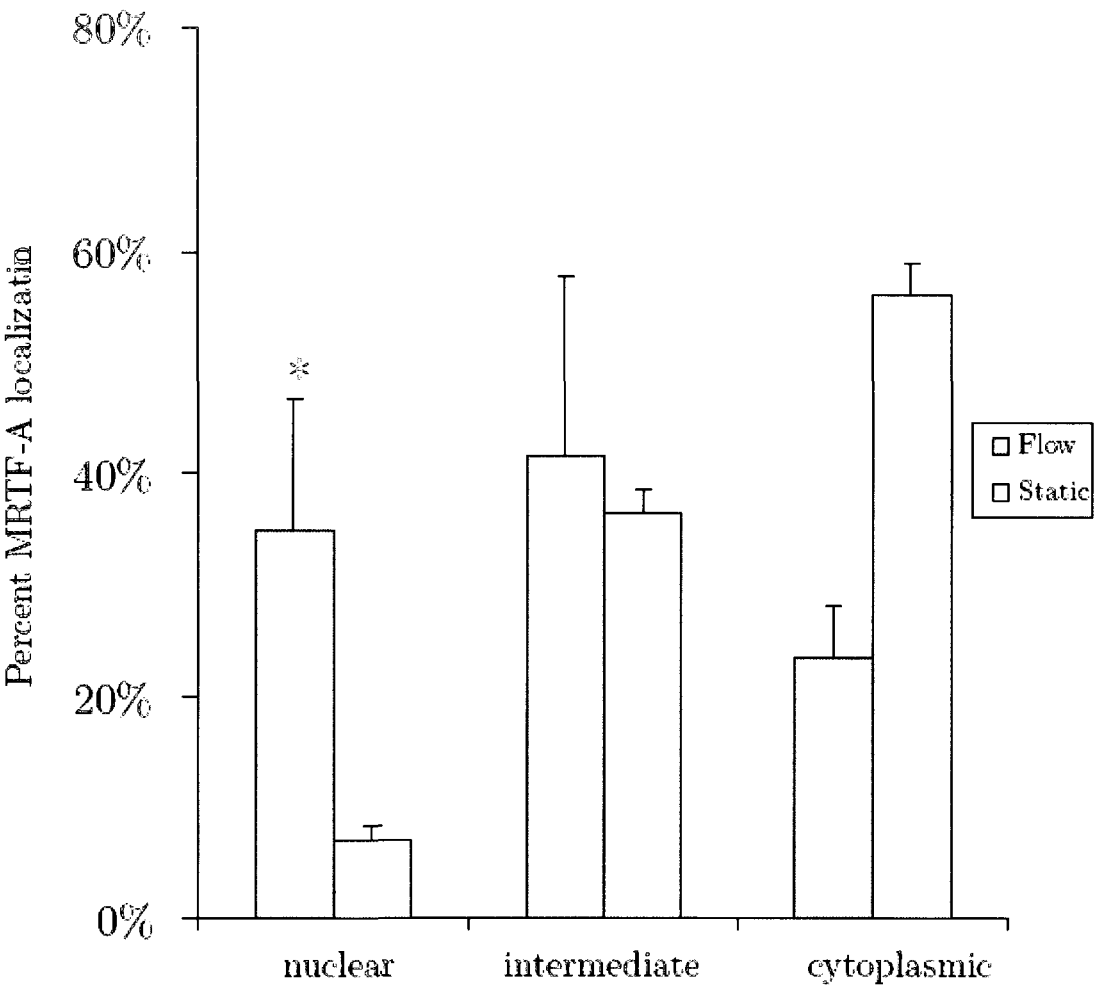

Figure 3.17. PI-3 kinase inhibitor LY294002 reduces shear induced MRTF-A nuclear translocation.

HUVEC were preincubated with 20μM of LY294002 for 1 hr prior to being subjected to 3hrs of shear stress (3 dynes/cm^2) in the presence of 20μM of LY294002. Error bars indicate standard deviation from the mean (>100 cells counted from two separate experiments). * indicates significant difference compared with percentage of cells with nuclear MRTF-A in untreated HUVEC subjected to flow $P<0.05$

(Figure 3.19). MRTF-A nuclear localization was also diminished in static control cells treated with LiCl. Less than 1% of static cells displayed nuclear MRTF-A. Most static cells had either an intermediate (49%) or cytoplasmic (50%) MRTF-A distribution (Figure 3.19).

3.3.4 MAP kinase

The onset of shear stress has been shown to activate MAP kinases (Azuma et al., 2000, Azuma et al., 2001). Shear induced cell alignment requires the activity of p38 MAP kinase (Kadohama et al., 2006). MRTF-A/SRF activation is known to occur independently of MAP kinase signalling in fibroblasts (Gineitis and Treisman, 2001). In order to verify that shear induced MRTF-A nuclear translocation occurs independently of MAP kinase signalling in HUVECs, cells were pre-treated with MEK inhibitor (U0126) and subjected to shear stress in the presence of U0126. The media as well as MEK inhibitor were replenished on control static cells. MRTF-A sub-cellular localization was assessed by immunofluoresence. MEK inhibitor had no effect on MRTF-A nuclear translocation or cytoskeletal remodeling. Cells subjected to shear stress were able to elongate and form parallel bundles of actin stress fibers (Figure 3.20). MRTF-A translocated to the nucleus in 65% of these cells (Figure 3.21). Furthermore, MRTF-A had an intermediate distribution in 18% of cells and a cytoplasmic distribution in 17% of cells. In static cultures, MRTF-A was largely cytoplasmic (79%) (Figure 3.21). These results indicate that shear induced MRTF-A nuclear translocation occurs independently of MAP kinase signalling.

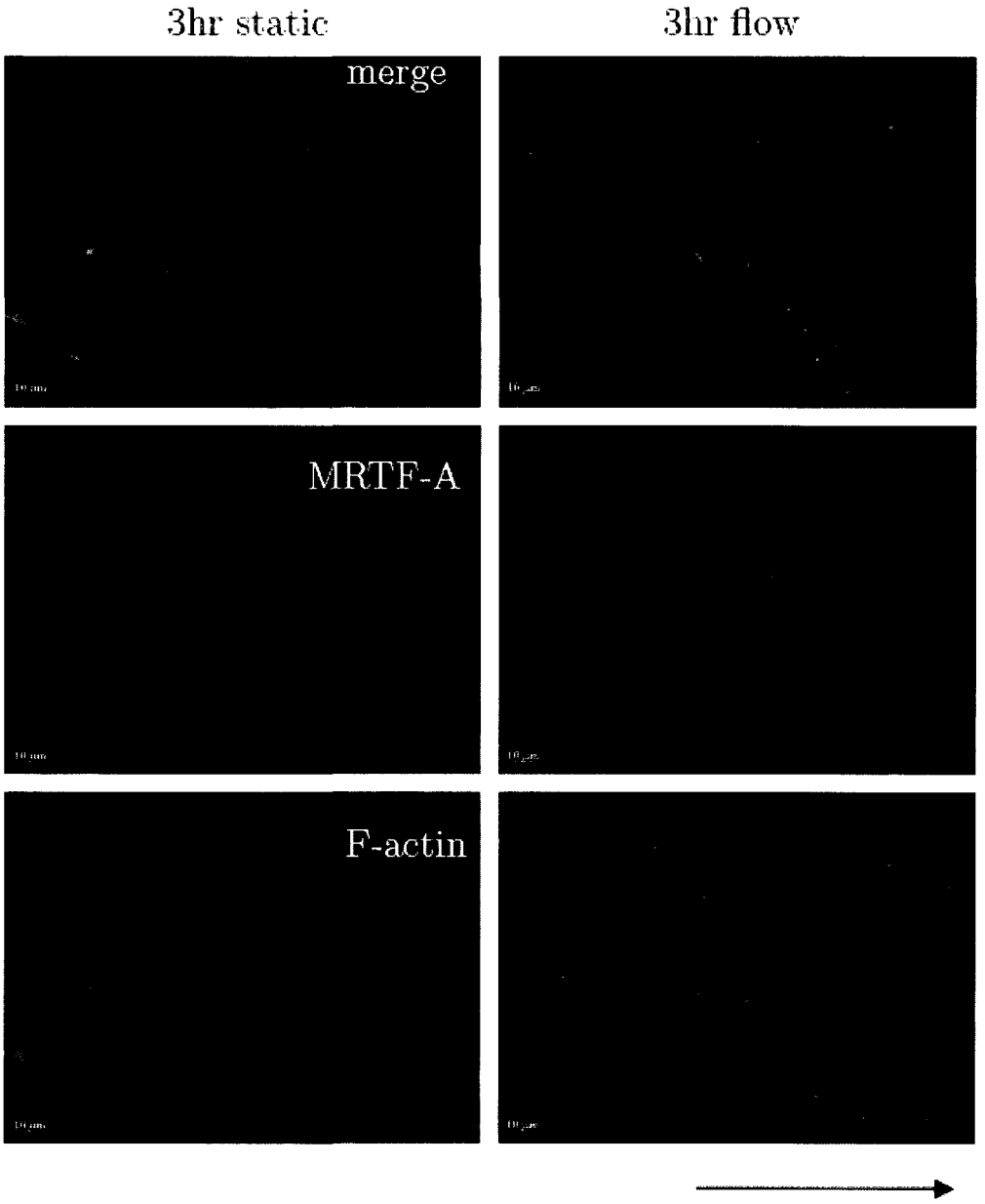

Figure 3.18. LiCl reduces shear induced MRTF-A nuclear translocation. HUVEC were preincubated with 30mM of LiCl for 2hr prior to being subjected to 3hrs of shear stress (3dynes/cm^2) in the presence of 30μM of LiCl. Endogenous MRTF-A was detected using anti-MRTF-A antibody (red); F-actin was detected with fluorescein phalloidin (green). Arrow indicates direction of flow.

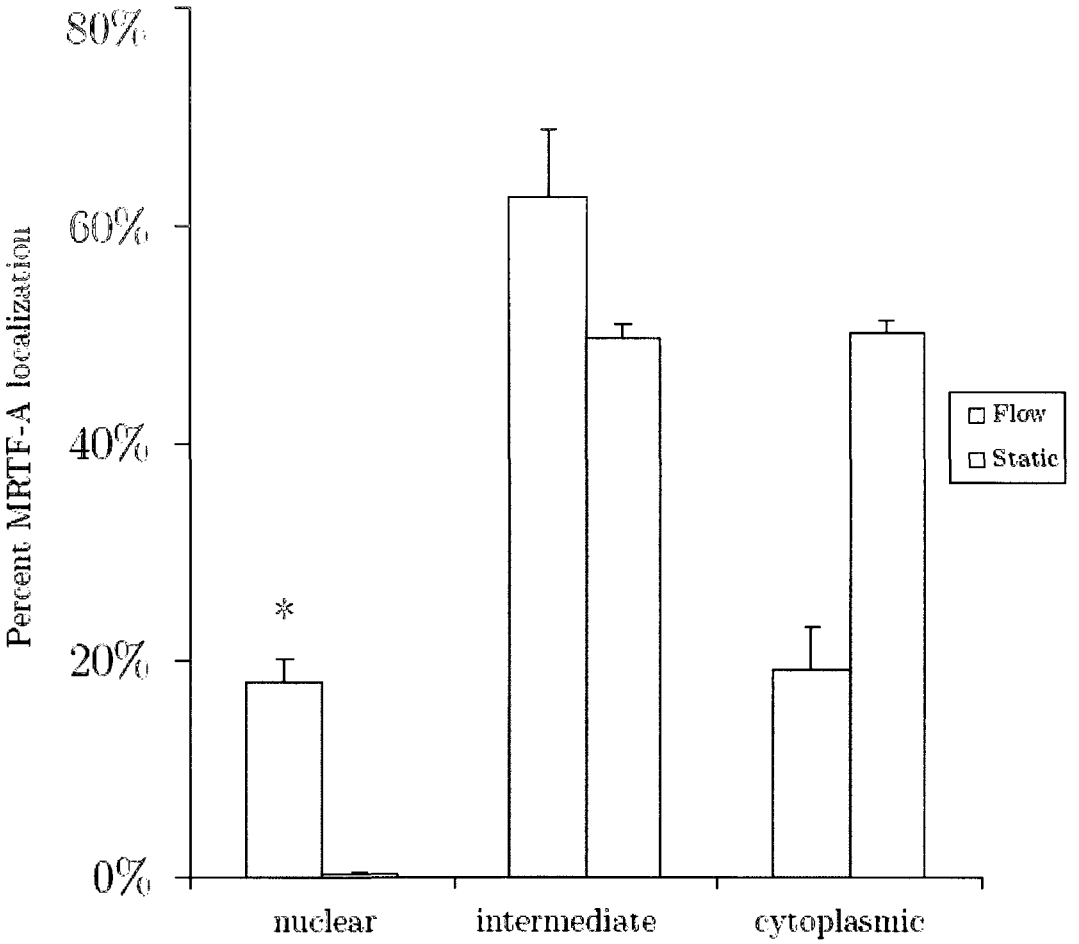

Figure 3.19. LiCl reduces shear induced MRTF-A nuclear translocation. HUVEC were preincubated with 30mM of LiCl for 2hr prior to being subjected to 3hrs of shear stress (3dynes/cm^2) in the presence of 30μM of LiCl. Error bars indicate standard deviation from the mean (>100 cells counted from two separate experiments). * indicates significant difference compared with percentage of cells with nuclear MRTF-A in untreated HUVEC subjected to flow $P<0.01$.

3.3.5 ROCK

ROCK is one of the direct downstream effectors of Rho in the MRTF-A/SRF pathway in NIH 3T3 cells. The expression of ROCK is sufficient to activate SRF and constitutively active ROCK induces stress fiber formation (Ishizaki et al., 1996). Moreover, ROCK inhibition blocks serum induced SRF activation (Sahai et al., 1998). Following shear stress application, a rapid increase in ROCK activation is observed (Lin et al., 2003). We wished to investigate the role of ROCK in shear induced MRTF-A nuclear translocation. HUVECs were pre-treated with ROCK inhibitor (Y27632) prior to shear stress application in the presence of Y27632. The majority of cells subjected to flow in the presence of Y27632 displayed cytoplasmic MRTF-A (64%). Nuclear MRTF-A was seen in only 2% of cells and intermediate MRTF-A was detected in 34% of cells (Figure 3.22 and Figure 3.23). Cytoskeletal remodeling was completely abolished and the actin cytoskeleton in cells subjected to shear stress resembled that of cells in static culture with actin condensed in a ring around the cell periphery (Figure 3.22). MRTF-A sub-cellular localization was not affected by Y27632 treatment in static controls. These results indicate that ROCK is an essential component acting upstream of MRTF-A in HUVECs.

3.3.6 Myosin II

ROCK acts to stabilize actin filaments via LIM kinase and cofilin and also plays a role in promoting stress fiber contractility via myosin II. In fibroblasts, it has been shown that ROCK requires the activity of both LIM kinase/cofilin and myosin II to activate MRTF-A/SRF (Geneste et al., 2002). We wished to investigate the role of

Figure 3.20. MEK inhibitor- U0126 has no effect on shear induced MRTF-A nuclear translocation.

HUVEC were preincubated with 10μM of U0126 for 1hr prior to being subjected to 3hrs of shear stress (3 dynes/cm^2) in the presence of 10μM of U0126. Endogenous MRTF-A was detected using anti-MRTF-A antibody (red); F-actin was detetcted with fluorescein phalloidin (green). Arrow indicates direction of flow.

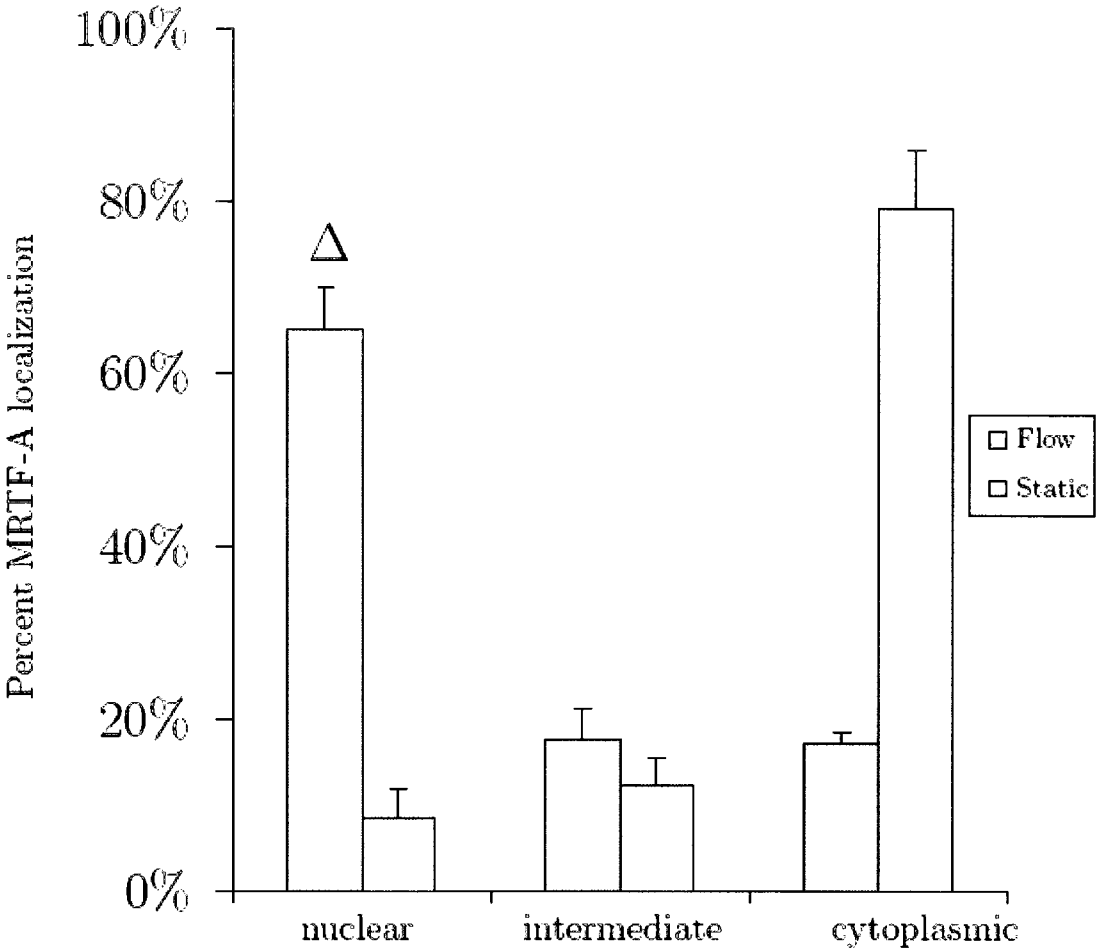

Figure 3.21. MEK inhibitor- U0126 has no effect on shear induced MRTF-A nuclear translocation.

HUVEC were preincubated with 10μM of U0126 for 1hr prior to being subjected to 3hrs of shear stress (3 dynes/cm^2) in the presence of 10μM of U0126. Error bars indicate standard deviation from the mean (>100 cells counted from two separate experiments). Δ Indicates no significant difference when compared with percentage of cells with nuclear MRTF-A in untreated HUVEC subjected to flow P=0.9

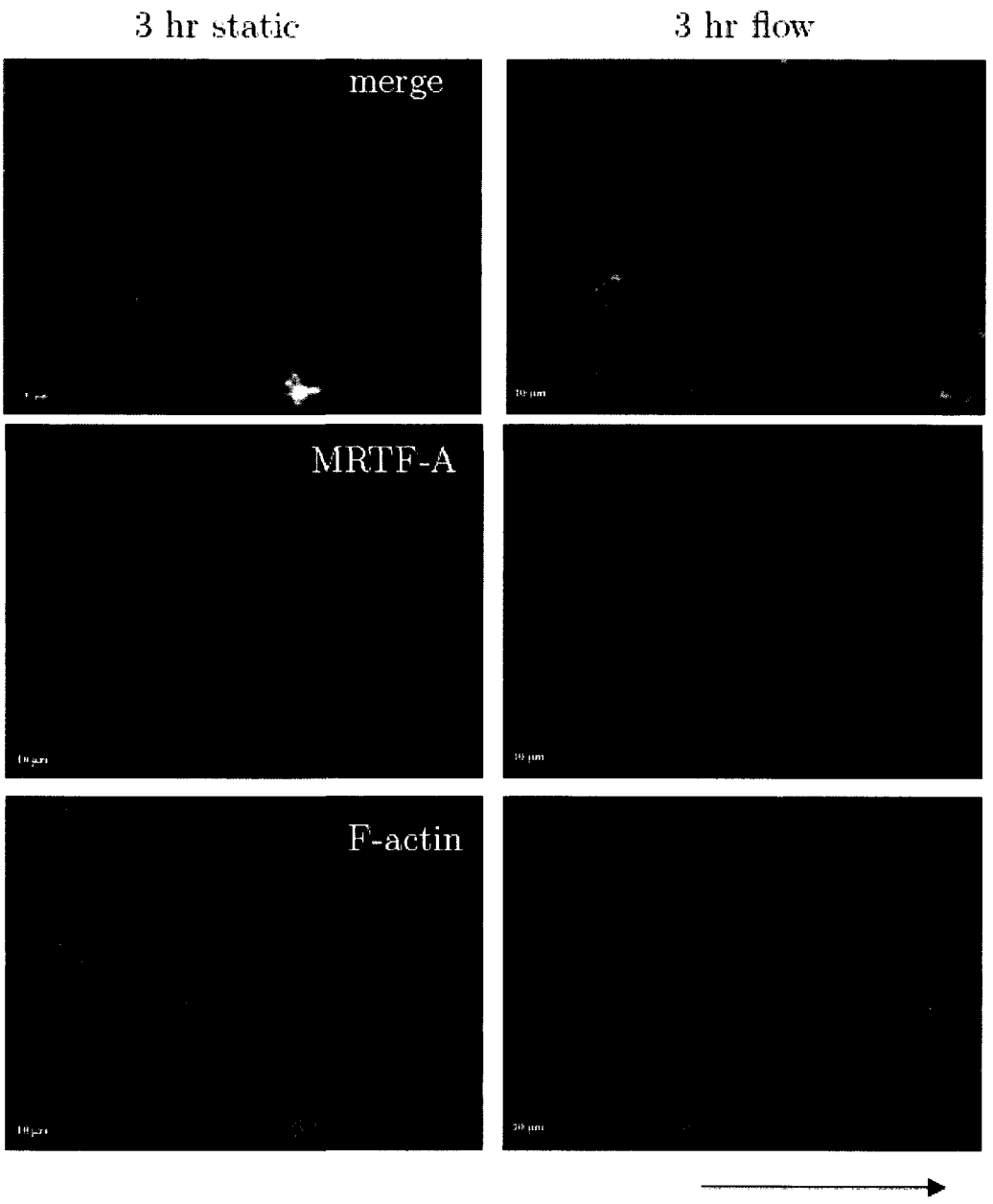

Figure 3.22. ROCK inhibitor- Y27632 prevents shear induced MRTF-A nuclear translocation.

HUVEC were preincubated with 10μM of Y27632 for 1hr prior to being subjected to 3hrs of shear stress (3dynes/cm^2) in the presence of 10μM of Y27632. Endogenous MRTF-A was detected using anti-MRTF-A antibody (red); F-actin was detected with fluorescein phalloidin (green). Arrow indicates direction of flow.

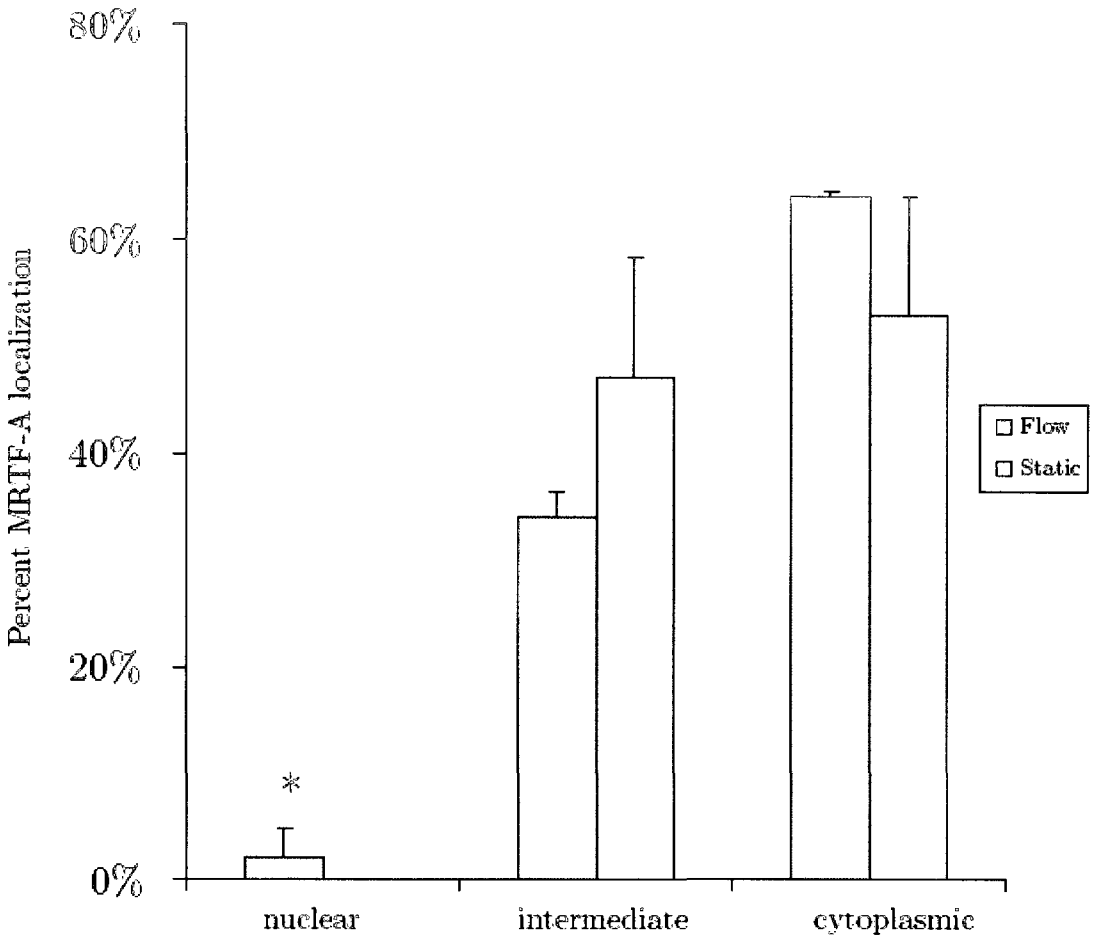

Figure 3.23. ROCK inhibitor- Y27632 prevents shear induced MRTF-A nuclear translocation.

HUVEC were preincubated with 10μM of Y27632 for 1hr prior to being subjected to 3hrs of shear stress (3dynes/cm^2) in the presence of 10μM of Y27632. Error bars indicate standard deviation from the mean (>100 cells counted from two separate experiments). * indicates significant difference compared with percentage of cells with nuclear MRTF-A in untreated

We wished to investigate the role of myosin II in shear induced MRTF-A nuclear translocation in HUVECs as above using blebbistatin an inhibitor of myosin ATPase activity. MRTF-A sub-cellular localization was assessed by immunofluoresence. MRTF-A was mostly either cytoplasmic (53%) or intermediate (43%) in static cells. A small proportion of static cells displayed nuclear MRTF-A (4%) (Figure 3.25). Blebbistatin treatment disrupted the actin cytoskeleton in static cells as actin was no longer in a distinct cortical ring but was distributed around the cell in a clumped and uneven manner (Figure 3.24). The actin cytoskeleton in cells subjected to shear stress resembled that in static cells. Very few parallel stress fibers were detected following shear stress (Figure 3.24) and nuclear MRTF-A was detected in only 25% of cells. A high proportion of cells subjected to shear stress had intermediate MRTF-A (57%) and 18% displayed cytoplasmic MRTF-A (Figure 3.24).

3.4 Requirement of MRTF-A for Shear Induced Cytoskeletal Remodeling

MRTF-A is required for stress fiber formation in NIH 3T3 cells. Cell lines expressing DN MRTF-A displayed defective formation of stress fibers and focal adhesions (Morita et al., 2007). To determine whether MRTF-A is required for shear induced cytoskeletal remodeling to occur, a DN MRTF-A construct lacking the basic regions (B1 and B2) necessary for nuclear translocation was used. This dominant negative construct works by dimerizing to endogenous MRTF-A and preventing MRTF-A nuclear accumulation resulting in a 70% inhibition of reporter gene activation (Miralles et al 2003). Cells were infected with either an adenovirus expressing this DN construct or an adenovirus expressing GFP which served as the control. Cells were

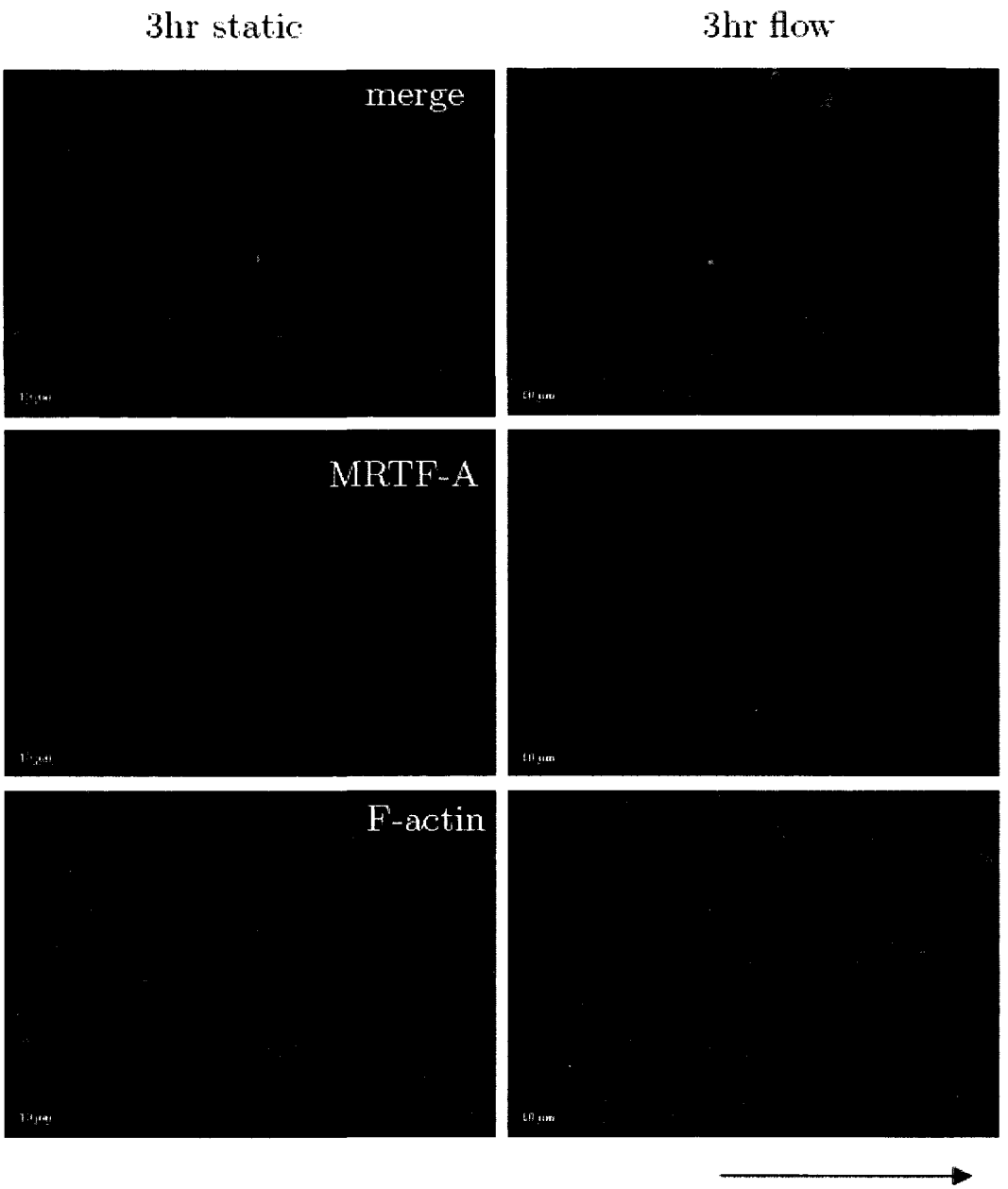

Figure 3.24. Blebbistatin reduces shear induced MRTF-A nuclear translocation. HUVEC were preincubated with 30μM of blebbistatin for 1hr prior to being subjected to 3hrs of shear stress (3dynes/cm^2) in the presence of 30μM of blebbistatin. Endogenous MRTF-A was detected using anti-MRTF-A antibody (red); F-actin was detected with fluorescein phalloidin (green). Arrow indicates direction of flow.

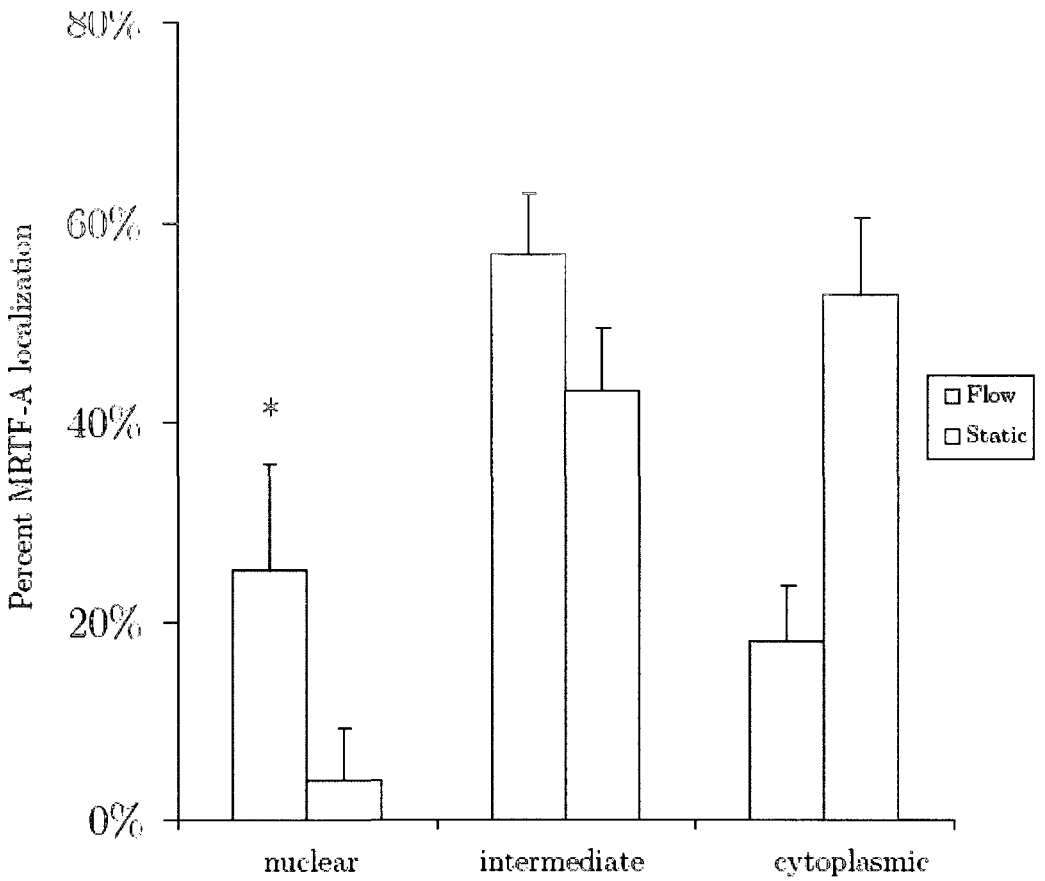

Figure 3.25. Blebbistatin reduces shear induced MRTF-A nuclear translocation.

HUVEC were preincubated with 30μM of blebbistatin for 1hr prior to being subjected to 3hrs of shear stress (3dynes/cm^2) in the presence of 30μM of blebbistatin. Error bars indicate standard deviation from the mean (>100 cells counted from two separate experiments). * indicates significant difference compared with percentage of cells with nuclear MRTF-A in untreated HUVEC subjected to flow $P<0.01$

incubated for 48hrs following infection and subsequently subjected to shear stress. Media on static control cells was also replenished. The sub-cellular localization of endogenous MRTF-A, as well as flag tagged DN MRTF-A, was assessed by immunofluoresence. Uninfected cells showed robust remodeling of the actin cytoskeleton in response to flow with thick actin stress fibers spanning the length of cells. Stress fibers were less pronounced in Ad ΔB1ΔB2 expressing cells. AdΔB1ΔB2 expressing cells in some areas had less actin than uninfected cells (Figure 3.26). Only a small number of cells were infected with the GFP-control virus, thus making it difficult to determine what effect DN MRTF-A expression had on shear induced cytoskeletal remodeling (See Discussion).

In order to determine whether MRTF-A is required for shear induced cytoskeletal remodeling, we wished to knockdown both MRTF-A and MRTF-B in HUVECs using siRNA and subject these cells to flow to assess the effects on cytoskeletal remodeling. We were able to establish conditions for efficient siRNA knockdown of MRTF-A (Figure 3.27) however, there have been some obstacles associated with MRTF-B knockdown by siRNA. We have been able to demonstrate efficient knockdown of MRTF-B by western blotting, but we have been unable to validate these results by immunofluoresence (Figure 3.28). In this case the remaining MRTF-B seems to be predominantly nuclear.

In order to further investigate the necessity of MRTF-A for shear induced cytoskeletal remodeling, a novel inhibitor of the MRTF-A/SRF pathway (CCG-1423) (Evelyn et al., 2007) was used. We first sought to determine the efficacy of CCG-1423 inhibition of MRTF-A/SRF activity. NIH3T3 cells were pre-treated with increasing

concentrations of CCG-1423 for 19hrs prior to serum stimulation. The inhibitor was not efficient at inhibiting serum-induced SRF activation. Also, SRFVP16-induced SRF activation was not completely inhibited (Figure 3.29). Moreover, MRTF-A nuclear translocation was still observed in the presence of the inhibitor in serum-stimulated cells and stress fibers were still evident (Figure 3.30 and Figure 3.31). Thus it appears that use of CCG-1423 would not further elucidate the role of MRTF/SRF activity in the shear stress response.

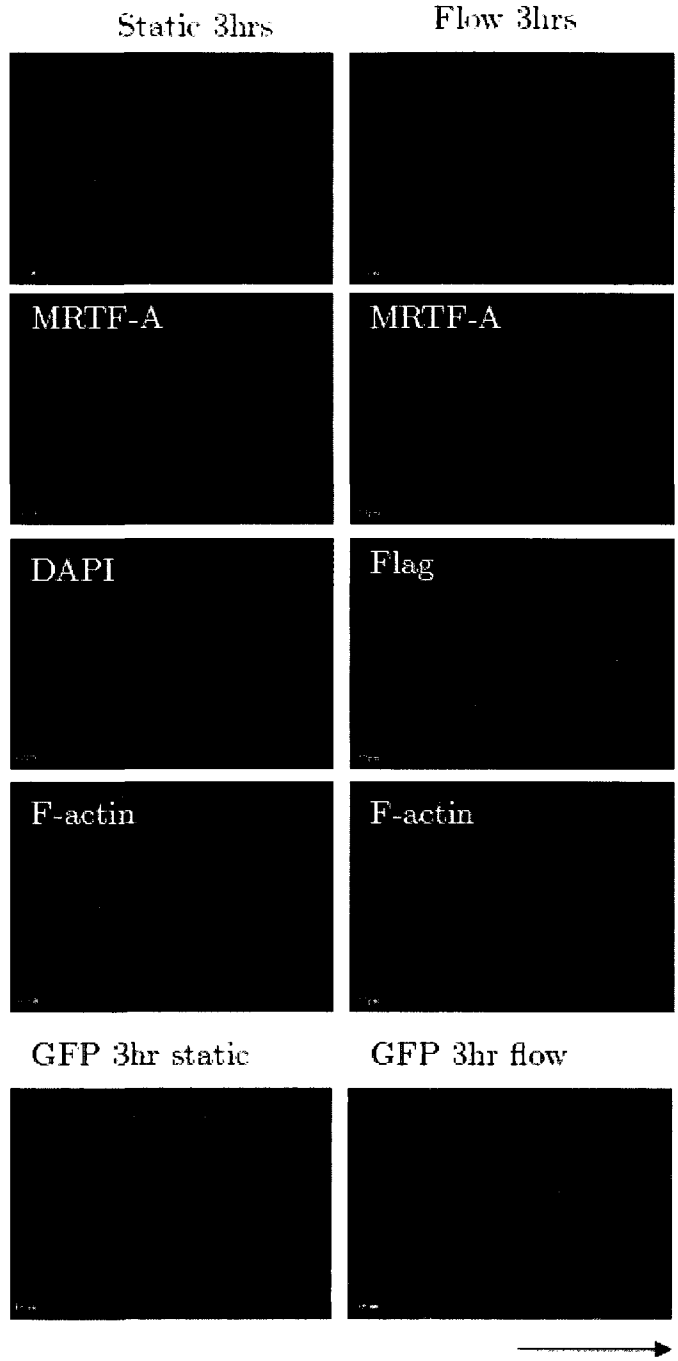

Figure 3.26. Effects of DN MRTF-A on shear induced stress fiber formation

Cells were transfected with either AdMRTF-AΔB1ΔB2 or AdGFP 48hrs after seeding and left to accumulate viral protein for 48hrs. Cells were then subjected to 3hrs of shear stress (3dynes/cm^2). Endogenous MRTF-A was detected using anti MRTF-A antibody (red), infected cells were detected using an anti-flag antibody (blue) and F-actin was detected using fluorescein phalloidin (green).

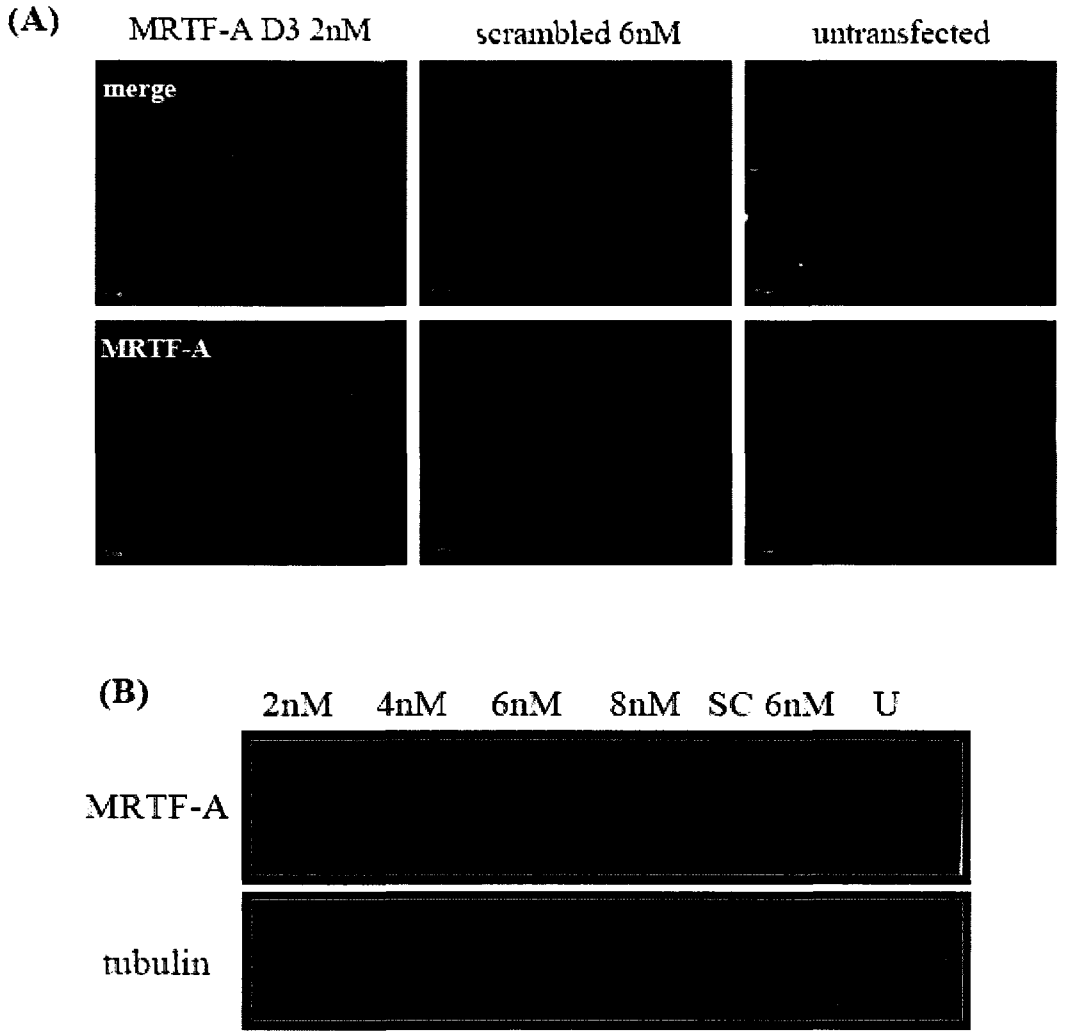

Figure 3.27 Verification of MRTF-A knockdown

HUVEC were transfected with either 2nM of MRTF-A siRNA, 2nM scrambled (SC) siRNA or left untransfected (U). (A) anti-MRTF-A antibody used to verify protein knockdown by immunofloresence. (B) Western blot probed with anti-MRTF-A antibody to verify protein knockdown. Tubulin blot served as a loading control.

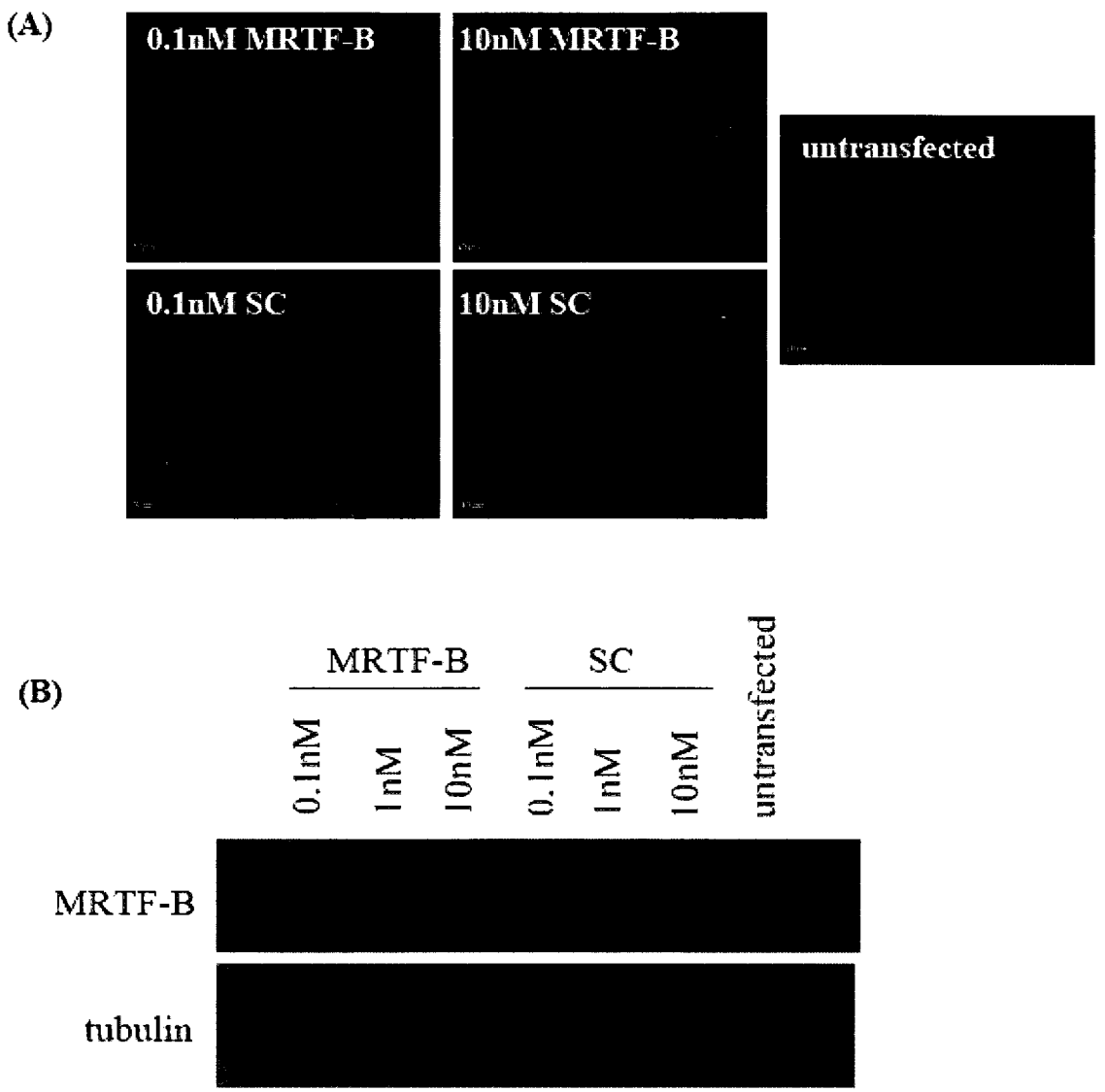

Figure 3.28 Verification of MRTF-B knockdown.

HUVEC were transfected with either MRTF-B siRNA, scrambled siRNA or left untransfected. (A) anti-MRTF-B antibody used to verify protein knockdown by immunofloresence. (B) western blot probed with anti-MRTF-B antibody to verify protein knockdown. Tubulin blot served as a loading control.

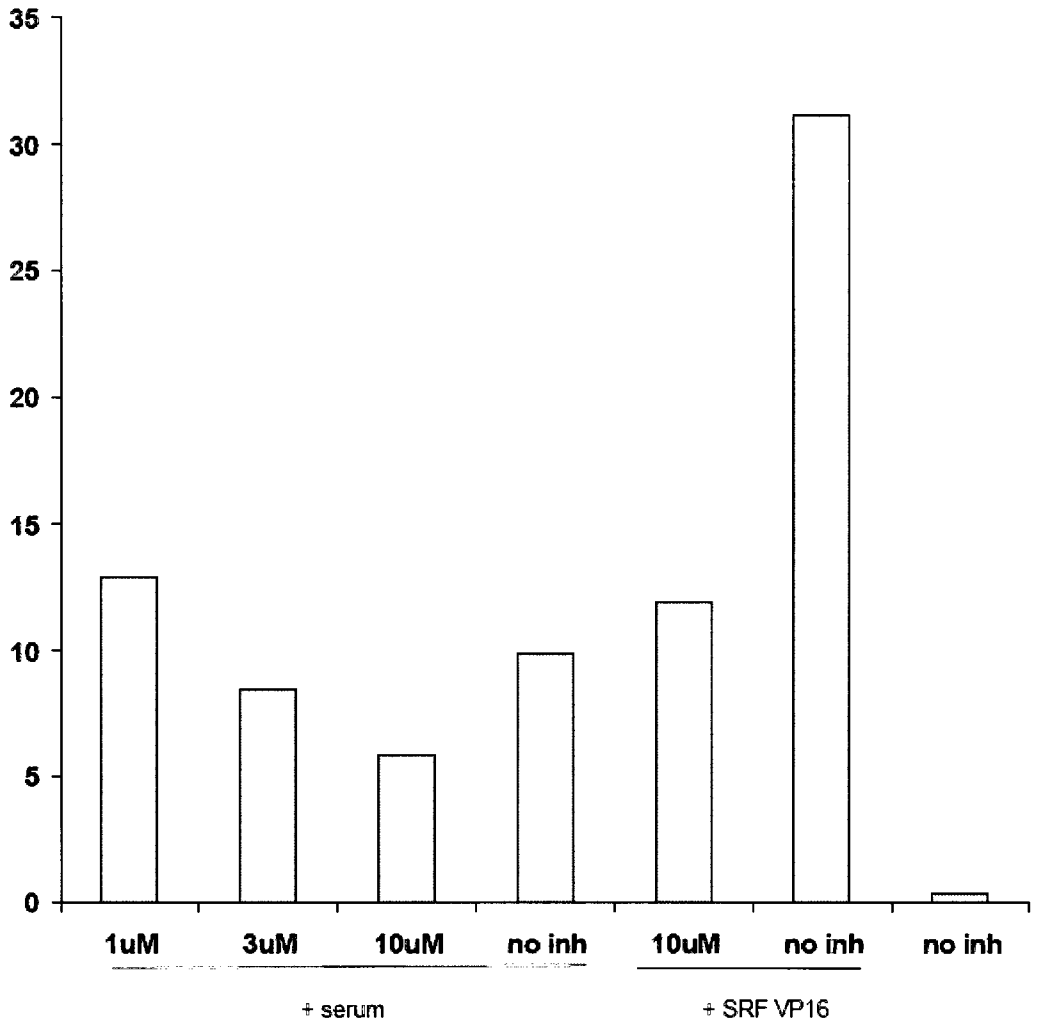

Figure 3.29 Testing of CCG-1423

NIH 3T3 cells were transfected with 3DA.luc reporter and MLV.lacZ expressing plasmids. During serum starvation, cells were preincubated with CCG-1423 for 19hrs. Selected samples were serum stimulated for 6hrs following the preincubation period. Cell lysates were collected and used in an SRF assay.

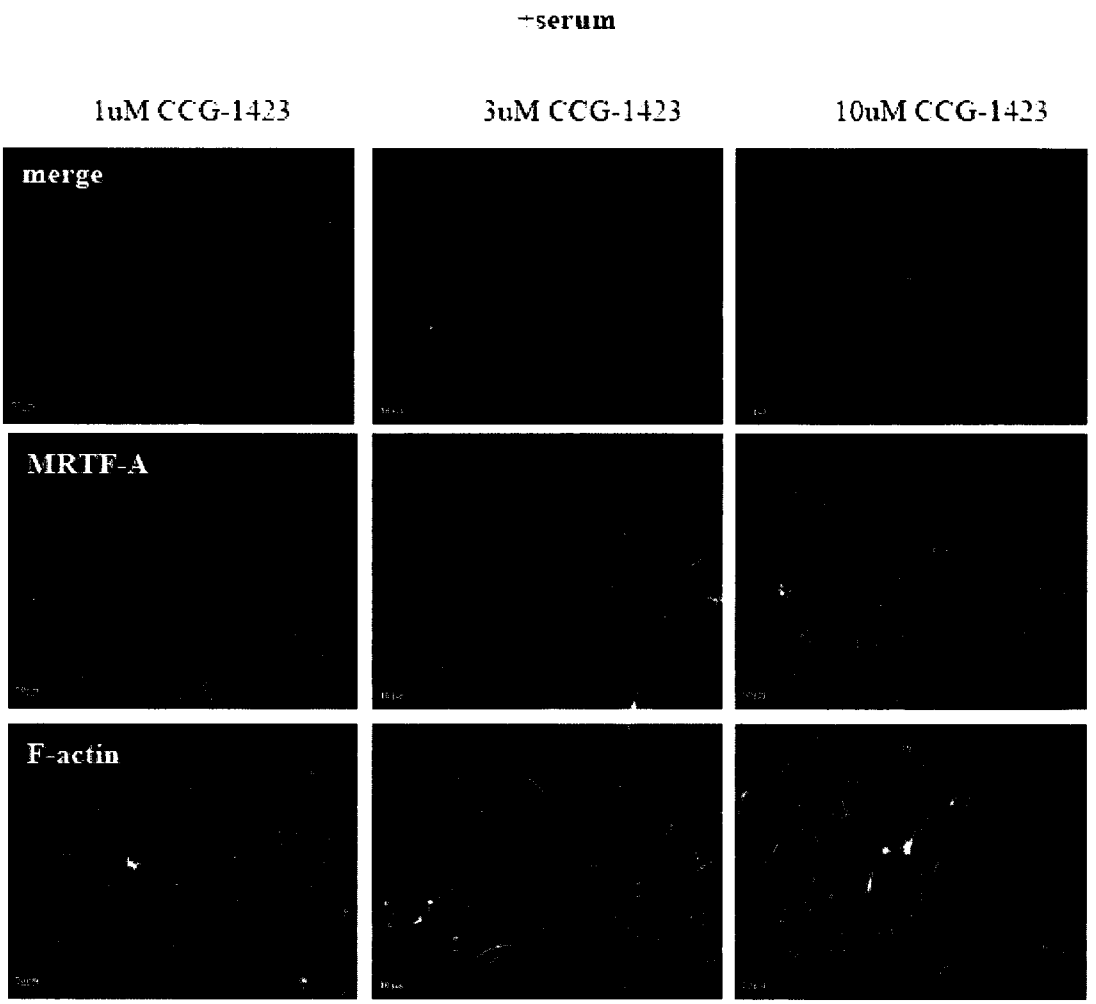

Figure 3.30 Testing of CCG-1423

NIH3T3 cells were grown on glass coverslips in 6 well plates. Cells were pre-incubated with CCG-1423 for 1 hr after being serum starved overnight. Selected samples were serum stimulated for 1hr prior to fixing. MRTF-A was visualized using goat-anti-MRTF-A. F-actin was visualized using fluorescein phalloidin. Nuclei were stained with DAPI.

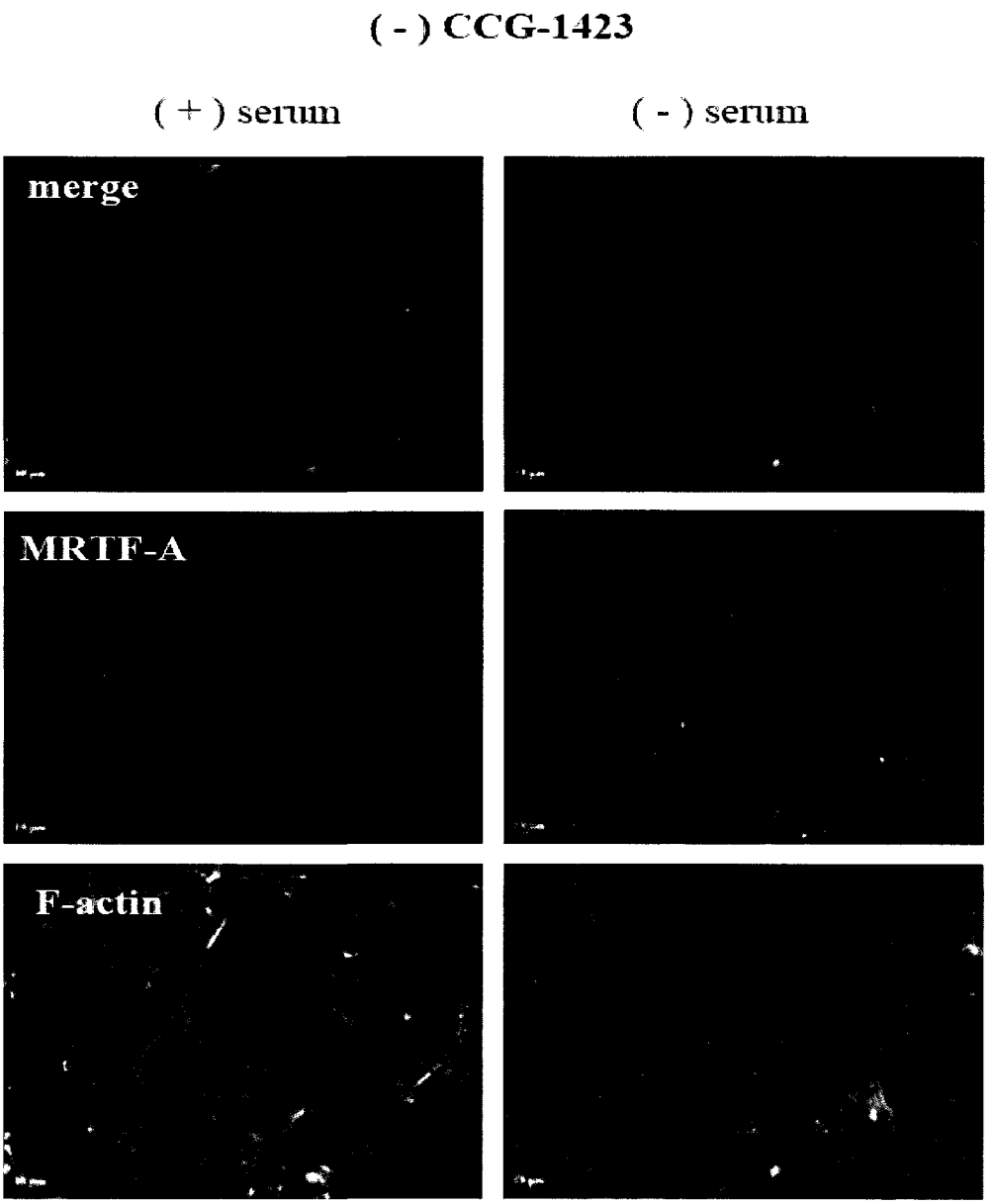

Figure 3.31. Testing of CCG-1423

NIH3T3 cells were grown on glass coverslips in 6 well plates. Cells were serum starved overnight. Selected samples were serum stimulated for 1hr prior to fixing. MRTF-A was visualized using goat-anti-MRTF-A. F-actin was visualized using fluorescein phalloidin. Nuclei were stained with DAPI.

3.5 Membrane Receptors Involved in MRTF-A Nuclear Translocation

3.5.1 Is PECAM-1 Required for Shear Induced MRTF-A Nuclear Translocation and Cytoskeletal Remodeling?

We wished to identify possible mechanoreceptors involved in activating the signalling cascade leading to MRTF-A nuclear translocation. PECAM-1 is a glycoprotein largely concentrated at cell-cell junctions in HUVECs. It is part of a mechanosensory complex necessary and sufficient to mediate shear induced cytoskeletal remodeling (Tzima et al., 2005). To determine if PECAM-1 is required for MRTF-A nuclear translocation and shear induced cytoskeletal remodeling, PECAM-1 expression was knocked down using 2nM PECAM-1 siRNA. Knockdown efficiency was determined by western blotting using anti-PECAM-1 antibody and confirmed by immunofluoresence (Figure 3.36 and Figure 3.32). Cells were subjected to shear stress after having been incubated for 48hrs following siRNA transfection and the media on static control cells was replaced. MRTF-A sub-cellular localization as well as PECAM-1 distribution were assessed by immunofluoresence. MRTF-A nuclear translocation was seen in a high proportion of cells in both PECAM-1 knock down (59%) and control (scrambled siRNA transfected) cells (63%) (Figure 3.33 and Figure 3.35). PECAM-1 knockdown cells displayed an intermediate distribution of MRTF-A in 35% of cells and a cytoplasmic distribution in 5% of cells (Figure 3.33). Scrambled siRNA transfected cells displayed an intermediate distribution in 36% of cells and a cytoplasmic distribution in less than 1% of cells (Figure 3.28). Robust parallel actin stress fibers were observed in both PECAM-1 knock down and scrambled siRNA transfected cells (Figure 3.32 and

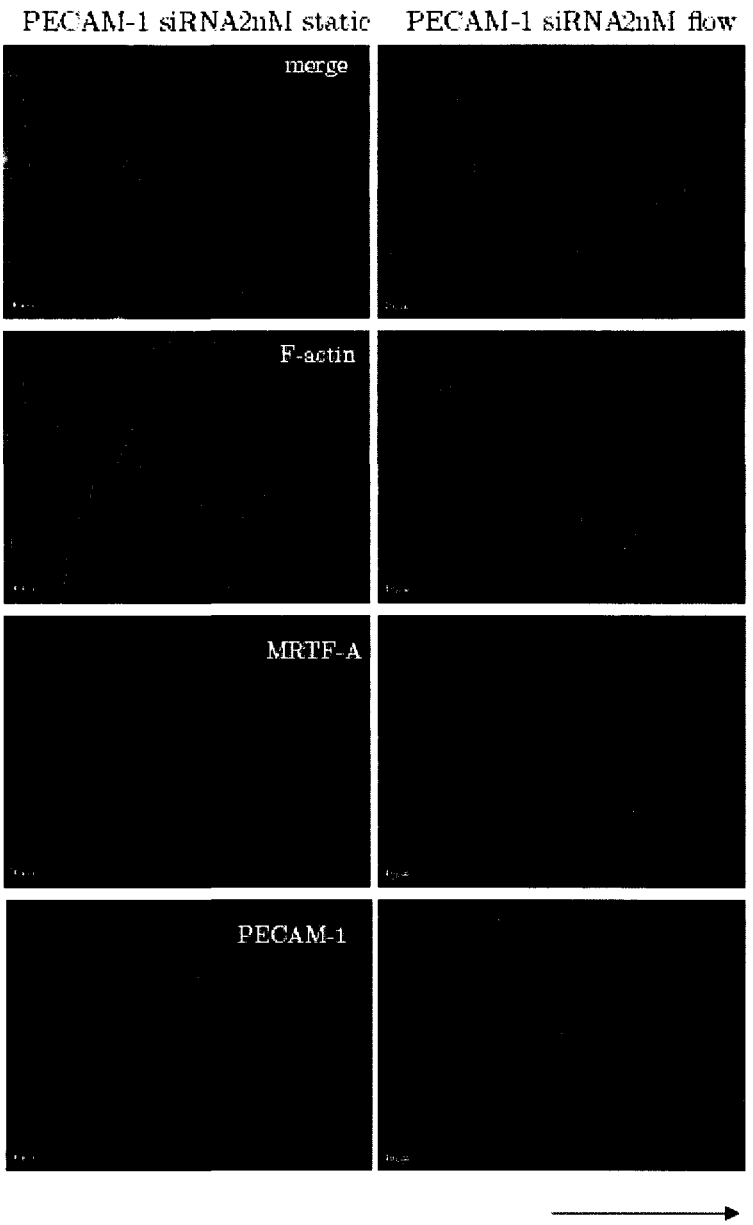

Figure 3.32. Effects of PECAM-1 knockdown on shear induced MRTF-A nuclear translocation.

HUVEC were transfected with 2nM PECAM-1 48 hrs prior to subjecting cells to 3hrs shear stress (3dynes/cm^2). Endogenous MRTF-A was detected using anti-MRTF-A antibody (red); F-actin was detetcted with fluorescein phalloidin (green). PECAM-1 was detected with anti-PECAM-1 antibody (blue). Arrow indicates direction of flow.

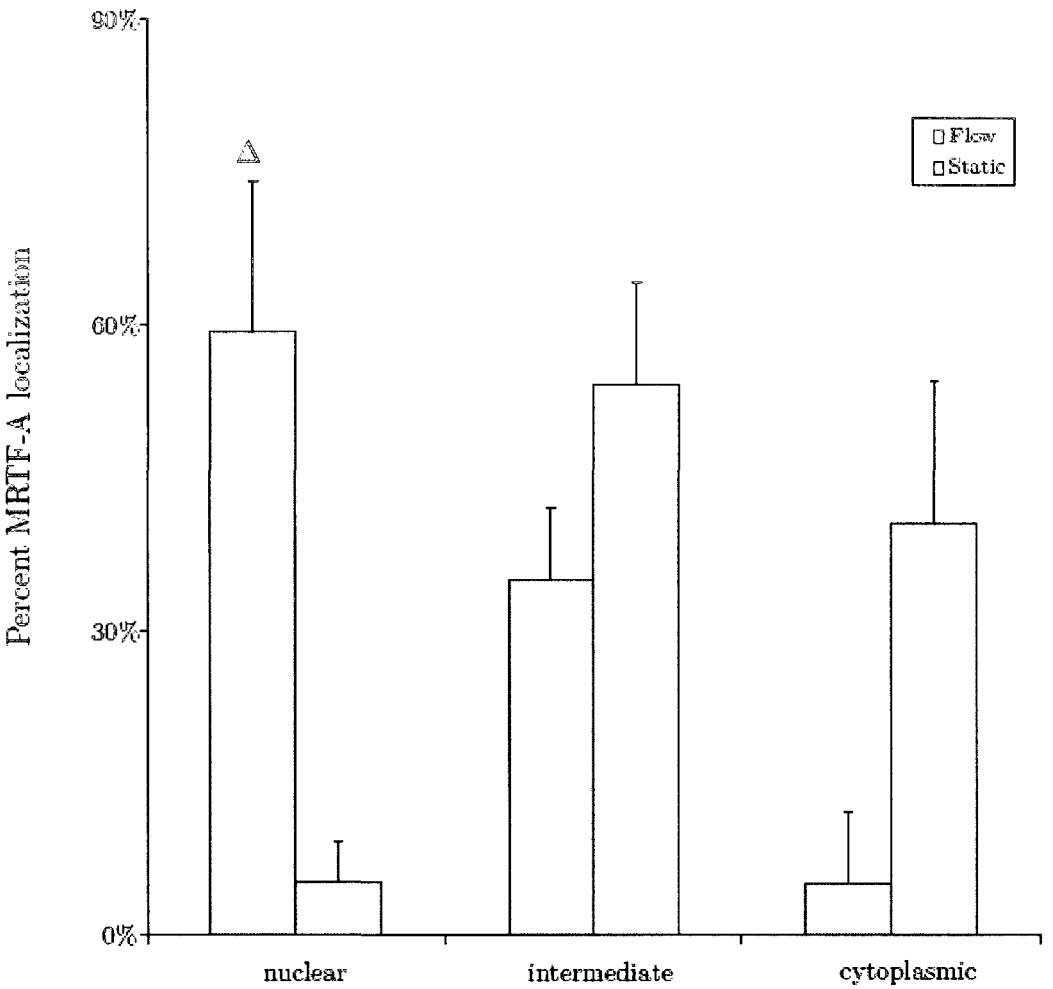

Figure 3.33. Effects of PECAM-1 knockdown on shear induced MRTF-A nuclear translocation.

HUVEC were transfected with 2nM PECAM-1 siRNA 48 hrs prior to subjecting cells to 3hrs shear stress (3dynes/cm2). Mean values are plotted from two separate experiments (>100 cells counted). Error bars indicate standard deviation from the mean. Δ Indicates no significant difference when compared with percentage of cells with nuclear MRTF-A in untreated HUVEC subjected to flow P=0.6

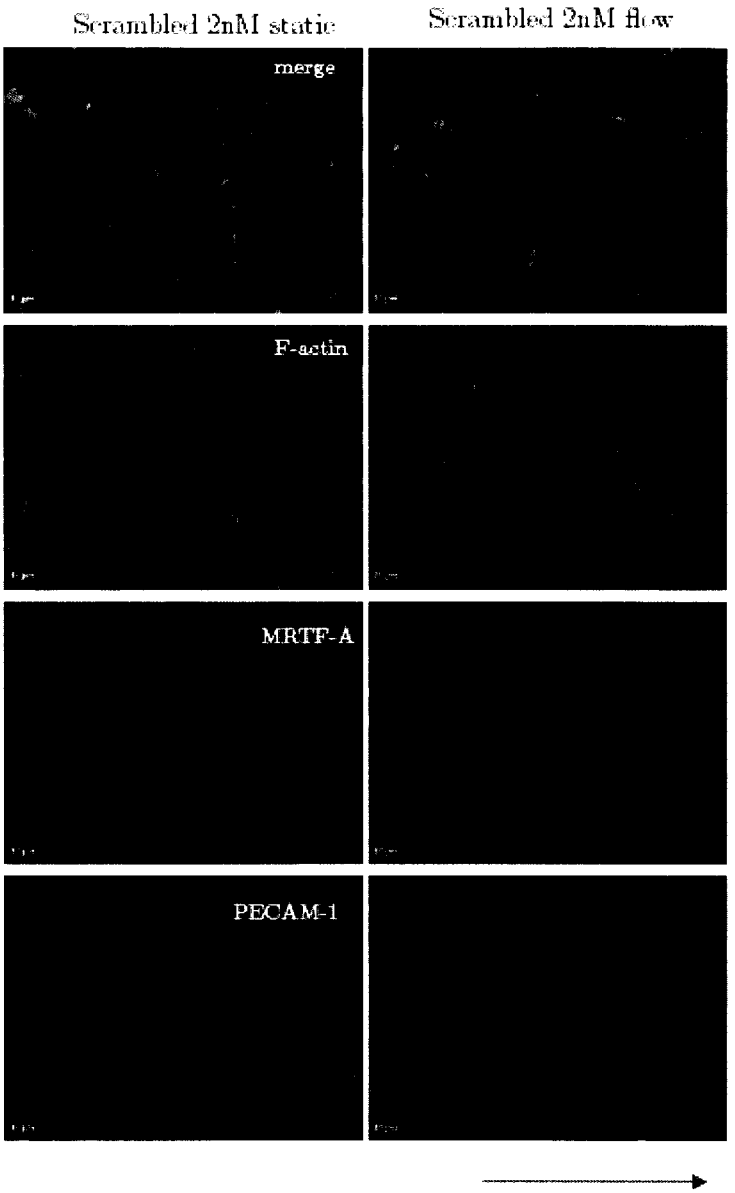

Figure 3.34. Effects of PECAM-1 knockdown on shear induced MRTF-A nuclear translocation.

HUVEC were transfected with 2nM scrambled siRNA 48 hrs prior to subjecting cells to 3hrs shear stress (3dynes/cm2). Endogenous MRTF-A was detected using anti-MRTF-A antibody (red); F-actin was detetcted with fluorescein phalloidin (green). PECAM-1 was detected with anti-PECAM-1 antibody (blue). Arrow indicates direction of flow.

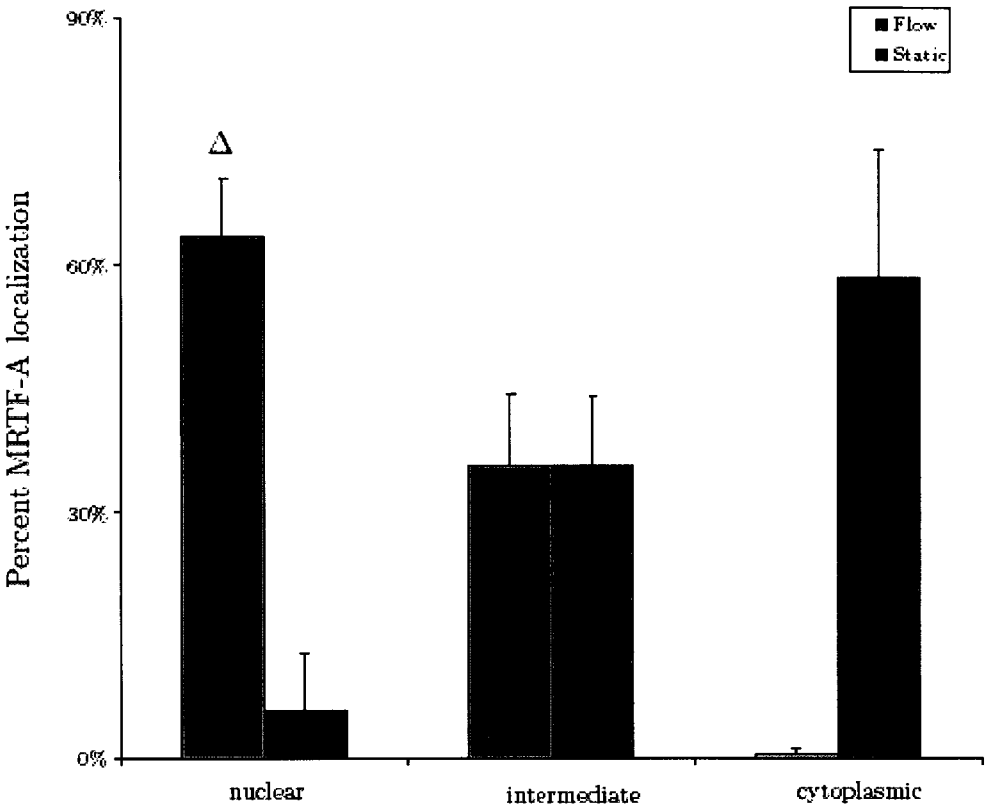

Figure 3.35. Effects of PECAM-1 knockdown on shear induced MRTF-A nuclear translocation.

HUVEC were transfected with 2nM scrambled siRNA 48 hrs prior to subjecting cells to 3hrs shear stress (3dynes/cm2). Mean values are plotted from two separate experiments (>100 cells counted). Error bars indicate standard deviation from the mean. Δ Indicates no significant difference when compared with percentage of cells with nuclear MRTF-A in untreated HUVEC subjected to flow P =0.8

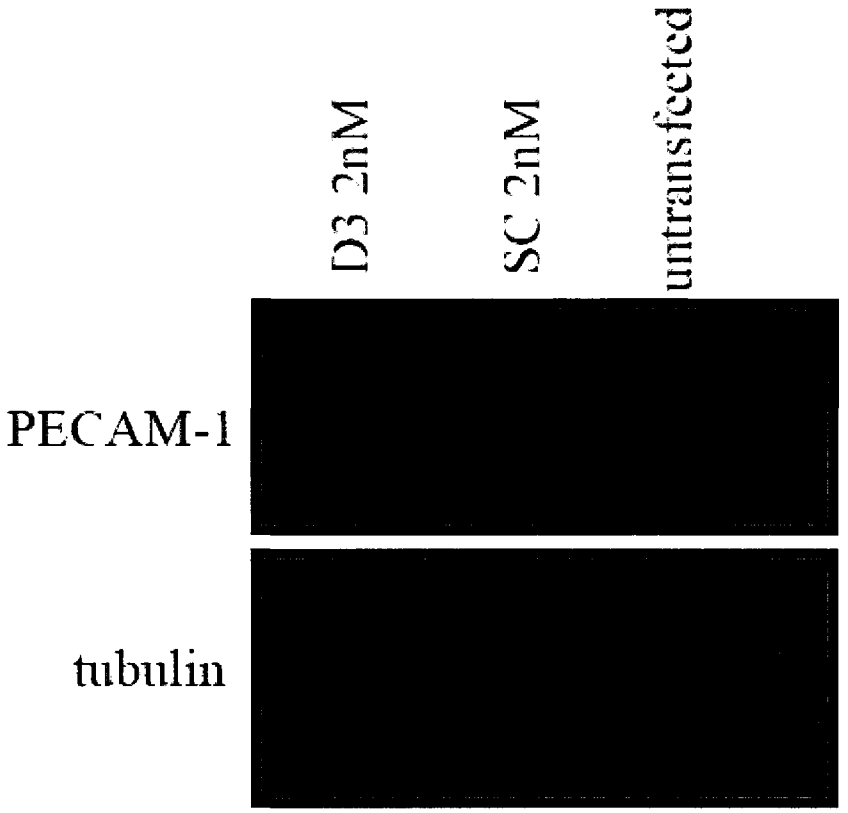

Figure 3.36. Verification of PECAM-1 knockdown.

HUVEC were transfected with 2nM PECAM-1, 2nM scrambled siRNA or left untransfected 48 hrs prior to subjecting cells to 3hrs shear stress (3dynes/cm2). HUVECs were harvested from slides with 1X SDS. Lysates were boiled for 3 minutes and loaded onto 10% SDS-PAGE gel. Western blot probed with anti PECAM-1 antibody to verify protein knockdown by siRNA. Tubulin blot served as a loading control.

Figure 3.34). A student *t*-test indicated that there is no significant difference in the percentage of cells with nuclear MRTF-A between PECAM-1 knockdown and untreated cells (Pvalue = 0.6 Figure 3.33).

3.5.2 MRTF-A Nuclear Translocation in Response to a Magnetic Field

In the pursuit of membrane receptors that activate signalling cascades leading to MRTF-A nuclear translocation in HUVECs, we performed experiments in which cells were incubated with ligand coated magnetic beads that allowed the magnetic beads to bind receptors specific to the ligand. The cells were then exposed to a magnetic field of constant force which would exert a force specifically on the receptor associated with the ligand bound bead. The magnetic field was applied in such a way that the resulting force was acting lateral to the cell surface in an effort to mimic as closely as possible the force exerted on the cell membrane by the application of shear. The sub-cellular localization of MRTF-A was assessed by immunofluoresence. HUVECs incubated with anti-PECAM-1 coated beads did not display any nuclear translocation of MRTF-A when a magnetic field was applied for 1hr, 2hrs and 4hrs (Figure 3.37). Similarly, HUVECs incubated with RGD peptide (ligand for integrins) coated beads did not display MRTF-A nuclear translocation when subjected to a magnetic field (Figure 3.38). In addition, F-actin remained in a cortical actin ring at the periphery of cells in both experiments. This suggests that either additional conditions are required to stimulate MRTF-A nuclear translocation or MRTF-A nuclear translocation is triggered by the activation of membrane receptors other than PECAM-1 and integrins.

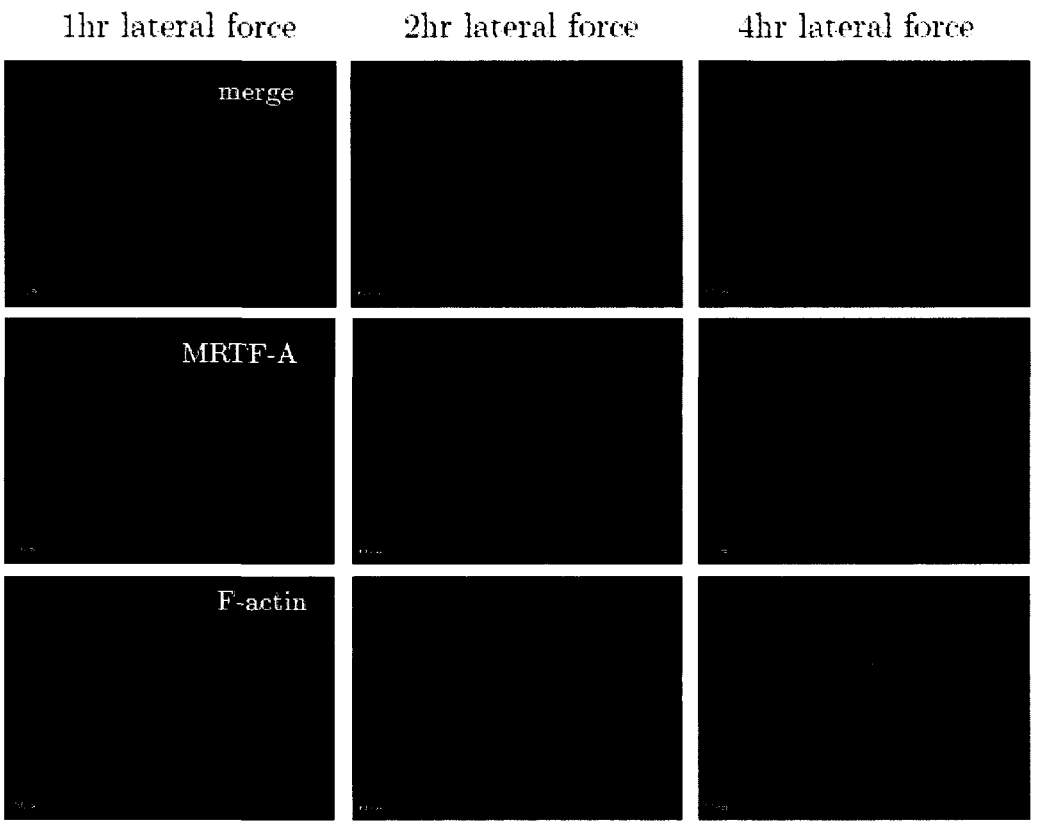

Figure 3.37. Effect of PECAM-1 activation by magnetic force on MRTF-A translocation.

HUVECs were grown to confluence and coupled to anti-PECAM-1 coated magnetic beads. Cells were then exposed to a magnetic field which exerted lateral force on the cells for 1hr, 2hrs and 4hrs. Endogenous MRTF-A was detected using anti-MRTF-A antibody (red); F-actin was detected with fluorescein phalloidin (green).

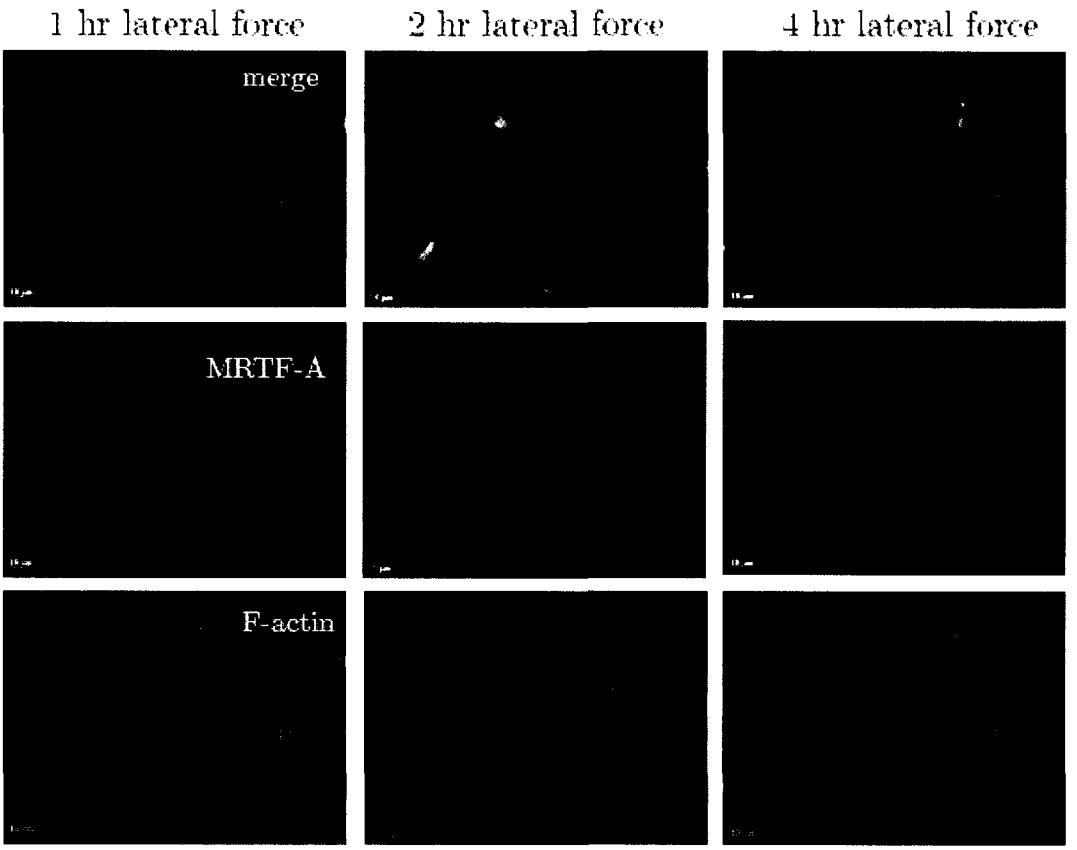

Figure 3.38. Effect of integrin activation by magnetic force on MRTF-A translocation.

HUVECs were grown to confluence and coupled to RGD peptide coated magnetic beads. Cells were then exposed to a magnetic field which exerted lateral force on the cells for 1hr, 2hrs and 4hrs. Endogenous MRTF-A was detected using anti-MRTF-A antibody (red); F-actin was detected with fluorescein phalloidin (green).

3.6 Does cell confluence influence MRTF-A and MRTF-B sub-cellular localization?

While performing flow experiments, we noticed that the sub-cellular distribution of MRTF-A varied depending on cell confluence. In sub-confluent areas, MRTF-A was nuclear in a large proportion of cells whereas in confluent regions, MRTF-A was predominantly cytoplasmic. This observation prompted us to verify whether cell confluence affects sub-cellular localization of MRTF-A. HUVECs were seeded onto glass coverslips and fixed 24hrs after seeding when cells were still sub-confluent, as well as 96hrs after seeding, when cells had reached confluence. MRTF-A sub-cellular localization was assessed by immunofluoresence. At 24hrs after seeding, MRTF-A was either nuclear or intermediate in most of the cells. At 96hrs after seeding, MRTF-A was almost exclusively cytoplasmic (Figure 3.39). We also examined the distribution of MRTF-B in sub-confluent and confluent HUVEC cultures. The distribution of MRTF-B was not affected by cell confluence. MRTF-B appeared to be evenly dispersed throughout the cell in both sub- confluent and confluent cell cultures (Figure 3.39).

3.7 Can the disruption of adherens junctions trigger MRTF-A nuclear translocation?

The changes that endothelial cells undergo after being subjected to shear stress include changes in cell shape and orientation. These changes require the disassembly followed by reassembly of adherens junctions. It has been reported that the disruption of cell-cell junctions in epithelial cells through calcium removal, induced nuclear localization of MRTF-A (Fan et al., 2007). Moreover, the dissociation of E-cadherin dependent junctions in epithelial cells resulted in MRTF-dependent SRF activation

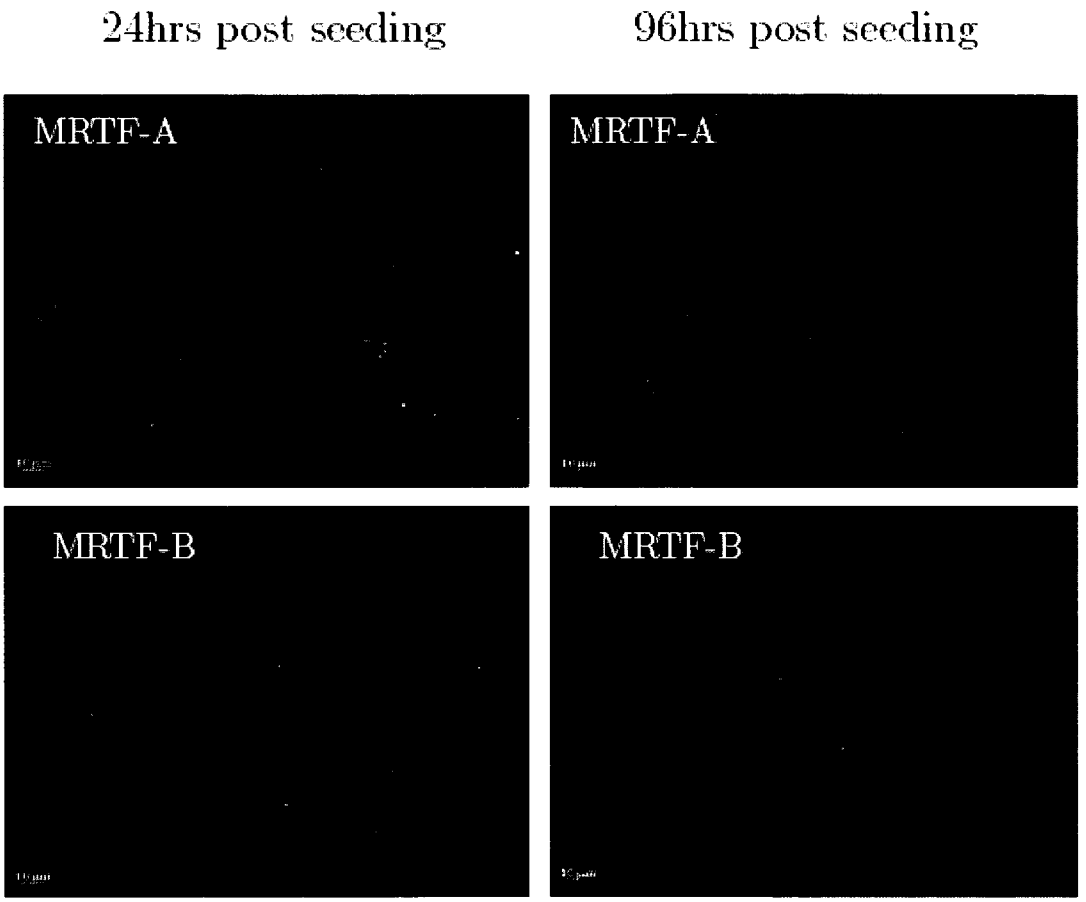

Figure 3.39. MRTF-A localization in subconfluent and confluent cell cultures. HUVECs were fixed either 24hr or 96hr post seeding. The distribution of endogenous MRTF-A and MRTF-B was determined using anti-MRTF-A and anti-MRTF-B antibodies. Nuclei were stained with DAPI.

(Busche et al., 2008). We wanted to test whether the disassembly of adherens junctions through calcium removal would be sufficient to trigger MRTF-A nuclear translocation in HUVECs. HUVECs were grown to confluence and the cells were treated with EGTA to chelate the calcium from the extracellular media to disrupt adherens junctions. Cells were fixed at different time points after the addition of DMEM-EGTA in order to monitor MRTF-A localization during adherens junction dissociation.

In a parallel experiment, cells were treated with EGM-2-EGTA for 40 mins to allow complete dissolution of adherens junctions. The media on the cells was then replaced with complete EGM-2 media in order to allow for junction reformation. Cells were fixed at different time points after media change in order to monitor MRTF-A localization during junction reformation. As a control, adherens junctions were left intact and fixed at the same time points as above. MRTF-A sub-cellular localization as well as VE cadherin distribution was assessed by immunofluoresence. Nuclear MRTF-A was detected in a few cells 15 mins after junction reformation (Figure 3.41). Also, 30 mins after the dissolution of adherens junctions, nuclear and intermediate MRTF-A was detected in a number of cells (Figure 3.40). MRTF-A appeared to be predominantly cytoplasmic at the remainder of time points during junction dissolution (Figure 3.40) as well as junction reformation (Figure 3.41). This indicates that the disruption of adherens junctions may trigger MRTF-A nuclear translocation.

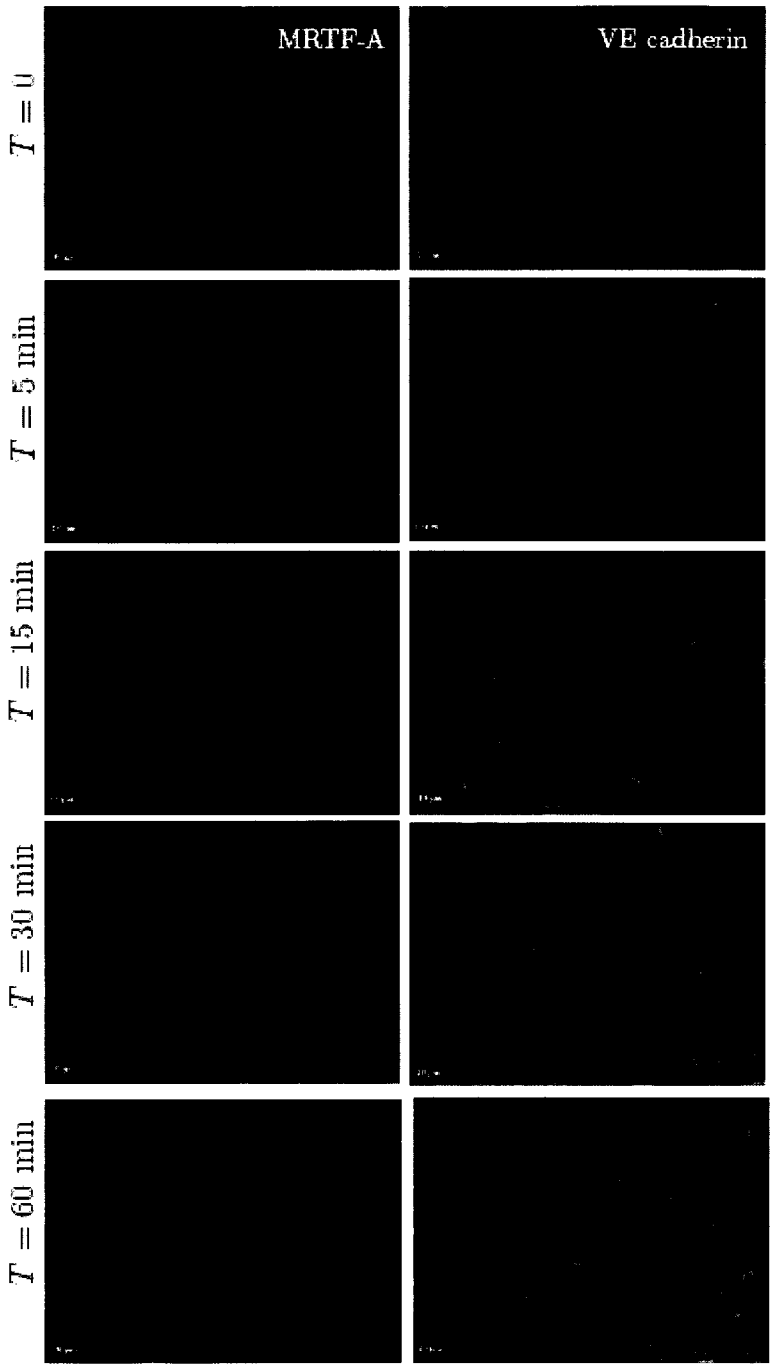

Figure 3.40 MRTF-A activation in response to formation of adherens junctions. Adherens junctions of a confluent cell monolayer were disrupted using 4mM EGTA and allowed to reform by reintroducing DMEM containing calcium. MRTF-A localization was monitered 5min, 15min, 30min and 60min after addition of calcium.

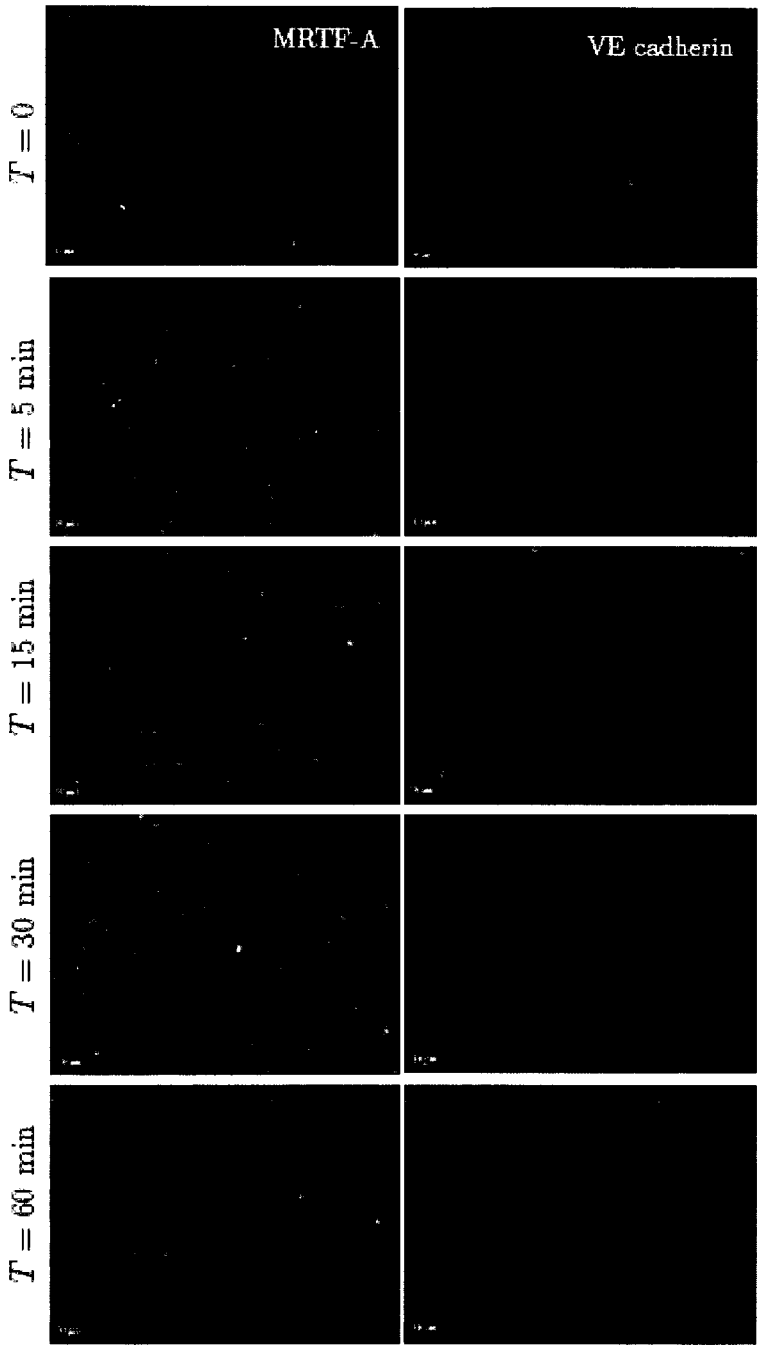

Figure 3.41. MRTF-A activation in response to dissolution of adherens junctions.

Adherens junctions of a confluent cell monolayer were disrupted using 4mM EGTA. MRTF-A localization was monitered 5min, 15min, 30min and 60min after addition of EGTA.

Part II: Requirement of MRTF-A in Endothelial Cell Migration

Aside from looking at the involvement of MRTF-A in shear induced cytoskeletal remodeling, we investigated the role of MRTF-A in cell migration. HUVECs were infected with either an adenovirus expressing a DN MRTF-A lacking the basic regions necessary for nuclear translocation (as described previously) or an adenovirus expressing GFP (AdGFP) as a control. Cell monolayers were wounded 48hrs after adenoviral infection and incubated for twenty nine hours after wounding to allow for wound closure. Localization of endogenous MRTF-A as well as adenoviral DN MRTF-A was assessed by immunofluoresence. AdGFP infected as well as uninfected cells migrated into the wounded area (Figure 3.42). In contrast, cells infected with adenovirus expressing the DN MRTF-A construct were unable to migrate into the wound (Figure 3.42). This suggests that MRTF-A is required for endothelial cell migration. MRTF-A sub-cellular localization in the different regions of the wound was investigated in uninfected cells. Sub-cellular localization of endogenous MRTF-A was assessed by immunofluoresence. MRTF-A was found to be nuclear exclusively in the first few rows of cells at the very edge of the wound. In contrast, MRTF-A was predominantly cytoplasmic in cells located in the unwounded area (Figure 3.43).

In an effort to further investigate the involvement of MRTF-A in cell migration, we attempted to determine whether cells expressing the DN MRTF-A construct were able to form capillary networks when plated on matrigel. As above, cells were infected with either adenovirus expressing DN MRTF-A, adenovirus expressing GFP or left uninfected. 48hrs later, cells were trypsinized and re-seeded onto matrigel and left to form capillary networks for 24 hrs before fixing. Cells expressing DN MRTF-A were

still able to form capillary networks. These networks, however, were denser (cells more tightly packed together) in comparison to networks formed by uninfected and GFP expressing cells (Figure 3.44). This may indicate a defect in cell migration in DN MRTF-A expressing cells. However, this defect is less manifested than that seen in the scratch wound model.

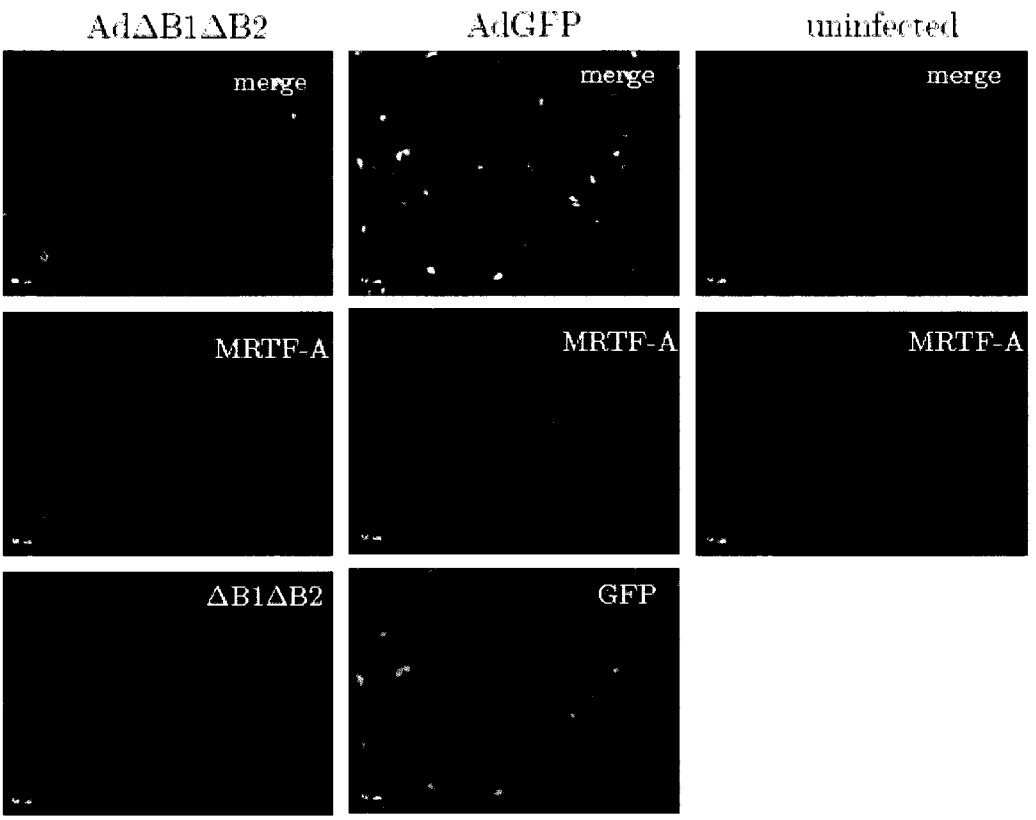

Figure 3.42. MRTF-AΔB1ΔB2 infected HUVEC are unable to migrate into wound.

HUVEC grown to confluence and either left uninfected or infected with AdGFP or DN.MRTF-A (MRTF-AΔB1ΔB2) expressing virus. Infected cells were left to accumulate viral protein for 48hrs and both infected and uninfected cells were subsequently wounded with a pipette tip and fixed 29hrs after wounding.

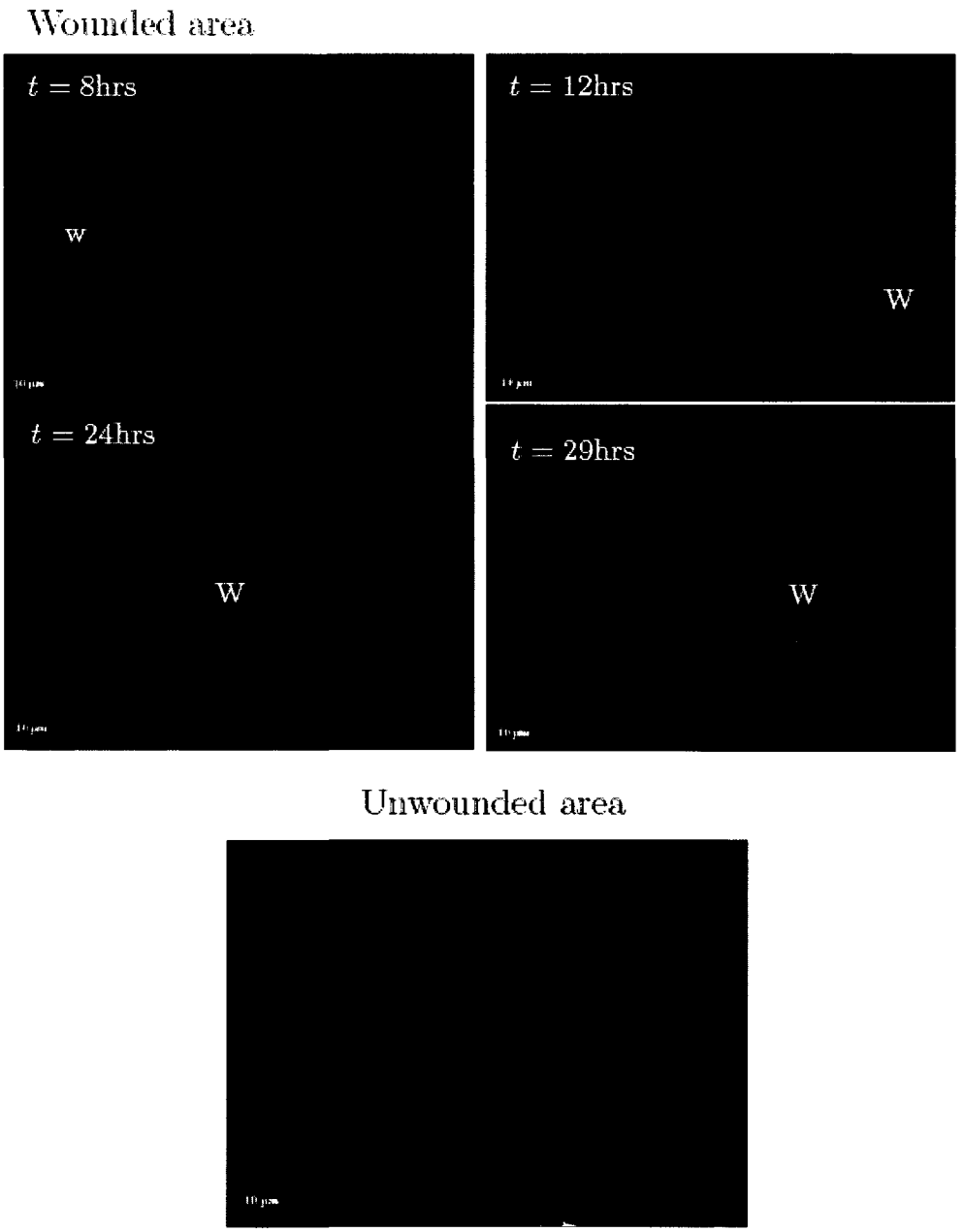

Figure 3.43. MRTF-A is activated in cells migrating towards the wound. HUVEC were grown to confluence and wounded with a pipette tip. Cells were fixed 8hrs, 12hrs, 24hrs and 29hrs after wounding. Endogenous MRTF-A was detected using anti MRTF-A antibody (red). The wounded area is indicated by (w).

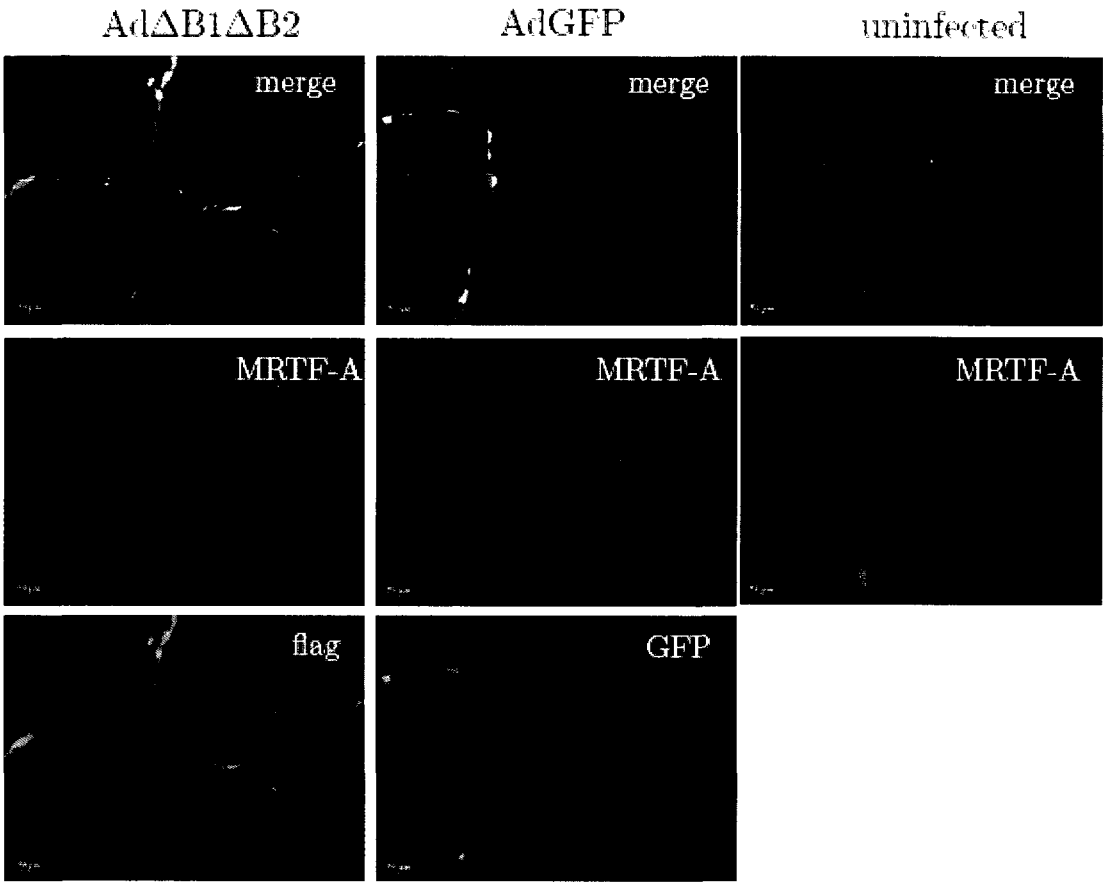

Figure 3.44. Effect of MRTF-AΔB1ΔB2 on formation of capillary networks
HUVEC were infected with adenovirus expressing either DN MRTF-A (MRTF-AΔB1ΔB2), control virus expressing GFP or left uninfected. Cells were left to accumulate viral protein for 48hrs before being trypsinized and reseeded onto matrigel. Cells were fixed 24hrs after seeding onto matrigel.

Chapter 4: Discussion

Part I: Shear Stress, MRTF Nuclear Translocation and Cytoskeletal Remodeling

The SRF cofactor MRTF-A has been shown to be necessary for several tension/force associated processes of development such as load induced muscle hypertrophy and border cell migration during Drosophila oogenesis. MRTF-A dependent SRF transcription gives rise to proteins that enable the cell to withstand force/tension. This leads us to believe that MRTF-A may be required for cytoskeletal remodeling in HUVECs enabling these cells to withstand the forces of shear.

We were able to show that after the application of 3 hrs of shear stress, MRTF-A nuclear accumulation is seen in about 65% of the cells subjected to shear stress. Shear stress also induced nuclear accumulation of MRTF-B although its translocation was weaker than that of MRTF-A (about 14% of cells subjected to shear stress). Serum stimulation of NIH 3T3 cells induces nuclear translocation of MRTF-B to a similar extent as that seen in HUVECs in response to flow (Morita el al, 2007).

MRTF-A and MRTF-B are suggested to be functionally redundant as both MRTF-A and MRTF-B function must be blocked in order to inhibit MRTF/SRF signalling (Cen at al., 2003). For this reason, it would be interesting to see whether MRTF-B would translocate to the nucleus to a greater extent in response to shear stress if we were to knockdown MRTF-A expression in HUVECs using siRNA.

Nuclear localization of MRTF-A is not necessarily synonymous with SRF activation. MAL nuclear accumulation induced by blocking the activity of Crm-1 nuclear exportin through leptomycin B treatment does not result in the activation of an SRF reporter gene nor does it activate the expression of MRTF-A dependent SRF genes

(Vartiainen et al., 2007). In addition, MRTF-A dependent gene transcription is transient in contrast to MRTF-A nuclear localization which can persist for several hours long after gene transcription has ceased. This suggests that there are additional regulatory mechanisms that control MRTF-A/SRF dependent gene transcription.

The expression of MRTF-A-NLS potentiates gene activation when co-expressed with wild type MRTF-A RPEL motif, but not when co-expressed with a mutant RPEL motif unable to bind actin (Vartiainen et al., 2007). This suggests that the activity of MRTF-A-NLS is repressed by actin. This repression appears to be at the level of transcription as apposed to DNA binding since ChIP studies show that leptomycin B treatment substantially increases MRTF-A recruitment to the promoters of target genes (Vartiainen et al., 2007). Therefore, in order to confirm whether MRTF-A nuclear localization is synonymous with gene activation ChIP studies should be performed to pinpoint the gene promoters MRTF-A is being recruited to in response to shear stress. ChIP studies should also be followed by qRT-PCR for target genes in order to confirm that MRTF-A recruitment to the promoter parallels gene activation. The first genes to be tested for MRTF-A recruitment would include genes encoding cytoskeletal proteins such as β-actin and vinculin.

Many pathways activated by shear stress are either sustained or down regulated with prolonged shear stress application. We wished to investigate whether MRTF-A would remain nuclear or return to its original cytoplasmic distribution with the sustained application of shear stress. MRTF-A nuclear accumulation was seen following 4hrs of flow and was somewhat sustained after 6hrs of flow where MRTF-A was either nuclear or dispersed evenly throughout the cell in the majority of cells. At the longer time points

MRTF-A was almost exclusively cytoplasmic. Thus MRTF-A activation is initiated 4hrs after the onset of flow and is down regulated between 6 hrs and 8 hrs. It appears that MRTF-A activation is required at the beginning of shear stress application in order to mount the remodeling response that will reduce the tension exerted on the cell. Maintenance of the cytoskeletal phenotype induced by shear stress, however, does not seem to require MRTF-A activity. This allows us to speculate on the requirement for MRTF-A activation in the endothelium in vivo. Since MRTF-A is seen to be down-regulated following extended periods of flow, it can be predicted that MRTF-A will be cytoplasmic in the endothelium of blood vessels being subjected to laminar flow. A surprising observation was that cells subjected to extended periods of shear stress aligned perpendicular to the direction of flow. We are still uncertain as to why cells aligned in this manner. We were however able to rule out our experimental setup as a cause for this strange alignment since in both trials attempted where two different flow setups were used, perpendicular alignment was observed. Endothelial cells have been seen to align perpendicular to the direction of flow in other instances. Porcine aortic endothelial cells align perpendicular to the direction of flow when subjected to flow in narrow microfluidics channels (1.5 mm width) (B.L. Langille pers. comm.). In addition, the level of shear stress we were applying to the cells was on the lower end of physiological shear. Perhaps higher levels of shear stress are required to achieve full alignment of cells in the direction of flow.

We were unable to obtain consistent results when cells were subjected to oscillating flow. This is largely due to technical difficulties associated with apparatus assembly. It would be expected however, that oscillating flow would cause the

continuous activation of MRTF-A resulting in MRTF-A nuclear localization. Indeed, immunofluoresence (using anti-MRTF-A antibody) performed on a section of a mouse artery subjected to turbulent flow showed nuclear localization of MRTF-A in most cells (Langille B.L pers. comm.).

Small molecule inhibitors were used to determine what signalling pathways act upstream to induce MRTF-A nuclear translocation. The inhibition of ROCK activity had the most dramatic effect in terms of inhibiting shear induced MRTF-A nuclear translocation and cytoskeletal remodeling implying that ROCK is an essential component acting upstream of the MRTF-A/SRF pathway in HUVECs. Exposing cells to shear stress in the presence of PI-3 kinase, and myosin II inhibitors resulted in a significant decrease in the number of cells with nuclear MRTF-A. However, MRTF-A nuclear translocation was not completely inhibited. Furthermore, cytoskeletal remodeling decreased significantly. These results are consistent with what is known about the MRTF-A/SRF pathway in fibroblasts where ROCK plays a crucial role in activation of the pathway and PI-3 kinase and myosin II have both been identified as upstream factors contributing to MRTF activation.

GSK-3β activity is required for proper cell elongation in response to flow as well as realignment in the direction of flow (McCue et al., 2006). Subjecting cells to shear stress in the presence of LiCl, an inhibitor of GSK-3β, prevented cytoskeletal remodeling and resulted in a significant decrease in the number of cells with nuclear MRTF-A. This suggests that GSK-3β is involved in shear induced cytoskeletal remodeling and plays a role upstream of MRTF-A in the MRTF-A/SRF pathway.

Rac1 inhibitor (NSC23766) had no effect on shear induced MRTF-A nuclear translocation and shear induced cytoskeletal remodeling remained intact. This indicates that the activation of the MRTF-A/SRF pathway in HUVECs is independent of Rac1 activity. However, we cannot exclude a peripheral role for Rac1 in the activation of the MRTF-A/SRF pathway based on these results. These results are consistent with what is known about the role of Rac1 in the MRTF-A/SRF pathway in fibroblasts where the expression of DN Rac1 does not affect serum or LPA-induced SRF transcriptional activation (Hill et al., 1995).

It is known that in fibroblasts, MRTF-A dependent SRF activation occurs independently of MAP kinases and MEK signalling (Treisman and Gineitis, 2001). This was also what we observed in HUVECs since the use of MEK inhibitor (U0126) did not affect shear induced MRTF-A nuclear translocation or cytoskeletal remodeling.

Further experiments using inhibitors of other components known to be important in the MRTF-A/SRF pathway in fibroblasts will have to be conducted to further delineate the pathway in HUVECs. Follow up experiments would include using TAT-C3 in the presence of flow to determine the involvement of Rho in shear induced MRTF-A nuclear localization and cytoskeletal remodeling. The TAT peptide permits cell permeability and the *Clostridium botulinum* exotoxin C3 inactivates Rho by ADP ribosylation.

Experiments previously conducted in our lab tested the involvement of formin proteins (effectors of RhoGTPase) in shear induced stress fiber formation and MRTF-A nuclear translocation. Infecting cells with a DN form of the formin Dia1 and subjecting these cells to shear stress did not inhibit MRTF-A nuclear translocation. However,

cytoskeletal remodeling was somewhat affected. Stress fiber formation did occur but was very minimal and the stress fibers that did form appeared significantly thinner than those in uninfected cells (Gaudet BM., pers. comm.). Expression of the DN Dia1 construct used in these experiments inhibits the activity of all previously tested formins (Copeland et al., 2004) due to its ability to bind to the barbed end of the actin filament as a monomer and prevent further polymerization. It would be interesting to see whether diaphanous related formins (DRF) other than those presumably inhibited by DN Dia1 are involved in shear induced cytoskeletal remodeling and MRTF-A nuclear translocation. A study by Gasteier et al. shows that a constitutively active form of the DRF FHOD1 (FHOD1ΔC) induced stress fiber formation as well as cell elongation (2005). These processes appear to be Rho/ROCK dependent in both HeLa and NIH3T3 cells (Gasteier et al., 2005, Gasteier et al., 2003). Inhibiting Rho function by overexpressing C3 trasnferase abolished FHOD1ΔC induced stress fiber formation. Moreover, ROCK inhibition using the ROCK inhibitor Y27632 also prevented FHOD1ΔC induced stress fiber formation. In contrast, DN Rac1 (N17Rac) was not able to block FHOD1ΔC induced stress fiber formation in HeLa cells (Gasteier et al., 2005). These data suggest a possible role for FHOD1 is shear induced cytoskeletal remodeling.

The results from our inhibitor studies along with recent findings in the literature allow us to propose a pathway through which shear stress activates MRTF-A/SRF dependent transcription. The onset of shear stress activates a shear receptor (other than PECAM-1) initiating downstream signaling leading to the activation of RhoA. RhoA in turn phosphorylates and activates its downstream target ROCK. Downstream of ROCK there are 3 candidate pathways that cooperate to activate MRTF-A/SRF. From our

inhibitor results it appears that ROCK and myosin II play an important role in shear induced MRTF-A nuclear localization and cytoskeletal remodeling. In fibroblasts, the active form of RhoA binds to and phosphorylates ROCK leading to its activation. ROCK acts either through phosphorylating myosin light chain (MLC) phosphatase thus increasing MLC phosphorylation or through LIM kinase where ROCK binds to and phosphorylates LIM kinase which in turn phosphorylates cofilin resulting in its inactivation. The inactivation of MLC phosphatase and subsequent increase in MLC phosphorylation is a prerequisite for stress fiber formation and increased cell contractility whereas inactivating cofilin leads to F-actin stabilization. Both roles mediated by ROCK appear important in shear induced cytoskeletal remodeling in endothelial cells.

We also propose a possible role for the formin FHOD1 in the activation of the MRTF-A/SRF pathway in endothelial cells in response to shear stress. ROCK has been shown to phosphorylate FHOD1 in endothelial cells at 3 residues found in the C terminus of the molecule. Phosphorylation of the C terminus of FHOD1 appears to relieve the molecule from the intermolecular N-C terminal autoinhibitory interaction. The involvement of FHOD1 in shear induced cytoskeletal remodeling can be assessed by knockdown of FHOD1 using siRNA and subjecting knockdown cells to shear stress. However, in the presence of two other cooperative pathways (myosin II and LIM kinase), it is difficult to tell whether the knocking down FHOD1 would have any effect on shear induced cytoskeletal remodeling.

The simple model of MRTF-A/SRF activation entails that MRTF-A is directly regulated by the G-actin pool. Increased amount of G-actin inhibit MRTF-A whereas the depletion of G-actin allows for nuclear localization of MRTF-A . This simple model however, does

not fit in the current proposed mechanism of MRTF-A activation by shear stress. MRTF-A is most probably regulated by a sub population of actin or actin protein complex which accumulates in response to the application of shear stress. The presence of this actin sub-population allows MRTF-A nuclear localization and MRTF-A/SRF dependent gene transcription (Figure 4.1). We are still uncertain as to which MRTF-A/SRF specific genes are activated in response to shear stress. However, it is likely that genes encoding cytoskeletal proteins such as β-actin and vinculin are up-regulated.

In order to determine whether MRTF-A is required for shear induced cytoskeletal remodeling, a dominant negative MRTF-A construct was used. An adenoviral vector expressing this construct was obtained from Dr. Robin Parks. This dominant negative construct dimerizes with endogenous MRTF-A and B and prevents their nuclear translocation. Expression of DN MRTF-A had a moderate effect on actin remodeling where infected cells in some areas had a less robust actin phenotype than uninfected or control cells. Unfortunately, control cells were not efficiently infected with a control adenovirus expressing GFP making it difficult to exclude that the observed effects on cell morphology were caused by the infection itself.

We sought to investigate possible mechanoreceptors functioning to activate the signalling cascade leading to MRTF-A nuclear translocation. We first tested PECAM-1 which is an essential component of the mechanosensory complex formed in association with VEGFR2 and VE-cadherin in endothelial cells (Tzima el al., 2005). PECAM-1 was knocked down in HUVECs using siRNA and cells were subjected to shear stress. MRTF-A nuclear translocation was not significantly different from that seen in untreated cells and cytoskeletal remodeling was still evident. This suggests that shear-induced MRTF-A

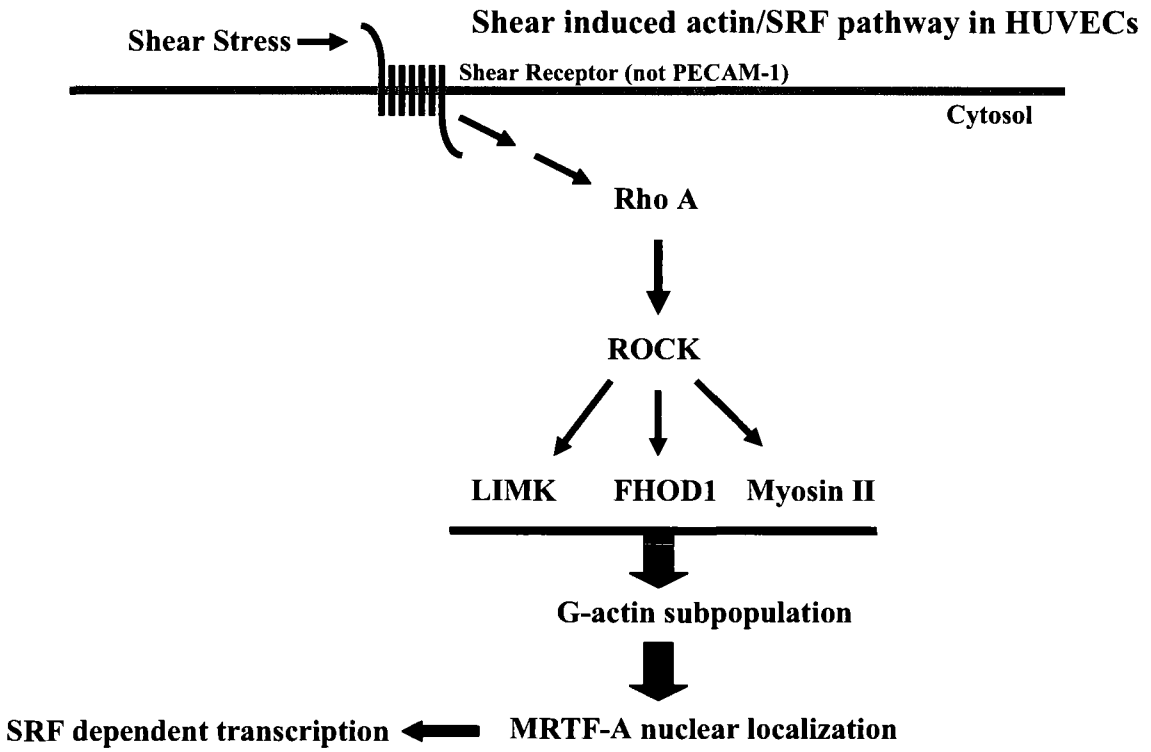

Figure 4.1. Proposed pathway for shear induced MRTF-A/SRF activation. The proposed pathway suggests that MRTF-A is induced through a Rho-A/ROCK dependent pathway. Downstream of ROCK LIM kinase, FHOD1 and myosin II cooperatively induce F-actin and stress fiber formation leading to MRTF-A nuclear localization.

nuclear translocation is independent of PECAM-1 and that there must be another mechanoreceptor acting upstream of this pathway. Possible candidates could include integrins, G-protein coupled receptors, and heterotrimeric G-proteins, all of which have been suggested to be mechanosensors activated in response to shear stress.

In order to further investigate possible receptors acting at the level of the membrane, we used magnetic beads coupled to known receptor ligands. PECAM-1 antibody and an integrin ligand, the RGD peptide, were coupled to magnetic beads. HUVECs were incubated with these ligand-coupled beads and exposed to a constant lateral magnetic force. Subjecting cells to 2hrs and 4hrs of magnetic force did not affect MRTF-A localization which remained predominantly cytoplasmic. This further confirms that MRTF-A nuclear translocation occurs independently of PECAM-1 activation. Moreover, MRTF-A nuclear translocation seems to be independent of integrin activation. One caveat to the interpretation of these results is the lack of a positive control (e.g. phosphorylation of ERK1/2) to confirm that the magnetic beads actually exerted mechanical force on our cells.

We noticed in our static controls that sub-confluent areas of culture slides showed on average more cells with nuclear MRTF-A than confluent areas. In order to confirm that cell density affects MRTF-A sub-cellular localization, we examined MRTF-A sub-cellular localization in sub-confluent (24 hours after plating) and confluent (96 hours) cultures. It was evident that when cells were sub-confluent (24hr time point), the number of cells with nuclear MRTF-A was higher than that in post confluent cultures. A possible explanation for these results is that when cells are subconfluent, they can migrate freely

thus activating the MRTF-A/SRF pathway. However, a more likely explanation for the nuclear localization of MRTF-A in subconfluent cells is the absence of contact inhibition.

This hypothesis was supported by a study showing that disrupting cell-cell junctions in epithelial cells through calcium removal was enough to induce MRTF-A nuclear translocation and SRF activation (Fan et al., 2007, Busche et al., 2008). In order to test this hypothesis in endothelial cells, we performed a "calcium switch" assay where HUVECs were grown until post confluent and MRTF-A localization was monitored while cell-cell contacts were disrupted (by adding EGTA) and while they were reformed (by removing EGTA from medium and adding back calcium). MRTF-A remained cytoplasmic at the majority of time points following contact dissolution and contact reformation. Unlike epithelial cells, disruption of adherens junctions is not sufficient to induce MRTF-A activation, although we cannot rule out that disruption of the adherens junctions during shear induced cytoskeletal remodeling may play a permissive role in the pathway.

Part II: MRTF-A and Angiogenesis

The process of angiogenesis involves multiple steps including invasion, migration, and differentiation. It has been shown previously that knocking down SRF in HUVECs resulted in a reduction in migration in a scratch wound assay (Chai et al., 2004). We investigated the role of the SRF cofactor MRTF-A in cell migration by means of a scratch wound assay. In this assay, HUVECs were grown to confluence and the cell monolayer was wounded with a pipet tip and left for 29hrs before fixing and staining. We were able to show that MRTF-A was activated in actively migrating cells at the wound periphery. In contrast, MRTF-A remained cytoplasmic in cells that were further away from the wound edge.

In order to assess the necessity of MRTF-A for cell migration in HUVECs, cells were infected with adenoviral vectors expressing either DN MRTF-A (ΔB1ΔB2) or GFP 48hrs after seeding. Cell monolayers were wounded 48hrs after viral infection. Cells infected with Ad ΔB1ΔB2 failed to migrate and the wound remained open. Cells infected with AdGFP were able to migrate but at a slower rate than uninfected cells. This suggests that adenoviral infection may itself have an affect on motility. These results contradict reports that adenoviral infection accelerates HUVEC motility. Our results do, however, show that ΔB1ΔB2 infected cells fail to migrate at all which suggests that MRTF-A is required for HUVEC migration. An interesting observation was that a high proportion of cells fixed 29hrs after wounding displayed nuclear MRTF-A despite still being infected with DN MRTF-A which is supposed to sequester endogenous MRTF-A in the cytoplasm. In contrast, cells fixed at earlier time points (8hrs after wounding) displayed predominantly cytoplasmic MRTF-A. It is possible that the expression of adenoviral

protein is down-regulated after an extended period following infection. Also, MRTF-A (ΔB1ΔB2) is known to cause only a 70% inhibition of reporter gene activation. Therefore, it would be expected to see cells where MRTF-A is nuclear. Since MRTF-A (ΔB1ΔB2) works by competitive inhibition, it is also possible that monolayer wounding up-regulates MRTF-A transcription preventing DN MRTF-A from efficient inhibition of endogenous MRTF-A.

A matrigel assay was performed with Ad ΔB1ΔB2 and Ad GFP infected cells to follow up on the results of the scratch wound assay. Ad ΔB1ΔB2, Ad GFP infected cells, and uninfected cells were all able to form capillary networks when plated onto matrigel. The networks formed by Ad ΔB1ΔB2 infected cells were denser where each capillary was formed of more tightly packed cells than networks formed by Ad GFP infected and uninfected cells. This may result from the defects in cell motility induced by Ad ΔB1ΔB2 expression resulting in the cells remaining clumped together on the matrigel and unable to spread out to form thin capillary networks.

Conclusion

We were able to show that MRTF-A translocates to the nucleus in response to shear stress. Nuclear translocation of MRTF-A occurs concomitantly with cell elongation and stress fiber formation. These changes in cell morphology are thought to be required to enable endothelial cells to withstand the forces associated with flow-induced shear. MRTF-A translocates to the nucleus within 4hrs of shear application and is then down regulated between 6 and 8hrs of shear application. ROCK was shown to be required for shear induced MRTF-A nuclear translocation and cytoskeletal remodeling. PI-3 kinase, myosin II and GSK-3β also contribute to activation of the pathway. Gasteier et al. have shown that a CA form of FHOD1 induces stress fiber formation and cell elongation through the Rho/ROCK pathway (2005). In light of these results, we favour a model where shear induced MRTF-A nuclear translocation in HUVECs occurs through a Rho-ROCK-(FHOD1-mysoin II- LIM kinase) pathway and that dissolution of adherens junctions could serve as a permissive signal.

Our findings could be clinically applied to screen for individuals predisposed to atherosclerosis. Individuals having mutations in MRTF-A and MRTF-B could potentially be at a higher risk for developing atherosclerosis since cells would be unable to mount the remodeling response typical of endothelial cells subjected to shear stress and would hence resemble cells subjected to turbulent flow.

References

Alberts, B., Johnson, A., Lewis, J., Raff, M., Roberts, K. and Walter, P. (2002). Molecular Biology of The Cell. (Fourth Edition). New York: Garland Science.

Arsenian, S., Weinhold, B., Oelgeschlager, M., Ruther, U. and Nordheim, A. (1998). Serum response factor is essential for mesoderm formation during mouse embryogenesis. *EMBO J.* **17,** 6289-6299.

Auerbach, R., Lewis, R., Shinners, B., Kubai, L. and Akhtar, N. (2003). Angiogenesis assays: A critical overview. *Clin. Chem.* **49,** 32-40.

Azuma, N., Akasaka, N., Kito, H., Ikeda, M., Gahtan, V., Sasajima, T. and Sumpio, B. E. (2001). Role of p38 MAP kinase in endothelial cell alignment induced by fluid shear stress. *Am. J. Physiol. Heart Circ. Physiol.* **280,** H189-97.

Azuma, N., Duzgun, S. A., Ikeda, M., Kito, H., Akasaka, N., Sasajima, T. and Sumpio, B. E. (2000). Endothelial cell response to different mechanical forces. *J. Vasc. Surg.* **32,** 789-794.

Busche, S., Descot, A., Julien, S., Genth, H. and Posern, G. (2008). Epithelial cell-cell contacts regulate SRF-mediated transcription via rac-actin-MAL signalling. *J. Cell. Sci.* **121,** 1025-1035.

Cen, B., Selvaraj, A., Burgess, R. C., Hitzler, J. K., Ma, Z., Morris, S. W. and Prywes, R. (2003). Megakaryoblastic leukemia 1, a potent transcriptional coactivator for serum response factor (SRF), is required for serum induction of SRF target genes. *Mol. Cell. Biol.* **23,** 6597-6608.

Cen, B., Selvaraj, A. and Prywes, R. (2004). Myocardin/MKL family of SRF coactivators: Key regulators of immediate early and muscle specific gene expression. *J. Cell. Biochem.* **93,** 74-82.

Chachisvilis, M., Zhang, Y. L. and Frangos, J. A. (2006). G protein-coupled receptors sense fluid shear stress in endothelial cells. *Proc. Natl. Acad. Sci. U. S. A.* **103,** 15463-15468.

Chai, J., Jones, M. K. and Tarnawski, A. S. (2004). Serum response factor is a critical requirement for VEGF signalling in endothelial cells and VEGF-induced angiogenesis. *FASEB J.* **18,** 1264-1266.

Chhabra, E. S. and Higgs, H. N. (2007). The many faces of actin: Matching assembly factors with cellular structures. *Nat. Cell Biol.* **9,** 1110-1121.

Chien, S. (2008). Effects of disturbed flow on endothelial cells. *Ann. Biomed. Eng.* **36,** 554-562.

Chien, S. (2008). Role of shear stress direction in endothelial mechanotransduction. *Mol. Cell. Biomech.* **5,** 1-8.

Copeland, J. W., Copeland, S. J. and Treisman, R. (2004). Homo-oligomerization is essential for F-actin assembly by the formin family FH2 domain. *J. Biol. Chem.* **279,** 50250-50256.

Copeland, J. W. and Treisman, R. (2002). The diaphanous-related formin mDia1 controls serum response factor activity through its effects on actin polymerization. *Mol. Biol. Cell* **13,** 4088-4099.

Davies, P. F. (1995). Flow-mediated endothelial mechanotransduction. *Physiol. Rev.* **75,** 519-560.

Evelyn, C. R., Wade, S. M., Wang, Q., Wu, M., Iniguez-Lluhi, J. A., Merajver, S. D. and Neubig, R. R. (2007). CCG-1423: A small-molecule inhibitor of RhoA transcriptional signalling. *Mol. Cancer. Ther.* **6,** 2249-2260.

Fan, L., Sebe, A., Peterfi, Z., Masszi, A., Thirone, A. C., Rotstein, O. D., Nakano, H., McCulloch, C. A., Szaszi, K., Mucsi, I. et al. (2007). Cell contact-dependent regulation of epithelial-myofibroblast transition via the rho-rho kinase-phospho-myosin pathway. *Mol. Biol. Cell* **18,** 1083-1097.

Flaherty, J. T., Pierce, J. E., Ferrans, V. J., Patel, D. J., Tucker, W. K. and Fry, D. L. (1972). Endothelial nuclear patterns in the canine arterial tree with particular reference to hemodynamic events. *Circ. Res.* **30,** 23-33.

Folgering, J. H., Sharif-Naeini, R., Dedman, A., Patel, A., Delmas, P. and Honore, E. (2008). Molecular basis of the mammalian pressure-sensitive ion channels: Focus on vascular mechanotransduction. *Prog. Biophys. Mol. Biol.* **97,** 180-195.

Franco, C. A., Mericskay, M., Parlakian, A., Gary-Bobo, G., Gao-Li, J., Paulin, D., Gustafsson, E. and Li, Z. (2008). Serum response factor is required for sprouting angiogenesis and vascular integrity. *Dev. Cell.* **15,** 448-461.

Frangos, J. A., McIntire, L. V. and Eskin, S. G. (1988). Shear stress induced stimulation of mammalian cell metabolism. *Biotechnol. Bioeng.* **32,** 1053-1060.

Fraser, A. G., Kamath, R. S., Zipperlen, P., Martinez-Campos, M., Sohrmann, M. and Ahringer, J. (2000). Functional genomic analysis of C. elegans chromosome I by systematic RNA interference. *Nature* **408,** 325-330.

Fujiwara, K., Masuda, M., Osawa, M., Kano, Y. and Katoh, K. (2001). Is PECAM-1 a mechanoresponsive molecule? *Cell Struct. Funct.* **26,** 11-17.

Gasteier, J. E., Madrid, R., Krautkramer, E., Schroder, S., Muranyi, W., Benichou, S. and Fackler, O. T. (2003). Activation of the rac-binding partner FHOD1 induces actin stress fibers via a ROCK-dependent mechanism. *J. Biol. Chem.* **278,** 38902-38912.

Gasteier, J. E., Schroeder, S., Muranyi, W., Madrid, R., Benichou, S. and Fackler, O. T. (2005). FHOD1 coordinates actin filament and microtubule alignment to mediate cell elongation. *Exp. Cell Res.* **306,** 192-202.

Geneste, O., Copeland, J. W. and Treisman, R. (2002). LIM kinase and diaphanous cooperate to regulate serum response factor and actin dynamics. *J. Cell Biol.* **157,** 831-838.

Gineitis, D. and Treisman, R. (2001). Differential usage of signal transduction pathways defines two types of serum response factor target gene. *J. Biol. Chem.* **276,** 24531-24539.

Gudi, S., Nolan, J. P. and Frangos, J. A. (1998). Modulation of GTPase activity of G proteins by fluid shear stress and phospholipid composition. *Proc. Natl. Acad. Sci. U. S. A.* **95,** 2515-2519.

Guillemin, K., Groppe, J., Ducker, K., Treisman, R., Hafen, E., Affolter, M. and Krasnow, M. A. (1996). The pruned gene encodes the drosophila serum response factor and regulates cytoplasmic outgrowth during terminal branching of the tracheal system. *Development* **122,** 1353-1362.

Han, Z., Li, X., Wu, J. and Olson, E. N. (2004). A myocardin-related transcription factor regulates activity of serum response factor in drosophila. *Proc. Natl. Acad. Sci. U. S. A.* **101,** 12567-12572.

Harada, N., Masuda, M. and Fujiwara, K. (1995). Fluid flow and osmotic stress induce tyrosine phosphorylation of an endothelial cell 128 kDa surface glycoprotein. *Biochem. Biophys. Res. Commun.* **214,** 69-74.

Harwood, A. J. (2001). Regulation of GSK-3: A cellular multiprocessor. *Cell* **105,** 821-824.

Hill, C. S., Wynne, J. and Treisman, R. (1995). The rho family GTPases RhoA, Rac1, and CDC42Hs regulate transcriptional activation by SRF. *Cell* **81,** 1159-1170.

Hinson, J. S., Medlin, M. D., Lockman, K., Taylor, J. M. and Mack, C. P. (2007). Smooth muscle cell-specific transcription is regulated by nuclear localization of the myocardin-related transcription factors. *Am. J. Physiol. Heart Circ. Physiol.* **292,** H1170-80.

Hoger, J. H., Ilyin, V. I., Forsyth, S. and Hoger, A. (2002). Shear stress regulates the endothelial Kir2.1 ion channel. *Proc. Natl. Acad. Sci. U. S. A.* **99,** 7780-7785.

Ishizaki, T., Maekawa, M., Fujisawa, K., Okawa, K., Iwamatsu, A., Fujita, A., Watanabe, N., Saito, Y., Kakizuka, A., Morii, N. et al. (1996). The small GTP-binding protein rho binds to and activates a 160 kDa Ser/Thr protein kinase homologous to myotonic dystrophy kinase. *EMBO J.* **15,** 1885-1893.

Jaffe, A. B. and Hall, A. (2005). Rho GTPases: Biochemistry and biology. *Annu. Rev. Cell Dev. Biol.* **21,** 247-269.

Jalali, S., del Pozo, M. A., Chen, K., Miao, H., Li, Y., Schwartz, M. A., Shyy, J. Y. and Chien, S. (2001). Integrin-mediated mechanotransduction requires its dynamic interaction with specific extracellular matrix (ECM) ligands. *Proc. Natl. Acad. Sci. U. S. A.* **98,** 1042-1046.

Kadohama, T., Akasaka, N., Nishimura, K., Hoshino, Y., Sasajima, T. and Sumpio, B. E. (2006). p38 mitogen-activated protein kinase activation in endothelial cell is implicated in cell alignment and elongation induced by fluid shear stress. *Endothelium* **13,** 43-50.

Li, F. and Higgs, H. N. (2003). The mouse formin mDia1 is a potent actin nucleation factor regulated by autoinhibition. *Curr. Biol.* **13,** 1335-1340.

Li, J., Zhu, X., Chen, M., Cheng, L., Zhou, D., Lu, M. M., Du, K., Epstein, J. A. and Parmacek, M. S. (2005). Myocardin-related transcription factor B is required in cardiac neural crest for smooth muscle differentiation and cardiovascular development. *Proc. Natl. Acad. Sci. U. S. A.* **102,** 8916-8921.

Li, S., Chang, S., Qi, X., Richardson, J. A. and Olson, E. N. (2006). Requirement of a myocardin-related transcription factor for development of mammary myoepithelial cells. *Mol. Cell. Biol.* **26,** 5797-5808.

Li, S., Czubryt, M. P., McAnally, J., Bassel-Duby, R., Richardson, J. A., Wiebel, F. F., Nordheim, A. and Olson, E. N. (2005). Requirement for serum response factor for skeletal muscle growth and maturation revealed by tissue-specific gene deletion in mice. *Proc. Natl. Acad. Sci. U. S. A.* **102,** 1082-1087.

Lin, T., Zeng, L., Liu, Y., DeFea, K., Schwartz, M. A., Chien, S. and Shyy, J. Y. (2003). Rho-ROCK-LIMK-cofilin pathway regulates shear stress activation of sterol regulatory element binding proteins. *Circ. Res.* **92,** 1296-1304.

Mack, C. P. and Hinson, J. S. (2005). Regulation of smooth muscle differentiation by the myocardin family of serum response factor co-factors. *J. Thromb. Haemost.* **3,** 1976-1984.

Mack, C. P., Somlyo, A. V., Hautmann, M., Somlyo, A. P. and Owens, G. K. (2001). Smooth muscle differentiation marker gene expression is regulated by RhoA-mediated actin polymerization. *J. Biol. Chem.* **276,** 341-347.

Maekawa, M., Ishizaki, T., Boku, S., Watanabe, N., Fujita, A., Iwamatsu, A., Obinata, T., Ohashi, K., Mizuno, K. and Narumiya, S. (1999). Signalling from rho to the actin cytoskeleton through protein kinases ROCK and LIM-kinase. *Science* **285,** 895-898.

McCue, S., Dajnowiec, D., Xu, F., Zhang, M., Jackson, M. R. and Langille, B. L. (2006). Shear stress regulates forward and reverse planar cell polarity of vascular endothelium in vivo and in vitro. *Circ. Res.* **98,** 939-946.

McCue, S., Noria, S. and Langille, B. L. (2004). Shear-induced reorganization of endothelial cell cytoskeleton and adhesion complexes. *Trends Cardiovasc. Med.* **14,** 143-151.

Miano, J. M. (2003). Serum response factor: Toggling between disparate programs of gene expression. *J. Mol. Cell. Cardiol.* **35,** 577-593.

Miralles, F., Posern, G., Zaromytidou, A. I. and Treisman, R. (2003). Actin dynamics control SRF activity by regulation of its coactivator MAL. *Cell* **113,** 329-342.

Mullins, R. D., Stafford, W. F. and Pollard, T. D. (1997). Structure, subunit topology, and actin-binding activity of the Arp2/3 complex from acanthamoeba. *J. Cell Biol.* **136,** 331-343.

Murai, K. and Treisman, R. (2002). Interaction of serum response factor (SRF) with the elk-1 B box inhibits RhoA-actin signalling to SRF and potentiates transcriptional activation by elk-1. *Mol. Cell. Biol.* **22,** 7083-7092.

Niu, Z., Yu, W., Zhang, S. X., Barron, M., Belaguli, N. S., Schneider, M. D., Parmacek, M., Nordheim, A. and Schwartz, R. J. (2005). Conditional mutagenesis of the murine serum response factor

gene blocks cardiogenesis and the transcription of downstream gene targets. *J. Biol. Chem.* **280,** 32531-32538.

Noria, S., Cowan, D. B., Gotlieb, A. I. and Langille, B. L. (1999). Transient and steady-state effects of shear stress on endothelial cell adherens junctions. *Circ. Res.* **85,** 504-514.

Noria, S., Xu, F., McCue, S., Jones, M., Gotlieb, A. I. and Langille, B. L. (2004). Assembly and reorientation of stress fibers drives morphological changes to endothelial cells exposed to shear stress. *Am. J. Pathol.* **164,** 1211-1223.

Norman, C., Runswick, M., Pollock, R. and Treisman, R. (1988). Isolation and properties of cDNA clones encoding SRF, a transcription factor that binds to the c-fos serum response element. *Cell* **55,** 989-1003.

Oh, J., Richardson, J. A. and Olson, E. N. (2005). Requirement of myocardin-related transcription factor-B for remodeling of branchial arch arteries and smooth muscle differentiation. *Proc. Natl. Acad. Sci. U. S. A.* **102,** 15122-15127.

Osawa, M., Masuda, M., Harada, N., Lopes, R. B. and Fujiwara, K. (1997). Tyrosine phosphorylation of platelet endothelial cell adhesion molecule-1 (PECAM-1, CD31) in mechanically stimulated vascular endothelial cells. *Eur. J. Cell Biol.* **72,** 229-237.

Osborn, E. A., Rabodzey, A., Dewey, C. F.,Jr and Hartwig, J. H. (2006). Endothelial actin cytoskeleton remodeling during mechanostimulation with fluid shear stress. *Am. J. Physiol. Cell. Physiol.* **290,** C444-52.

Pruyne, D., Evangelista, M., Yang, C., Bi, E., Zigmond, S., Bretscher, A. and Boone, C. (2002). Role of formins in actin assembly: Nucleation and barbed-end association. *Science* **297,** 612-615.

Rizzo, V., Morton, C., DePaola, N., Schnitzer, J. E. and Davies, P. F. (2003). Recruitment of endothelial caveolae into mechanotransduction pathways by flow conditioning in vitro. *Am. J. Physiol. Heart Circ. Physiol.* **285,** H1720-9.

Sagot, I., Rodal, A. A., Moseley, J., Goode, B. L. and Pellman, D. (2002). An actin nucleation mechanism mediated by Bni1 and profilin. *Nat. Cell Biol.* **4,** 626-631.

Schratt, G., Philippar, U., Berger, J., Schwarz, H., Heidenreich, O. and Nordheim, A. (2002). Serum response factor is crucial for actin cytoskeletal organization and focal adhesion assembly in embryonic stem cells. *J. Cell Biol.* **156,** 737-750.

Schratt, G., Philippar, U., Berger, J., Schwarz, H., Heidenreich, O. and Nordheim, A. (2002). Serum response factor is crucial for actin cytoskeletal organization and focal adhesion assembly in embryonic stem cells. *J. Cell Biol.* **156,** 737-750.

Schratt, G., Weinhold, B., Lundberg, A. S., Schuck, S., Berger, J., Schwarz, H., Weinberg, R. A., Ruther, U. and Nordheim, A. (2001). Serum response factor is required for immediate-early gene activation yet is dispensable for proliferation of embryonic stem cells. *Mol. Cell. Biol.* **21,** 2933-2943.

Schratt, G., Weinhold, B., Lundberg, A. S., Schuck, S., Berger, J., Schwarz, H., Weinberg, R. A., Ruther, U. and Nordheim, A. (2001). Serum response factor is required for immediate-early gene activation yet is dispensable for proliferation of embryonic stem cells. *Mol. Cell. Biol.* **21,** 2933-2943.

Selvaraj, A. and Prywes, R. (2003). Megakaryoblastic leukemia-1/2, a transcriptional co-activator of serum response factor, is required for skeletal myogenic differentiation. *J. Biol. Chem.* **278,** 41977-41987.

Shay-Salit, A., Shushy, M., Wolfovitz, E., Yahav, H., Breviario, F., Dejana, E. and Resnick, N. (2002). VEGF receptor 2 and the adherens junction as a mechanical transducer in vascular endothelial cells. *Proc. Natl. Acad. Sci. U. S. A.* **99,** 9462-9467.

Smith, M. L., Long, D. S., Damiano, E. R. and Ley, K. (2003). Near-wall micro-PIV reveals a hydrodynamically relevant endothelial surface layer in venules in vivo. *Biophys. J.* **85,** 637-645.

Somogyi, K. and Rorth, P. (2004). Evidence for tension-based regulation of drosophila MAL and SRF during invasive cell migration. *Dev. Cell.* **7,** 85-93.

Sotiropoulos, A., Gineitis, D., Copeland, J. and Treisman, R. (1999). Signal-regulated activation of serum response factor is mediated by changes in actin dynamics. *Cell* **98,** 159-169.

Sumpio, B. E., Yun, S., Cordova, A. C., Haga, M., Zhang, J., Koh, Y. and Madri, J. A. (2005). MAPKs (ERK1/2, p38) and AKT can be phosphorylated by shear stress independently of platelet endothelial cell adhesion molecule-1 (CD31) in vascular endothelial cells. *J. Biol. Chem.* **280,** 11185-11191.

Sun, Y., Boyd, K., Xu, W., Ma, J., Jackson, C. W., Fu, A., Shillingford, J. M., Robinson, G. W., Hennighausen, L., Hitzler, J. K. et al. (2006). Acute myeloid leukemia-associated Mkl1 (mrtf-a) is a key regulator of mammary gland function. *Mol. Cell. Biol.* **26,** 5809-5826.

Takeya, R., Taniguchi, K., Narumiya, S. and Sumimoto, H. (2008). The mammalian formin FHOD1 is activated through phosphorylation by ROCK and mediates thrombin-induced stress fibre formation in endothelial cells. *EMBO J.* **27,** 618-628.

Thoumine, O., Nerem, R. M. and Girard, P. R. (1995). Oscillatory shear stress and hydrostatic pressure modulate cell-matrix attachment proteins in cultured endothelial cells. *In Vitro Cell. Dev. Biol. Anim.* **31,** 45-54.

Treisman, R. (1986). Identification of a protein-binding site that mediates transcriptional response of the c-fos gene to serum factors. *Cell* **46,** 567-574.

Treisman, R. (1994). Ternary complex factors: Growth factor regulated transcriptional activators. *Curr. Opin. Genet. Dev.* **4,** 96-101.

Tzima, E., Del Pozo, M. A., Kiosses, W. B., Mohamed, S. A., Li, S., Chien, S. and Schwartz, M. A. (2002). Activation of Rac1 by shear stress in endothelial cells mediates both cytoskeletal reorganization and effects on gene expression. *EMBO J.* **21,** 6791-6800.

Tzima, E., del Pozo, M. A., Shattil, S. J., Chien, S. and Schwartz, M. A. (2001). Activation of integrins in endothelial cells by fluid shear stress mediates rho-dependent cytoskeletal alignment. *EMBO J.* **20,** 4639-4647.

Tzima, E., Irani-Tehrani, M., Kiosses, W. B., Dejana, E., Schultz, D. A., Engelhardt, B., Cao, G., DeLisser, H. and Schwartz, M. A. (2005). A mechanosensory complex that mediates the endothelial cell response to fluid shear stress. *Nature* **437,** 426-431.

Vartiainen, M. K., Guettler, S., Larijani, B. and Treisman, R. (2007). Nuclear actin regulates dynamic subcellular localization and activity of the SRF cofactor MAL. *Science* **316,** 1749-1752.

Vink, H. and Duling, B. R. (2000). Capillary endothelial surface layer selectively reduces plasma solute distribution volume. *Am. J. Physiol. Heart Circ. Physiol.* **278,** H285-9.

Wang, D., Chang, P. S., Wang, Z., Sutherland, L., Richardson, J. A., Small, E., Krieg, P. A. and Olson, E. N. (2001). Activation of cardiac gene expression by myocardin, a transcriptional cofactor for serum response factor. *Cell* **105,** 851-862.

Wang, D., Chang, P. S., Wang, Z., Sutherland, L., Richardson, J. A., Small, E., Krieg, P. A. and Olson, E. N. (2001). Activation of cardiac gene expression by myocardin, a transcriptional cofactor for serum response factor. *Cell* **105,** 851-862.

Wang, D. Z., Li, S., Hockemeyer, D., Sutherland, L., Wang, Z., Schratt, G., Richardson, J. A., Nordheim, A. and Olson, E. N. (2002). Potentiation of serum response factor activity by a family of myocardin-related transcription factors. *Proc. Natl. Acad. Sci. U. S. A.* **99,** 14855-14860.

Weinhold, B., Schratt, G., Arsenian, S., Berger, J., Kamino, K., Schwarz, H., Ruther, U. and Nordheim, A. (2000). Srf(-/-) ES cells display non-cell-autonomous impairment in mesodermal differentiation. *EMBO J.* **19,** 5835-5844.

Yu, J., Bergaya, S., Murata, T., Alp, I. F., Bauer, M. P., Lin, M. I., Drab, M., Kurzchalia, T. V., Stan, R. V. and Sessa, W. C. (2006). Direct evidence for the role of caveolin-1 and caveolae in mechanotransduction and remodeling of blood vessels. *J. Clin. Invest.* **116,** 1284-1291.

Zaromytidou, A. I., Miralles, F. and Treisman, R. (2006). MAL and ternary complex factor use different mechanisms to contact a common surface on the serum response factor DNA-binding domain. *Mol. Cell. Biol.* **26,** 4134-4148.

Zumbrunn, J., Kinoshita, K., Hyman, A. A. and Nathke, I. S. (2001). Binding of the adenomatous polyposis coli protein to microtubules increases microtubule stability and is regulated by GSK3 beta phosphorylation. *Curr. Biol.* **11,** 44-49.